INVESTIGATIONS OF THE MECHANISM AND MODULATION OF GABA(A) RECEPTORS AND THEIR POTENTIATION BY DIHYDROPYRIMIDINONES

A Dissertation

Presented to the Faculty of the Graduate School

of Cornell University

In Partial Fulfillment of the Requirements for the Degree of

Doctor of Philosophy

by

Ryan Wade Lewis

January 2011

INVESTIGATIONS OF THE MECHANISM AND MODULATION OF GABA(A) RECEPTORS AND THEIR POTENTIATION BY DIHYDROPYRIMIDINONES

Ryan Wade Lewis, Ph. D.

Cornell University 2011

Gamma-aminobutyric acid type-A ($GABA_A$) receptors are ligand-gated chloride channels essential for regulating signal transmission within the mammalian central nervous system (CNS). The chloride currents due to these pentameric receptors can be positively modulated (potentiated) by a variety of molecules including barbiturates, diazepams, and endogenous neurosteroids, some of which are used as therapeutics. Molecules that selectively modulate $GABA_A$ receptors of specific subunit compositions are scarce but would be valuable tools for elucidating the function of $GABA_A$ receptor subtypes within the CNS and may aid in developing therapeutics with greater target specificity.

Described here is the discovery of several dihydropyrimidinone (DHPM) small molecules that preferentially potentiate GABA induced whole-cell currents from δ subunit-containing $GABA_A$ receptors. Some of the DHPMs, such as JM-II-43A, had potentiation efficacies comparable to those of non-subtype selective modulators phenobarbital and tracazolate, but the DHPMs did not directly induce receptor currents. JM-II-43A was further tested with α1β2δ $GABA_A$ receptors using flash-photolysis transient kinetic techniques as well as single-channel and multi-channel current recording patch-clamp techniques to determine how DHPMs modulate

these receptors. The results lead to the proposal of a novel mechanism of receptor function involving an equilibrium of $GABA_A$ receptors between an active and inactive state before the presence of agonist. This equilibrium is shifted by potentiating compounds, such as DHPMs, towards the active state to increase the total number of receptors that reach an open-channel (ion conducting) state. This hypothesis also explains the characteristic lack of desensitization and low peak current amplitudes associated with δ subunit-containing receptors.

Also discussed is the purification and characterization of several photo labile GABA derivatives containing a coumarin-based caging group for their quantum yield, rate of photolysis, solubility, thermal stability and sensitivity to visible light in the 350- to 450-nm region. These compounds were intended for transient kinetic investigations of the modulation of $GABA_A$ receptors by DHPMs discussed above. One of these compounds was determined to have a quantum yield of 0.1, however the rate of photolysis was not suitable for transient kinetic measurements in the micro- to milli-second time region.

BIOGRAPHICAL SKETCH

Ryan Wade Lewis was born in Oklahoma City on October 28th, 1980. At the age of 3 Ryan moved with his family to Foxborough, Massachusetts. Thanks to his parents and wonderful teachers in the Foxborough School system Ryan developed a keen interest in both the arts and the sciences while growing up. Ryan graduated from Foxborough High School in May 1999 and went on to Syracuse University where he obtained his Bachelor of Science in Chemistry from the School of Arts and Sciences in May of 2003. Since then, he has lived in Ithaca, New York as a graduate student working on the mechanism of ion channels in George Hess' laboratory in the graduate field of Biochemistry, Molecular and Cell Biology at Cornell University.

Dedicated to my family and friends,

who have been instrumental in supporting me throughout the years.

ACKNOWLEDGMENTS

I would like to thank my advisor Professor George Hess for his mentorship and support in my research project. I wish to thank Susan Coombs for her continual help in keeping the lab functional and for her very helpful assistance with editing abstracts, papers, presentations and more over the years. Thank you to Professor Bruce Ganem, Dr. Lijun Fan, Dr. John Mabry, Jason Polisar and Kyle Eagen who have contributed to the synthesis of DHPMs, caged compounds, and the investigation of how these compounds act on $GABA_A$ receptors. I wish to thank Cornell University for funding through the many teaching assistantships that allowed me to continue my research over the years. I also wish to thank the NIH for funding my studentship for two years of my graduate career through the training grant given to the field of Biochemistry, Molecular and Cell Biology and for research funding through the NIH GM grant awarded to Geroge Hess. Finally, I wish to thank all the lab members, Cornell faculty and all my friends that have had scientific discussions with me, assisted me with experiments, helped me trouble shoot problems, and been moral support over the years. Your contributions to this work, while perhaps seemingly small, make a large difference to me. Thank you.

TABLE OF CONTENTS

BIOGRAPHICAL SKETCH iii

DEDICATION iv

ACKNOWLEDGEMENTS v

TABLE OF CONTENTS vi

LIST OF FIGURES ix

LIST OF TABLES xi

LIST OF ABBREVIATIONS xii

LIST OF SYMBOLS xiv

PREFACE xv

CHAPTER 1: GENERAL INTRODUCTION 1

1.1 General Overview of Neuronal Signaling and $GABA_A$ Receptors in the Central Nervous System 1

1.2 $GABA_A$ Receptor Subunits and Structure 4

1.3 Disease-linked Mutations of $GABA_A$ Receptors 8

Anxiety Disorders 8

Autism Spectrum Disorders 9

Epilepsy 10

1.4 The Mechanism of $GABA_A$ Receptors 13

1.5 Agonists, Antagonists and Modulators of $GABA_A$ Receptors 25

Benzodiazepines 29

Barbiturates 30

Neurosteroids 30

Subunit-specific Modulators 31

1.6 Receptors Containing the Delta Subunit 32

1.7 Techniques and Tools for Investigating Ligand-gated Ion Channels 35

Voltage-Clamp 36

Patch-Clamp Techniques 36

Systems for Solution Application 39

Laser- and Flash-Photolysis 40

CHAPTER 2: DISCOVERY OF DIHYDROPYRIMIDINONE SELECTIVE POTENTIATION OF GABA(A) RECEPTOR CURRENTS 49

Abstract 49

Introduction 50

Methods and Materials 55

Results 60

Discussion 80

CHAPTER 3: MECHANISM OF DIHYDROPYRIMIDINONE POTENTIATION OF DELTA SUBUNIT CONTAINING GABA(A) RECEPTORS 88

Abstract 88

Introduction 89

Methods and Materials 93

Results 97

Discussion 111

CHAPTER 4: CHARACTERIZATION OF VISIBLE-LIGHT-SENSITIVE PHOTOLABILE CAGED-GABA COMPOUNDS 121

Introduction 121

Methods and Materials 126

Results and Discussion 131

APPENDIX 144

A.1 Equations 144

REFERENCES 150

LIST OF FIGURES

Figure 1.1	Various Proposed Mechanisms of Action for Cys-Loop Receptors	15
Figure 1.2	Relation of Whole-Cell Current Recordings of GABA(A) Receptors to the Cash and Hess Mechanism	18
Figure 1.3	Examples of Agonists, Inhibitors and Modulators of GABA(A) Receptors	27
Figure 1.4	Schematic drawings of the Arrangements needed for Patch-Clamp, Cell-Flow and Flash-Photolysis Methods	41
Figure 1.5	Structures of Several Generic Photolabile Leaving Groups	45
Figure 2.1	The Cash and Hess Mechanism and a Proposed Mechanism Showing Phenobarbital Modulation of GABA(A) Receptors	52
Figure 2.2	Examples of GABA(A) Receptor Modulators and a Family of Dihydropyrimidinones that Potentiate GABA(A) Receptors	61
Figure 2.3	Results Demonstrating the Selectivity of Dihydropyrimidinone Potentiation of GABA(A) Receptors Containing the Delta Subunit	64
Figure 2.4	A Dose-Dependent Current Trace Demonstrating Both the Extent, Reversibility and Rate of Induced Potentiation by JM-II-43A at Low GABA Concentrations	67
Figure 2.5	Dose-Dependent Current Responses of GABA, JM-II-43A and Monastrol on α1β2δ GABA(A) Receptors for Obtaining Apparent Binding Affinities	72
Figure 2.6	Examining the Potentiation of JM-II-43A on the α1β2δ(E177A) Mutant GABA(A) Receptor Associated with GEFS+	78
Figure 3.1	Flash-Photolysis Data Indicates No Apparent Change in the Open-Channel Equilibrium Constant in the Presence of JM-II-43A	100
Figure 3.2	Single-Channel Measurements Demonstrate No Change in Channel Conductance or Rate of Channel Closing in the Presence of JM-II-43A	102

Figure 3.3 JM-II-43A Increases the Average Current Amplitudes Measured from a Small Population of Ion Channels using Multi-Channel Patch-Clamp Methods 107
Figure 3.4 JM-II-43A Increases the Stacking of Channel-Opening Events from a Small Population of Ion Channels using Multi-Channel Patch-Clamp Methods 109
Figure 3.5 Proposed Mechanism for Delta Subunit-Containing GABA(A) Receptors 113
Figure 4.1 Synthetic Scheme Used to Create Three Novel Visible-Light-Sensitive Caged-GABA Derivatives 124
Figure 4.2 Electrophysiological Measurements of Coumarin Caged-GABA Derivatives to Test Purity, Photo-Sensitivity to Visible Light, Inertness Prior to Photolysis and Thermal Stability 132
Figure 4.3 Absorption Scans of Compound 6 Before and After Light Exposure 136
Figure 4.4 HPLC Separation of Compound 6 from Coumarin Caging Group After Photolysis 138
Figure 4.5 Determination of the Quantum Yield of Compound **6** was Obtained by Estimation of the GABA Concentration Released Upon Photolysis as Measured with Flash-Photolysis 141

LIST OF TABLES

Table 1.1	Agonists, Antagonists and Modulators of $GABA_A$ Receptors	26
Table 1.2	Reagents and Equipment Used for Patch-Clamp and Flash-Photolysis Techniques	38
Table 2.1	Apparent Dissociation Constants Obtained for α1β2δ and α1β2δ(E177A) Mutant GABA(A) Receptor Subtypes	70
Table 2.2	Parameters Obtained from Exponential Fitting of Current Desensitization Phase	76
Table 3.1	Equilibrium and Rate Constant Values Obtained with Patch-Clamp and Flash-Photolysis Techniques	106

LIST OF ABBREVIATIONS

5α-THDOC - 3α, 21-dihydroxy-5α-pregnan-20-one, a neurosteroid

5-HT3 receptor - Family of serotonin receptors

αCNB - Alpha-carboxy-2-nitrobenzyl

ACBP - Acetylcholine binding protein

ATCC - American Type Culture Collection

CNS - Central nervous system

Cpd. - Compound

d.f. - Degrees of freedom

DHPM - Dihydropyrimidinone

DMEM - Dulbecco's modified Eagle's medium

DMSO - Dimethyl sulfoxide

ELIC - Ligand gated ion channel of *Erwinia chrysanthemi*

EM - Electron microscopy

ER - Endoplasmic reticulum

EGTA - Ethylene glycol bis(β-aminoethyl ether)-*N,N,N',N'* tetraacetic acid

FBS - Fetal bovine serum

GABA - γ-Aminobutyric acid

$GABA_A$ receptor - gamma amino butyric acid type-A receptor

GEFS+ - Generalized epilepsy with febrile seizures plus

GFP - Green fluorescent protein

GLIC - Ligand gated ion channel of *Gloeobacter violaceus*

GlyR - Glycine receptor

HEK293T - Human embryonic kidney cell line 293

HEPES - 4-(2-hydroxyethyl)-1-piperazineethanesulfonic acid

HPLC - High pressure liquid chromatography

IGE - Idiopathic generalized epilepsies

JM-II-43A - A dihydropyrimidinone synthesized by John Mabry

MNP - 2-Methoxy-5-nitrophenyl

MRS - Magnetic resonance spectroscopy

nAChR - Nicotinic acetylcholine receptor

NMDA - *N*-methyl-D-aspartic acid

NMR - Nuclear magnetic resonance spectroscopy

PEI - Polyethylenimine

Rf - Retention factor

RuBi - Ruthenium-bipyridine-triphenylphosphine

SPECT - Single photon emission computer tomography

TFA - Trifluoroacetic acid

THDOC - 3α,21-Dihydroxy-5α-pregnan-20-one

THIP - Gaboxadol, or 4,5,6,7-tetrahydroisoxazolo[5,4-c]pyridin-3-ol

THP - Allopregnanolone

uPAR - Plasminogen activator, urokinase receptor

LIST OF SYMBOLS

α - alpha, subunit of the $GABA_A$ receptor

β - beta, subunit of the $GABA_A$ receptor

γ - gamma, subunit of the $GABA_A$ receptor

δ - delta, subunit of the $GABA_A$ receptor

μ - mu; used as a prefix designating micro

Φ^{-1} - inverse of phi; designated as the channel-opening equilibrium constant

τ - tau, used to denote time constants

PREFACE

Over my graduate career I have had a variety of projects, with this dissertation discussing only one of these projects that eventually became fruitful. The other projects that I worked on, while not yielding a cohesive story or not working out the way I anticipated, did permit me the opportunity to learn many techniques that I might never have otherwise. However, I have come to realize that what one truly learns during a successful graduate student's studies are not the techniques and the details of projects an individual has pursued, but the process of learning how to learn about a topic and ask relevant questions. While this may sound fundamentally simple, it is a step that cannot be taught in a text book or a classroom. These are skills that no one can give through lectures and discussion. Mentors, advisors, and peers can only help an individual obtain these skills by demonstrating their use, but in the end it is the act and struggle of research that truly teaches a student to become a researcher. So I give to you, the reader, this dissertation; a small research story that is only such a small fraction of the experiences and labor that have transformed me into a scientist.

CHAPTER 1

GENERAL INTRODUCTION

The mammalian central nervous system is composed of roughly one trillion (10^{12}) neurons that are constantly receiving, propagating and transmitting signals to other cells through the collective contribution of a diverse class of proteins called ion channels. The transmission and regulation of neuronal signaling occurs in part through the use of ion channels that are activated by small molecules called neurotransmitters. The neurotransmitter γ-aminobutyric acid (GABA) is the primary inhibitory neurotransmitter of the vertebrate central nervous system (CNS) (*19, 20*). This ligand represses signaling in the CNS through activation of two major classes of receptors; $GABA_A$ receptors, which are ligand-gated ion channels, and $GABA_B$ receptors, which are heterotrimeric G protein coupled receptors (*20*). While both receptor types modulate neuronal signaling, this disertation focuses on $GABA_A$ receptors, a family of ligand-gated ion channels.

1.1 General Overview of Neuronal Signaling and $GABA_A$ Receptors in the Central Nervous System

The neurons of the CNS primarily rely on ion gradients and ion permeability across the plasma membrane for signal transmission. The low levels of Na^+ and high levels of K^+ inside cells, as compared to the extracellular environment, create ion gradients established by the P-type Na^+/K^+ ATPase, also known as the Na^+/K^+ pump. Gradients established by ion pumps, such as the Na^+/K^+ pump, and selective ion permeability

provided by transmembrane ion channels, collectively establish an electric potential across the membrane that is essential for neuronal signaling (*23*). The magnitude of this membrane potential (E_M) is described by the Nernst equation (*24*)

$$E_S = (RT/zF)\ln([S]_{out}/[S]_{in}) \quad [1.1]$$

for a single ion (S) with charge (z), or by the Goldmann/Hodgkin/Katz equation (*25, 26*)

$$E_M = (RT/F)\ln((\sum P_C[C]_{out} + \sum P_A[A]_{in})/(\sum P_C[C]_{in} + \sum P_A[A]_{out})) \quad [1.2]$$

for multiple monovalent cations (C) and anions (A). The other parameters in these equations are the universal gas constant (R), absolute temperature in Kelvin (T), Faraday's constant (F), and the permeability of a cation (P_C) or anion (P_A) through the membrane. In the case of neurons, the membrane potential commonly resides at -60 to -80 mV due to the presence of constitutively open potassium 'leak' channels. As ion permeability changes with the opening or closing of ion channels, the membrane potential changes accordingly. Changes in the membrane potential also activate voltage-sensitive ion channels, which further alter the membrane potential. The synchronized opening and closing of voltage-sensitive Na^+ and K^+ channels generates and propagates waves of electric potential, called action potentials (*29*). These action potentials are the fundamental signals of the CNS. The signals rapidly travel the length of a neuron, from its dendrites, through the soma and axon, to the axon terminals at conduction velocities up to 21.5 m/s for non-myelinated neurons (*30*). However, for these signals to be transmitted from the axon terminals of one neuron to the dendrites of the next, small molecules called neurotransmitters are needed. Upon reaching an axon terminal, an action potential ultimately causes vesicles

containing neurotransmitter to fuse with the plasma membrane. Neurotransmitter is released into the space between two juxtaposed neuronal membranes, called a synapse. The membrane of the post-synaptic dendrite contains ligand-gated ion channels that bind the neurotransmitter and rapidly open. Depending upon the ion selectivity of the ligand-gated channel, the neurotransmitter may raise the membrane potential to stimulate a new action potential, or lower it to prevent excitation.

The pentameric $GABA_A$ receptor is an anion-selective, ligand-gated ion channel that facilitates the flux of both Cl^- and bicarbonate (HCO_3^-) into the cell, which makes the membrane potential more negative (hyperpolarization) and diminishes the ability of voltage-sensitive ion channels to open. Thus, $GABA_A$ receptors are considered inhibitory or repressive and are critical for regulating neuronal signaling. Various subtypes of these ion channels are present at either neuronal synapses to receive inhibitory signals or throughout extrasynaptic areas to mediate regional modulation of the CNS by responding to extracellular levels of GABA and endogenous neurosteroids. The importance of $GABA_A$ receptors is exemplified by the numerous mental diseases that have been linked to the malfunction of these receptors, including insomnia, anxiety, autism, depression, schizophrenia and epilepsy. Additionally, endogenous steroids and many anesthetics and small molecule drugs, such as benzodiazepines, barbiturates, ethanol and gaboxadol, target $GABA_A$ receptors, emphasizing the importance of understanding the structure and function of these receptors.

1.2 $GABA_A$ Receptor Subunits and Structure

The pentameric structure of $GABA_A$ receptors is a common attribute of all members of the cys-loop receptor super-family, which includes nicotinic acetylcholine (nAChRs), glycine (GlyRs) and serotonin (5-HT3) receptors (*20*). These receptors can be composed of many combinations of subunits; in the case of the $GABA_A$ receptors, there are 19 different $GABA_A$ receptor subunits in the human genome (α1-6, β1-3, γ1-3, δ, ε, π, τ, ρ1-3). Classes of $GABA_A$ receptor subunits (*e.g.* α, β, etc.) are based on amino-acid sequence identity, with subunits within a single class having > 70% identity, and 30-40% identity between classes (*32, 33*). The combinations of these subunits dictate the pharmacology, kinetic mechanism, localization and even the cellular function of different $GABA_A$ receptors (*21, 33-40*). The variety of subunits is further expanded by different mRNA splice variants, such as the long (γ2L) and short (γ2S) forms of the γ2 subunit (*41*). With 19 different subunits, several with splice variants, the number of theoretical permutations is immense.

Though many different subtypes of $GABA_A$ receptors are theoretically possible, not all the possible combinations are found in the CNS (*42*). Receptors consist of at least two α and two β subunits (*20, 43*). A bias for specific combinations of subunits was demonstrated by using immunoaffinity columns of rat brain $GABA_A$ receptors (*44*). These studies specifically highlighted that γ and δ subunits were not found together in a receptor complex. These and many other studies (*32, 38, 45-47*) have attempted to identify endogenous receptor subtypes and their localization in the CNS (see review (*37*)). Immunocytochemistry studies have localized 13 different subunits in the rat CNS (*48*): α1, β1, β2, β3 and γ2 subunits are

found throughout the CNS whereas α2, α3, α4, α5, α6, γ1, γ3 and δ subunits are localized to specific areas of the brain. These results also supported previous evidence that the α1β2γ2 receptor subtype is the most abundant and is expressed ubiquitously in the CNS. Many other less abundant subtypes are localized to specific regions or neurons within the CNS. For example, the α1β2δ subtype is found in hippocampal interneurons (*6*), α1α6βδ and α1α6βγ receptors in cerebellum granule cells (*49*), and receptors containing α3, θ, and ε localize to the dorsal raphe as well as the locus coeruleus regions of the brain (*46, 50*). While various $GABA_A$ receptor subtypes may have overlapping roles in the CNS, the unique localizations, pharmacology and mechanisms of some subtypes suggest they have specialized functions.

The current structural understanding of subunit interactions with one another and with small molecule ligands is based entirely on techniques other than x-ray crystallography, as no full length eukaryotic cys-loop receptor has been crystallized. Primary sequence analysis indicates that all cys-loop receptors (nAChRs, GlyRs, 5-HT3 and $GABA_A$ receptors) have evolved from a single ancestral receptor and, therefore, are thought to have similarities in both structure and function (*51-53*). To date, the best atomic structures of eukaryotic cys-loop receptors are electron microscopy 3-dimensional reconstructions of nACh receptors from a *Torpedo* species (*54*). The 4 Å resolution structure of the receptor transmembrane domain has revealed several residues critical for gating ion flux. Additional structural information has come from the x-ray crystal structure of the acetylcholine-binding protein (AChBP) from the mollusk *Lymnaea stagnalis* (*55, 56*). AChBP is a cytosolic protein reported to have moderate sequence similarity

to the extracellular domain of nAChRs and was identified by its ability to bind acetylcholine and α-bungarotoxin, a specific inhibitor of muscle type and α7 nAChRs (*55*). Although the AChBP subunits lack transmembrane domains, their crystal structure shows the assembly of its subunits into a pentameric structure (*56*).

The structural information about cys-loop receptors has grown substantially with three recently reported x-ray structures of pentameric ligand-gated ion channels from prokaryotes; the ELIC receptor from *Erwinia chrysanthemi* was reported at 3.3 Å resolution (*57*), and two structures of the GLIC receptor were reported from *Gloeobacter violaceus* at 3.1 Å and 2.9 Å resolutions (*58, 59*). What is particularly interesting about these structures is that they give examples of full protein complexes that are in apparent open- and closed-channel states. Such structures are likely to be very helpful to identify important amino-acid residues and binding domains for all cys-loop receptors.

In the case of the $GABA_A$ receptor, the best structural data has been obtained by using the AChBP as a template to overlay the protein sequence of the extracellular domain of a $GABA_A$ receptor with two α, two β, and one γ subunit (*60*). This structural modeling prompted the hypothesis that there is a preferred absolute arrangement of the subunits within the $GABA_A$ receptor pentamer. This model was supported by studies that characterized the expression and electrophysiology of α1, β2, and γ2L subunits that were artificially linked to one another as dimers or trimers (*61*). These 'tethered' or concatenated subunits force the receptors to assemble into an absolute arrangement, which permits examining the effect of subunit position within a $GABA_A$ receptor complex. While a preferred arrangement for α1β2γ2L

was identified with both concatenated subunits and modeling of subunits based on the AChBP structure, it is still not known what absolute subunit arrangements exist for other $GABA_A$ receptor subtypes (i.e. non-α1β2γ2L receptor subtypes). Indeed, investigations using concatenated subunit constructs have shown several alternate arrangements in δ subunit-containing receptors (*10*).

$GABA_A$ receptor structure and function has also been investigated by mutagenesis techniques, which identified critical residues within $GABA_A$ receptors for the anion selectivity of the receptor (*62*), the binding of GABA (*63*), the binding of modulatory compounds (*64-67*), and mechanistic steps for channel function (*68*). Natural mutations within $GABA_A$ receptors have been instrumental to understanding the structure and function of $GABA_A$ receptors. Point mutations in receptor subunits genetically linked to diseases, such as epilepsy (*3, 69-71*), have greatly contributed to understanding both the role of $GABA_A$ receptors within the CNS and of individual residues in receptor function. These point mutations influence $GABA_A$ receptor pharmacology (*70*), mechanism (*1, 4*), subunit assembly (*72*), cellular trafficking (*43*) and surface expression (*73, 74*).

The combination of natural point mutations, artificial mutations, structural modeling, EM structural data, and analysis of homologous ligand-gated ion channels has given researchers a general understanding of the structural organization of subunits, domains, and residues needed for receptor function. However, the many possible subunits that compose these receptors complicate this general picture. Since receptor subtypes have different biophysical and pharmacological properties, the ability to extrapolate structural information from one particular subtype to another, or

from nAChRs to $GABA_A$ receptors, may be limited.

1.3 Disease-linked Mutations of $GABA_A$ Receptors

$GABA_A$ receptors are important components for the regulation of neuronal signaling, thus it is little surprise that their malfunction or altered function has been implicated in diseases. Anxiety, autism, depression, epilepsy, insomnia and some cases of schizophrenia are all mental disorders that have been linked to $GABA_A$ receptor function or expression within the CNS (reviewed in (*75*) and (*76*)). This section will briefly discuss what is currently known for the three best understood mental disorders: anxiety, autism and epilepsy. While $GABA_A$ receptors are implicated in other mental afflictions, the evidence is indirect or limited.

Anxiety Disorders

Anxiety as a neurological disorder has a great socioeconomic impact and is highly prevalent with roughly 4.7% of individuals fitting criteria for lifetime panic disorders (*77, 78*). Because $GABA_A$ receptors regulate and repress signaling in the CNS, it is thought that anxiety may be due to decreased GABAergic signaling (*79*). Genetic components of anxiety disorders have not been found with any genes, including $GABA_A$ receptor subunits (*80, 81*); however, several lines of evidence support a contribution of $GABA_A$ receptors. Several benzodiazepines, a class of compounds that target and modulate $GABA_A$ receptors, are commonly used as anxiolytics (anti-anxiety drugs) (*77, 82*). Positron emission tomography (PET) studies using the benzodiazepine flumazenil to bind $GABA_A$ receptors, suggest that the brains of patients with anxiety disorders have a decrease in $GABA_A$

receptor expression (*83, 84*). This apparent reduction of $GABA_A$ receptors was supported by a study using single photon emission computer tomography (SPECT) with iomazenil, an analog of flumazenil (*85*). These results indicate reduced GABAergic regulation of CNS signaling. Other studies using magnetic resonance spectroscopy (MRS) measurements show a considerable (22%) reduction in cortical GABA concentrations in patients with anxiety disorders, again suggesting a decrease in GABAergic regulation (*86*). Mouse models have shown that decreased $GABA_A$ receptor expression in the CNS leads to increased anxiety. Mice heterozygous for the γ2 subunit, which is important for keeping receptors in the plasma membrane, displayed increased anxiety and threat response when examined for their response to fear stimuli (*87*). Further studies are needed to elucidate and understand the connection of $GABA_A$ receptors to anxiety disorders.

Autism Spectrum Disorders

Autism is largely inherited in a non-Mendelian (idiopathic) manner, but there are several indications the function and expression levels of $GABA_A$ receptors have a role in autism spectrum disorders (*88*). While the genetic link of $GABA_A$ receptors to autism is still debated (*89, 90*), mutations in and around genes for β3, α5, and γ3 subunits, found within the q11-13 regions of chromosome 15, have been genetically associated with autism (*91-94*). It should be noted that the 15q11-13 region is also implicated in the Prader Willi/Angelman Syndrome and in autistic individuals often having chromosomal duplications of this region (*88, 95*). Non-genetic evidence from binding assays, using radio-labeled muscimol and flunitrazepam, indicates a decrease in $GABA_A$ receptor expression in

brains of autistic individuals, particularly in the anterior cingulate cortex (*96*). Epigenetic dysregulation of the expression levels of $GABA_A$ receptor genes has also been implicated as a possible cause of autism-spectrum disorders (*97*). Dramatic changes in the expression levels of various $GABA_A$ receptor subunits have been observed in knockout mice for the protein uPAR (*98*), a protein implicated in autism (*99*). Thus, a growing amount of data supports the notion that $GABA_A$ receptors, particularly their expression levels, have a significant role in autism-spectrum disorders.

Epilepsy

Epilepsy was estimated to affect 42 million people worldwide and 2.5 million Americans in 1993 with an estimated annual cost of $2.5 billion (*100*), making epilepsy a significant societal and economic burden (*101*). Of all the disorders linked to $GABA_A$ receptors, epilepsy is the best established, as several mutations leading to susceptibility for epilepsy have been identified. Although these mutations have been correlated with inheritance of particular forms of epilepsy in families, mutations in $GABA_A$ receptors are not common in most epileptic patients, and other unknown susceptibility factors must exist (*102-106*). Regardless, more than ten mutations found in the $GABA_A$ receptor subunits correlate with inheritable forms of epilepsy, clearly demonstrating that $GABA_A$ receptors contribute to this disease.

The first genetic evidence implicating $GABA_A$ receptors in epilepsy was reported in 2001 when two distinct missense mutations coding for either a lysine-to-methionine change at residue 289 (K289M) or an arginine-to-glutamine change at residue 43 (R43Q) were found within a γ2 subunit gene of a family displaying traits similar to generalized epilepsy with febrile

seizures plus (GEFS+)(*69*) or childhood absence epilepsy and febrile seizures(*70*), respectively. The K289M mutation is located in a conserved amino-acid loop between the second and third transmembrane domains, a region implicated in the gating of the receptor (*107*) and resulting in decreased current amplitudes of mutant receptors (*1, 69, 108*). The K289M mutation is believed to decrease the receptor mean-open time (the period that the receptor stays in an open-channel state) to 10% that of wild type (*108, 109*) and to reduce the channel-opening equilibrium constant by 5-fold (*1*). The R43Q mutation is located in the extracellular N-terminal domain of the γ2 subunit and was reported to abolish the modulatory effects of the benzodiazepine diazepam (*70*). It was later revealed that lower currents from mutant receptors result from decreases in cell-surface expression (*108, 109*). By inserting enhanced yellow fluorescent protein in between the fourth and fifth amino-acid of the γ2 subunit, confocal microscope studies were able to visualize retention of the γ2(R43Q) subunit in the endoplasmic reticulum (ER) (*73*), likely the result of an inability to assemble into functional receptors (*72*).

Since the first report in 2001 many other $GABA_A$ receptor mutations have been linked to cases of epilepsy and seizures. The R139G mutation in the γ2 subunit of $GABA_A$ receptors was associated with febrile seizures in 47 unrelated patients (*110*). Receptors containing the γ2(R139) subunit have an increased rate of receptor desensitization and decreased sensitivity to diazepam.

Another point mutation in the γ2 gene was identified in a family with a genetically heritable form of childhood absence epilepsy and febrile seizures (*111*). This mutation, denoted as γ2(IVS6+2T→G), abolishes

mRNA processing at the 5' splice-site of intron-6. While never experimentally confirmed, it is predicted that the IVS6+2T→G mutation will result in the merging of exon 5 and 7 in a process called 'exon skipping', which would result in a premature stop codon (*111*).

The γ2(Q351X) point mutation found in an Australian GEFS+ family codes for a premature termination codon (*112*) and creates a truncated subunit that acts as a dominant-negative by retaining α and β subunits in the ER (*113*). Furthermore, the generation of both a yellow fluorescent protein tagged γ2(Q351X) subunit and a pH sensitive enhanced GFP (pHluorin) tagged γ2(Q351X) subunit clearly indicate reduced expression of the mutant subunit on the cell plasma membrane (*114*).

Recently, a Chinese family with a record of GEFS+ was found to carry a γ2 gene with a W390X truncation mutation, which is located between the third and fourth transmembrane helixes of the subunit (*115*). It is not known whether the γ2(W390X) subunit has any functional activity; it is likely retained in the ER and shuttled into the degradation pathway.

An A322D mutation found in the α1 subunit within a family with autosomal dominant juvenile myoclonic epilepsy (*71*) was determined to have significant retention in the ER and reduced expression in the plasma membrane (*74, 116*). Any functional receptors containing the α1(A322D) subunit were found to have significantly altered mechanisms (*117, 118*) and to undergo more rapid endocytosis and targeting to the lysosome for degradation (*119*).

A screen of 98 unrelated patients with idiopathic generalized epilepsies (IGE) revealed a frame-shift mutation at residue 326 of the α1 subunit, creating an early termination codon two positions later

(S326fs328X) (*120*). The α1(S326fs328X) subunit is truncated three-quarters through the third transmembrane helix and likely does not give rise to functional receptors. Accordingly, it was determined that the α1(S326fs328X) subunit was retained in the ER and no currents were observed when it was expressed with other subunits in HEK293 cells.

Three point mutations (P11S, S15F, and G32R) in the β3 subunit gene were associated with childhood absence epilepsy in four families from Mexico, Honduras and El Salvador (*121*). These mutations result in decreased currents in transiently expressed receptors, with preliminary results indicating that increased glycosylation of β3(P11S, S15F, and G32R) mutant receptors may play a role. While glycosylation does alter the mechanism of $GABA_A$ receptors (*122*), it is not entirely clear how hyper-glycosylation would decrease channel currents.

The E177A and R220H point mutations within the δ subunit gene were identified in two separate GEFS+ families and lead to reduced currents from whole-cell, patch-clamped cells transiently expressing α, β, and mutant δ subunits (*3*). Further characterization of the δ(E177A)- and δ(R220H)-containing receptors revealed reduced open-times of the channel and a slight reduction in cell surface expression (*4*).

1.4 The Mechanism of $GABA_A$ Receptors

Electrophysiological techniques established by Sakmann and Neher (*123-125*) have allowed many researchers to investigate the mechanism of ion channels through analysis of both whole-cell and single-channel current measurements. (These techniques are described in Section 1.7.2.) These techniques permitted researchers to build upon previously proposed

mechanisms resulting in a diversity of potential mechanisms for nACh and $GABA_A$ receptors (*15, 27, 28, 31, 126-128*). Several mechanisms are shown in Figure 1.1, the upper three proposed from voltage clamp measurements and ion flux measurements (*12, 15, 22*), and the lower three proposed based on single channel analysis techniques (*27, 28, 31*). However, the underlying components of all these mechanisms can be traced back to the mechanisms proposed for nAChRs by Del Castillo, Katz and Thesleff based on voltage-clamp measurements of frog neural muscle endplates (*12, 22*). Because all cys-loop receptors ($GABA_A$ receptors, nAChRs and GlyRs) are likely of the same origin (*52, 53*), many principles of the nAChR mechanism also apply to $GABA_A$ receptors. The first mechanism proposed for nAChRs, by Del Castillo and Katz, described the nAChR in a ligand-free state (R), a ligand-bound state with the channel closed (RL), a ligand-bound state with the channel open ($\overline{\text{RL}}$), and a desensitized state with a closed-channel (DL) (Figure 1.1). This mechanism was refined by Katz and Thesleff to generate two cyclic mechanisms where an active (R) and inactive (D) form of the receptor can both bind a ligand (one of these mechanisms is shown in Figure 1.1). These cyclic mechanisms were the foundation on which the Cash and Hess mechanism (*15*) was derived. Differences in the Cash and Hess mechanism include the receptor binding two ligand molecules. This widely accepted modification to the mechanism of cys-loop receptors is based on the presence of high (nM) and low (μM) affinity ligand-binding sites observed in both purified and cloned nACh and $GABA_A$ receptors (*52, 129-131*). The Cash and Hess mechanism also explicitly describes the channel-opening equilibrium constant (Φ^{-1}), which is defined as the channel-opening rate constant (k_{open}) divided by the channel-closing rate constant (k_{close}) (*15*).

Figure 1.1 Shown are only a few of the many mechanisms of action that have been proposed for cys-loop receptors, which include $GABA_A$ and nAChRs receptors. These mechanisms demonstrate the diversity of how voltage-clamp, single-channel, and whole-cell patch-clamp data can be interpreted to explain the function of these receptors. The mechanism proposed by Cash & Hess (*15*) is the mechanism primarily focused on in this dissertation because it is a minimalistic mechanism that still describes the observed behaviors of ligand-gated channels. It is based largely on the mechanism of Del Castillo (*22*) and the refinements by Katz & Thesleff (*12*). Other mechanisms shown have been proposed by Jones & Westbrook (*27*), Macdonald & Twyman (*28*) and Bianchi et al.(*31*).

These mechanisms have been adapted to use a uniform set of symbols. These include, ligand-free receptor states (R), ligand-bound states with the channel closed (RL and RL_2), ligand-bound states with the channel open ($\overline{\mathrm{RL}}$, $\overline{\mathrm{RL}_2}$, etc.), and desensitized states with a closed-channel (various 'D' states) (Figure 1.1). Shown in only some of the mechanisms are rate constants (k), dissociation constants for GABA (K) and the channel open equilibrium constant (Φ^{-1}). In fact, all of the arrows are associated with rate constants, but these are not shown for aesthetic purposes.

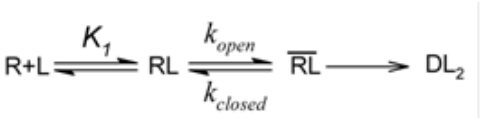

Del Castillo & Katz (1957)

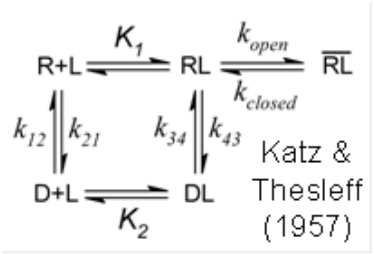

Katz & Thesleff (1957)

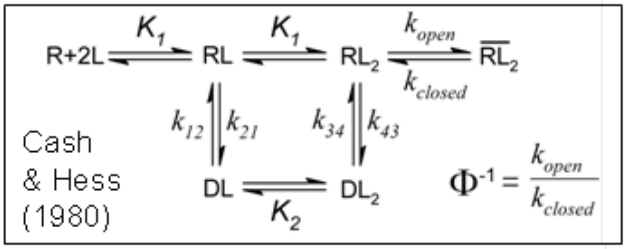

Cash & Hess (1980)

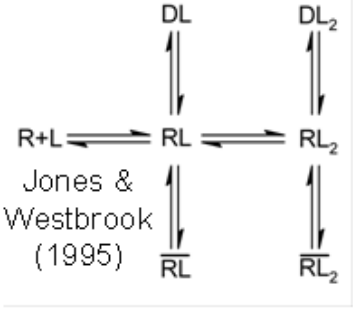

Jones & Westbrook (1995)

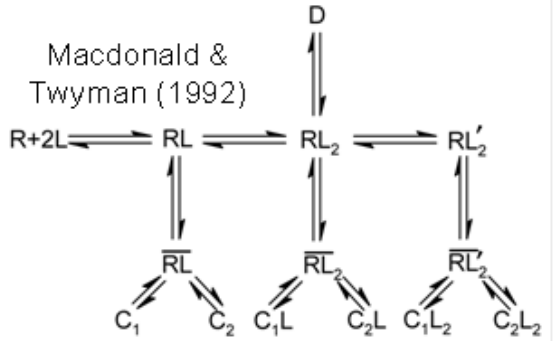

Macdonald & Twyman (1992)

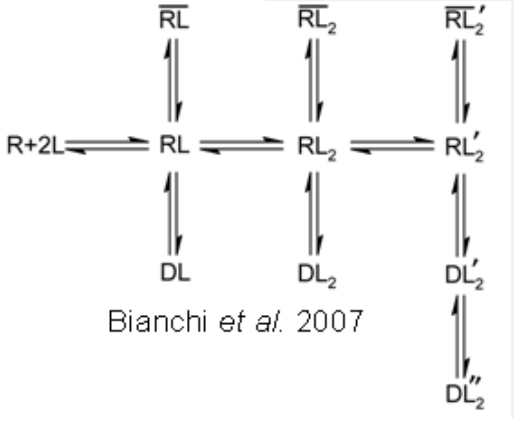

Bianchi *et al.* 2007

Many mechanisms have been proposed for both $GABA_A$ receptors and nAChRs (*15, 27, 31, 126-128, 132*). The Cash and Hess mechanism (Figure 1.1) has been used in the research described in this dissertation, because it is a minimalistic model and fits well with observed data for these receptors. The current trace in Figure 1.2A, obtained with a cell expressing α1β2γ2L $GABA_A$ receptors and voltage-clamped at -60 mV using whole-cell patch-clamp recording, clearly displays the individual receptor states that are described in the Cash and Hess mechanism. Note that the membrane potential (E_M) is clamped at -60 mV across the cell membrane and that the currents observed will be negative. This is due to the relationship between electric potential (V), current (I) and conductance (g), as described by Ohm's law ($V = I / g$), which dictates that as $GABA_A$ receptor ion channels open or close, the current amplitude will change with the same sign as the electric potential. It is important to realize that the potential (V) is actually the difference between the set E_M and the electric potential generated by the concentrations of Cl^- ions on both sides of the membrane (E_{CL}). Thus Ohm's law can be written as $(E_M - E_{CL}) = I / g$.

In the current trace in Figure 1.2A, the receptors start in a non-conducting state (R) in the absence of GABA (L), which is observed as the baseline current (Roman numeral I). Upon application of GABA, the receptors rapidly bind a first (RL) and second (RL_2) molecule of GABA. The ligand bound, closed-channel state then enters a rapid equilibrium with the conducting, open-channel state ($\overline{RL_2}$). This is observed in the current trace as the rapid increase in current to ~ -4 nA, referred to as the 'rising' phase of the current trace (Roman numeral II). The population of receptors in the RL_2 state also slowly reaches an equilibrium with a non-conducting,

Figure 1.2 Attributes observed in whole-cell patch-clamp current recordings of $GABA_A$ receptors related to the mechanism proposed by Cash & Hess (*16*). **A.** Whole-cell patch-clamp currents recorded from α1β2γ2L (left) and α1β2δ (right) receptor subtypes that were transiently expressed in HEK293T cells. Currents were evoked by application of 1 mM GABA while the membrane was voltage-clamped at -60 mV. The differences observed between the receptor subtypes include absence of a desensitization phase from α1β2δ receptors as well as lower current amplitudes as compared to α1β2γ2L receptors. Different stages of both current traces are identified as baseline current (I), the current rising phase (II), the desensitization phase (III), and GABA dissociation from the receptor upon cessation of application (IV). Also shown is the current corrected for desensitization (V) obtained for the α1β2γ2L receptor subtype by using equation [1.8]. **B.** These different phases of the whole-cell current traces can be related to the receptor mechanism proposed by Cash & Hess (*16*). $GABA_A$ receptors starting in a closed-channel state (R) can rapidly bind two molecules of GABA (L). This ligand-bound, but closed-channel, state (RL_2) then undergoes a conformational change to enter an open-channel state ($\overline{RL_2}$). The population of receptors in this equilibrium between the open- and closed-channel states decreases as receptors more slowly enter a desensitized closed-channel state that does not readily respond to GABA (DL_2).

A

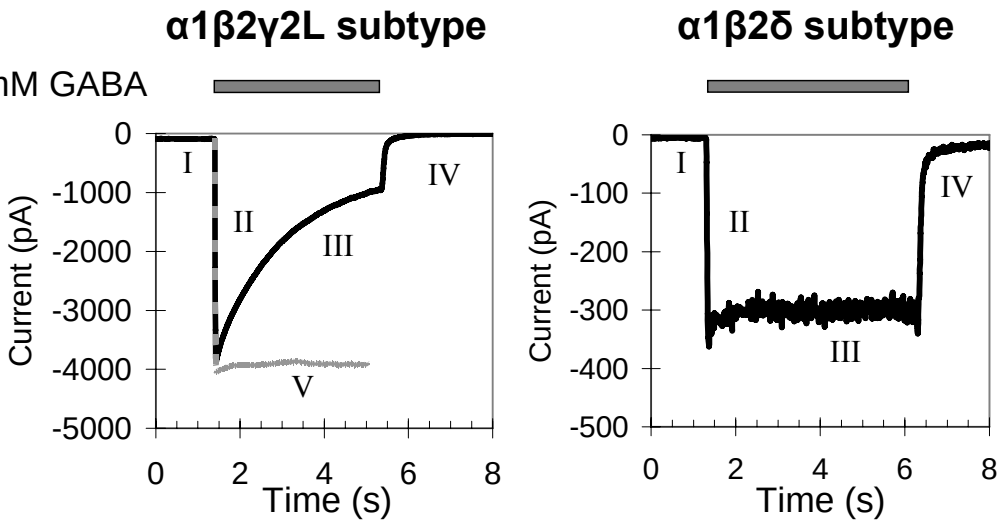
α1β2γ2L subtype
α1β2δ subtype
1 mM GABA
Current (pA)
Time (s)
I
II
III
IV
V

B

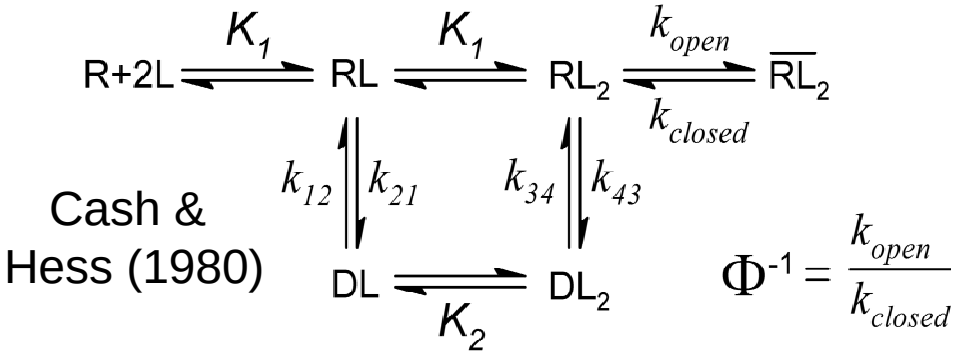
R+2L
RL
RL2
DL
DL2
K1
K2
kopen
kclosed
k12
k21
k34
k43
Cash & Hess (1980)
Φ-1 = kopen / kclosed

desensitized state (DL_2), which is observed as the exponential decrease in current with time (Roman numeral III). When GABA application is stopped and replaced with buffer (Roman numeral IV), GABA quickly dissociates from the receptor and the receptors return to the R state.

The equilibrium constants and rate constants ultimately dictate how a population of receptors is distributed among the conformational states of a mechanism. As such, experiments are conducted and mathematical relationships are calculated to determine these kinetic parameters of a mechanism. A few of these important constants include: the ligand dissociation constant (K_1); the rate of desensitization, which is often described by two or more exponential time constants (τ); the channel-opening equilibrium constant (Φ^{-1}); channel conductance ($g_{channel}$); and the term $I_M R_M$, which is the product of the maximal current obtained from one mole of receptors (I_M) multiplied against the molar concentration of functional receptors (R_M). These parameters, in combination with a mechanism, allow one to describe and make predictions about the behavior of receptors, such as the expected current amplitudes for specific agonist concentrations. Additionally, the mechanism of modulation by small molecules or point mutations linked to diseases can be determined by changes observed in these kinetic parameters. For instance, it was originally thought that inhibitors of the nAChRs, such as cocaine, bind to the open-channel state of the receptor and directly block ion flux (*133*). However it was later determined that these inhibitors act by binding to the closed-channel state of the receptor with a higher affinity (*134*), and that molecules that bind to the open-channel state with a higher affinity can alleviate this inhibition (*135, 136*). Thus, understanding the kinetic mechanism of

receptors is quite useful for explaining how these complexes contribute to signaling within the CNS.

To determine the values of the kinetic parameters, it is necessary to mathematically describe several predictions from the proposed mechanism. The Cash and Hess mechanism permits the derivation of two such equations (below) for calculating the fraction of receptors in an open-channel state (F_{open}) relative to the concentration of agonist (*15*). At the time of GABA application, before receptor desensitization ($t = 0$), F_{open} is described as

$$F_{open\ t=0} = [\overline{RL_2}]_{t=0} / [R_M] = ([L]) / ([L]^2 + \Phi([L] + K_1)^2) \qquad [1.3]$$

where $[R_M]$ is the molar concentration of all functional $GABA_A$ receptors and K_1 is the binding affinity of the receptor for GABA ($K_1 = k_{off} / k_{on}$). At infinite time ($t = \infty$) after application of GABA the open-channel concentration is

$$F_{open\ t=\infty} = [\overline{RL_2}]_{t=\infty} / [R_M] = ([L]K_{D2}) / (K_{D2}([L]^2 + \Phi([L] + K_1)^2 + \Phi[L]([L] + 2K_2)) \qquad [1.4]$$

where K_{D2} is an equilibrium constant between $[RL_2]$ and $[DL_2]$ and K_2 is the binding affinity of the desensitized receptor for GABA. Equations [1.3] and [1.4] were originally determined by Cash and Hess (*15*), and their derivations can be found in the appendix of this dissertation. These equations are based on several assumptions: i) only an active receptor can form an open-channel, ii) although the two GABA binding sites have unique affinities for GABA, the binding of both GABA molecules occurs at rates much faster than the conformational change that leads to an open-channel and faster than the rate of desensitization, thus can be described by two equivalent binding affinities (K_1), iii) all receptors start in an unbound active state. While the first two assumptions were explicitly stated when the model

was originally proposed (*15*), the third assumption was revealed by work described in Chapter 3 of this dissertation. The Cash and Hess mechanism is a general kinetic mechanism, and it is likely the rates of channel opening and closing, desensitization, and the binding of GABA to the receptor will vary for different receptor subtypes, such as α1β2δ $GABA_A$ receptors, which lack a desensitization phase (Figure 1.2A).

Equations [1.3] and [1.4] can be used to calculate the expected currents observed when using single-channel and/or whole-cell patch-clamp electrophysiological techniques. Patch-clamping applies a voltage-clamp across a cellular membrane (membrane potential, E_m), permitting the visualization of current increases and decreases directly due to channel opening and closing. When using whole-cell patch-clamp measurements, the expected current can be calculated by multiplying the fraction of channels in the open-channel state (F_{open}) by the molar concentration of functional receptors on the cell surface (R_M) and the current obtained from one mole of receptors in the open-channel state (I_M). This relationship,

$$I_{obs} = I_M R_M F_{open\ t=0} = I_M R_M ([\overline{RL_2}]_{t=0} / [R_M]) \qquad [1.5]$$

was originally described by Hess et al. (*137*). The parameter I_M for a $GABA_A$ receptor can then be estimated for a patch-clamped current recording by multiplying E_M-E_{CL} (the electric potential, V), against both the maximal channel conductance ($g_{channel}$), and Avogadro's number (N_A), $I_M = (E_M - E_{CL}) g_{channel} N_A$. Substituting this relationship into equation [1.5] yields a more complete equation of

$$I_{obs} = I_M R_M ([\overline{RL_2}]_{t=0} / [R_M]) = (E_M - E_{CL}) g_{channel} N_A [\overline{RL_2}] \qquad [1.6]$$

where the molar concentrations $[R_M]$ are cancelled and the parameters needed to calculate I_M have been inserted. The single channel conductance

($g_{channel}$) is a parameter that is specific for the receptor examined and must be experimentally obtained, typically by single-channel current measurements. As discussed in Section 1.2 the various subtypes of $GABA_A$ receptors have different biophysical properties, one of these being channel conductance.

An additional aspect to consider when mechanistically examining ligand-gated ion channels is the desensitization of the receptors with time. Desensitization results in an exponential decay of current, clearly observed in whole-cell current measurements (Figure 1.2A). The desensitization of ion channels can be described by fitting the decaying whole-cell current (I) with the exponential function

$$I(t) = \sum A_n e^{-t/\tau_n} \qquad [1.7]$$

which can have one or more exponential components, denoted by the subscript '*n*'. The parameters A_n represents the current amplitude for the n^{th} exponential component, t represents time and τ_n is the time constant for the n^{th} exponential component. A time constant in the context of $GABA_A$ receptor current can be thought of as the time that it takes for a current amplitude of the n^{th} exponential component (A_n) to decrease to A_n / e (or ~ 36.79% of A_n). [For example, if a current is obtained that starts at 100 nA of current and decreases to 0 nA, and this decrease can be fit with a function using only a single exponential, then τ would be the time it takes for the current to become ~ 36.79 nA.] Thus, τ parameters are good descriptors for desensitization and can be used to examine how this desensitization changes under various conditions. For example, when subunits α1-6 are individually expressed with a β and γ subunit, the resulting $GABA_A$ receptors have different desensitization rates, which are reflected in the different

values of τ measured (*39*).

The maximum amount of current evoked with saturating ligand concentrations, effectively described by $I_M R_M$, is useful for calculating other kinetic constants. This parameter is also useful for estimating the total number of receptors present in a single cell (if the channel conductance is known for a single channel) and the receptor density on a cell membrane. The value of $I_M R_M$ must be calculated rather than using peak current amplitudes measured with saturating GABA concentrations, due to the rapid rate of desensitization for some receptors. This desensitization may significantly reduce the peak current amplitude observed. The time resolution for ligand-gated ion channel measurements is often limited to the rate of neurotransmitter application and diffusion. A fluid mechanics principle first discussed by Landau and Lifshitz (*138*) states that a thin, but static, layer of solution will develop on the surface of spherical objects in a laminar flow of liquid. The exchange of solutions on a patch-clamped cell will also result in a static layer of buffer, which will act as a diffusion barrier for neurotransmitters in a solution flowing around the cell. Thus, the rate of change of ligand concentrations surrounding the receptors is limited to the rate of diffusion. Ultimately, this principle affects the rate of the current rising phase and the peak current amplitude, as some ion channels will be desensitizing before GABA is bound to others. To account for this, a "current correction" method was developed (*137*) to estimate what the amplitudes of whole-cell current recordings would be if the receptors did not undergo desensitization. This method largely relies on fitting the desensitization phase of the receptor current trace with equation [1.7] and then using the values of A_n and τ_n to extrapolate the desensitization phase of

the current back to the time that GABA was initially applied to the receptor ($t = 0$). The current that would be observed in the absence of receptor desensitization (I_A) is then calculated from

$$I_A = (e^{-\Delta t/\tau_n}) \sum_{i=1}^{j} (I_{obs})_{t_i} + (I_{obs})_{t_j} \qquad [1.8]$$

the product of an exponential function based on the time constants obtained using equation [1.7] with the sum of observed currents (I_{obs}) over a time interval (Δt) from the beginning to the end of the current trace (*i*=1 to *i*=*j*). The resulting corrected current is then plotted; see Figure 1.2A (Roman numeral V). The average of this "corrected current" is used for all further data analysis. Therefore, the $I_M R_M$ parameter is obtained from "current corrected" measurements of receptors applied with saturating ligand concentrations. Measurements from receptors that do not display receptor desensitization, such $GABA_A$ receptors containing the δ subunit (Figure 1.2A), cannot be "current corrected" and their $I_M R_M$ value is the observed peak current amplitude.

1.5 Agonists, Antagonists and Modulators of $GABA_A$ Receptors

$GABA_A$ receptors are activated, modulated and inhibited by a wide array of molecules, from zinc ions and endogenous neurosteroids, to toxins and drugs such as barbiturates and benzodiazepines (*21, 33, 139, 140*) (Table 1.1). These molecules cover a wide range of different structures (Figure 1.3), and have several, sometimes overlapping, binding sites on the receptor. An inclusive review of all $GABA_A$ receptor agonists, inhibitors and modulators is beyond the scope of this section, but it is of interest to point out several major pharmacological classes of compounds used in $GABA_A$ receptor

Table 1.1 A variety of different small molecules that act on the $GABA_A$ receptor as activators (agonists), inhibitors (antagonists), positive modulators (potentiators) and negative modulators (inverse agonists). This list is not inclusive, but does attempt to include most of the well known compounds as well as represent a diversity of structurally different compounds. Compounds listed as 'non-selective' may bind with a higher affinity or have more dramatic effects on specific subtypes, but they do act on most $GABA_A$ receptor subtypes.

	Endogenous	**Non-selective**		**Selective** [subunit specified]
Agonists	GABA Alphaxolone Ganaxolone Taurine GABOB β-alanine Imidazole-4-acetic acid	Muscimol THIP (Gaboxadol) Isoguvacine (+)-TACP Zapa 4-PIOL ThioTHIP		
Antagonists	Cortisone	RU5135 Pitrazepin SR95531 (+)-Hydrastine Bicuculline Securinine (+)-Tubocurarine Gabazine	Benxylpenicillin Picrotoxinin TBPS Enoxacin Cunaniol β-CCE Flumaxenil	Zinc ion [δ > γ]
Potentiators & Partial Agonists	Cortisol Allopregnanolone (3α-OH-DHP) 3α-THDOC	Diazepam ZK93423 Phenobarbital Pentobarbital Propofol Etomidate Valerenic acid	Bretazenil	Ethanol [δ] Ketamine [α6βxδ] TPA-023 [α2,α3] L838417 [α2,α3] Zolpidem [α1] NS11394 [α2,α3] Benzamide DS1 / DS2 [δ] JM-II-43A [δ] Monastrol [δ]
Inverse Agonists	Epipregnanolone	Flumazenil (Ro15-1788) ZK93426 DMCM Ro19-4603	CHEB FG7142	α5IA [α5] L-655708 [α5] α3IA [α3] RO4938581 [α5] RO154513 [α5]

Figure 1.3 Structures of various different agonists, inhibitors, and modulators of $GABA_A$ receptors. Several compounds fall into prominent categories of compounds known to interact with the $GABA_A$ receptor, such as benzodiazepines (diazepam and flumazenil), barbiturates (phenobarbital and pentobarbital) and neurosteroids (alphaxolone and 5α-THDOC). While several subtype-selective compounds are shown, the examples primarily show molecules that modulate receptors containing the δ subunit. Of all subtype-selective modulators, modulators of α subunit-containing receptors are most abundant (Table 1.1)(*21*). The discovery and modulation of $GABA_A$ receptors by dihydropyrimidinones (JM-II-43A and monastrol), are discussed in more detail in Chapters 2 and 3.

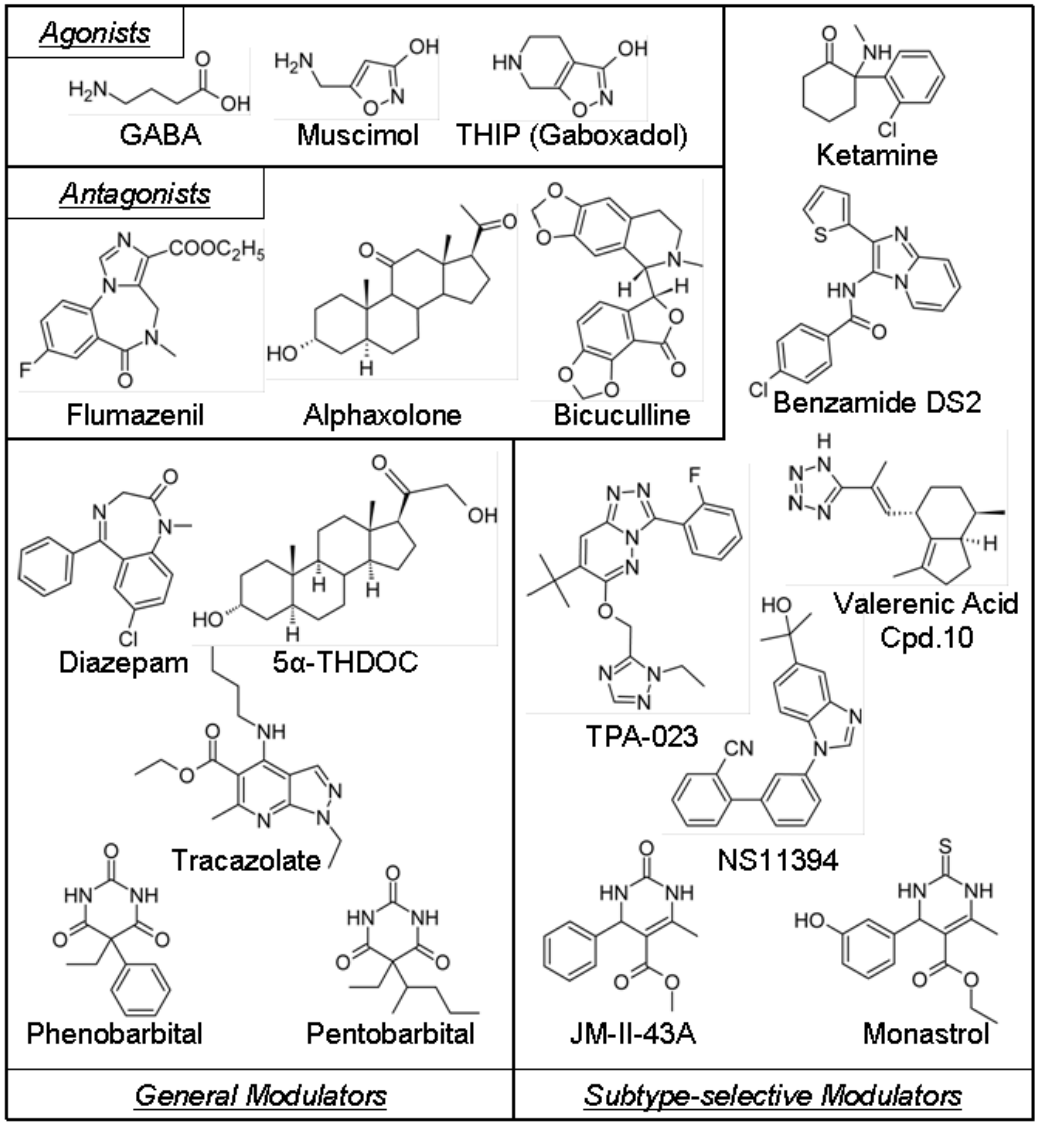
Agonists
GABA
Muscimol
THIP (Gaboxadol)
Antagonists
Flumazenil
Alphaxolone
Bicuculline
Ketamine
Benzamide DS2
Diazepam
5α-THDOC
Tracazolate
Phenobarbital
Pentobarbital
TPA-023
Valerenic Acid
Cpd.10
NS11394
JM-II-43A
Monastrol
General Modulators
Subtype-selective Modulators

investigations and briefly discuss subtype-selective compounds in the field of $GABA_A$ receptors.

Benzodiazepines

$GABA_A$ receptors were first identified as receptors for both GABA and benzodiazepines in the CNS (*130, 131*). The eventual cloning of the $GABA_A$ receptor confirmed that these were indeed the same receptor (*52*). As such, benzodiazepines are perhaps the most widely used of all $GABA_A$ receptor modulators. Benzodiazepines are positive modulators of $GABA_A$ receptor currents that allosterically bind to receptor subtypes containing a γ subunit.

It has been proposed that benzodiazepines modulate $GABA_A$ receptors by binding to a separate, yet structurally similar site as that of GABA to lower the energy barrier to forming an open-channel conformation (*128*). This differs from the popular view that benzodiazepines act by increasing the affinity of the channel for GABA (*22, 141, 142*). The hypothesis for lowering the channel-opening energy barrier is quite enticing as it agrees with a large amount of data showing that GABA acts as only a partial agonist for some receptor subtypes, such as δ subunit-containing receptors (*6, 8, 143-145*). While the mechanism of action for benzodiazepines and other modulators is far from understood, the identification of residues that make up the benzodiazepine-binding pocket and transduce binding to channel gating supports this mechanism (*146*).

While it is thought that most $GABA_A$ receptors are sensitive to these compounds, a small number of receptor subtypes, such as those containing α4, α6 and δ subunits, are benzodiazepine insensitive (*20, 147*). This

selective modulation of receptor subtypes is believed to limit the physiological side effects of these compounds compared to other $GABA_A$ receptor modulators. Thus, benzodiazepines, such as the well known diazepam (Valium), have been commonly used for medications as anticonvulsants, anxiolytics, and sedatives (*82*). However, these molecules are not free from side effects, and it is known that constant use of benzodiazepines causes individuals to develop dependencies (*148*), a topic of ongoing research.

Barbiturates

Another class of small molecules that modulate most $GABA_A$ receptors subtypes are the barbiturates. These compounds were used as anticonvulsants, anxiolytics and sedatives well before the $GABA_A$ receptor was identified (*149*). While barbiturates have many undesirable side effects and an inherent toxicity, they are still widely used as therapeutics (*150*). These molecules potentiate currents of $GABA_A$ receptors as do benzodiazepines (*151*) but have distinct binding sites. In fact, barbiturates can increase the binding affinity of the receptors for benzodiazepines (*152*). The mechanism of action for barbiturates on $\alpha1\beta2\gamma2L$ receptors is preferential binding to and stabilization of the open-channel receptor state (*2, 153*). Barbiturates are also known to act as partial agonists at high concentrations, inducing the $GABA_A$ channel to open (*2, 154-157*).

Neurosteroids

A variety of endogenous progesterone derivatives and metabolites activate and modulate $GABA_A$ receptors. Two commonly used

neurosteroids that act as agonists are alphaxolone and ganaxolone. Two of the most commonly studied and used potentiating neurosteroids of the $GABA_A$ receptors are allopregnanolone (THP) and 5α-THDOC (*151, 158*). THP modulation of some receptor subtypes, particularly δ subunit-containing receptors, is quite dramatic (*6*). Although electrophysiological measurements clearly demonstrate that THP and other allopregnanolone analogs modulate $GABA_A$ receptors, the binding sites and exact mechanism of action for these neurosteroids has not been reported.

Subunit-specific Modulators

Recently, pharmacological investigations of $GABA_A$ receptors, as well as most other ion channels, are focusing on the discovery of small molecules that specifically modulate receptor subtypes. More specific compounds will permit examining the contribution of specific subsets of $GABA_A$ receptors to neuronal processes. The primary drive for such compounds is ultimately the discovery of better, more selective pharmaceuticals with less risk of detrimental side effects. Several new subtype-selective compounds have been reported including: TPA-023, which is specific for receptors containing α2 and α3 subunits (*159, 160*); NS11394, also selective for receptors containing α2 and α3 subunits (*161*); zolipidem, which preferentially binds to receptors containing α1 (*162*); a class of benzamides that may be selective for δ subunit-containing receptors in the presence of low GABA concentrations (although only three different receptor subtypes – α1β3γ2S, α4β3γ2S, and α4β3δ – were examined) (*11*); and a novel set of dihydropyrimidinones (DHPMs) that selectively modulate δ subunit-containing receptors (see Chapter 2) (*163*). A more complete list of modulatory compounds as well as

subtype-selective compounds can be found in Table 1.1.

Most subtype-selective compounds have not been examined on a mechanistic level, as many of them were only recently discovered. However, the mechanism of action for these various compounds may be markedly different than others reported and may vary depending upon the receptor subtypes involved. Thus the search for subtype-selective compounds is far from over. In addition, understanding how the compounds function, and why they function selectively is an area of research that is virtually untouched. The data presented in Chapter 3 of this dissertation is perhaps the first investigation of the mechanism for subtype-selective compounds and demonstrates a novel mechanism of action.

1.6 Receptors Containing the Delta Subunit

A significant portion of chapters 2 and 3 of this dissertation focuses on understanding the differences in the mechanism and characteristics of δ subunit-containing receptors compared to other $GABA_A$ receptor subtypes. Thus, this section is intended to give a background on what is presently known regarding this $GABA_A$ receptor subunit.

The δ subunit was identified in 1989 (*45*), two years after the first α and β subunits were cloned and examined using voltage-clamp current recordings from *Xenopus laevis* oocytes (*52*). Delta subunit-containing receptors have a distinct extrasynaptic localization on the membranes of CNS neurons. This localization is thought to make receptors containing the subunit important for regulating a continuous (or 'tonic') chloride conductance that changes with fluctuations in extracellular GABA and neurosteroid concentrations. Such tonic currents are likely important for

regional CNS modulation and repression.

Delta subunits are ubiquitously expressed throughout the CNS, but are found in higher densities in the cerebellar granular cells, thalamus, cortex, striatum, and dentate gyrus regions of the human (*48*) and rat (*164, 165*) brain. Examination of the δ subunit localization also demonstrated that α4 and α6 subunits tend to colocalize with δ subunits (*48*). This was recapitulated with a study using mouse models, immunoprecipitation, and with ligand binding studies to show that α4 and α6 preferentially associate with the δ subunit in the forebrain and cerebellum, respectively (*166*). Immunopurification studies demonstrate that the δ subunit associates with a variety of subunits to form receptors, but there is a preference for interaction with α1, α3, β2, and β3 subunits, in addition to α4 and α6 (*44, 167*). Several additional reports have suggested that $GABA_A$ receptors have mutually exclusive incorporation of γ or δ subunits, which agrees with the distinct synaptic *versus* extrasynaptic localization observed for these two subunits in neurons of the CNS (*168, 169*).

An elaborate electrophysiological characterization of the δ subunit was conducted by expression of the subunit with α1, β1 and/or γ2 subunits in *X. laevis* oocytes to examine responses to GABA, zinc, diazepam and pentobarbital (*170*). Delta subunit-containing receptor currents were enhanced by pentobarbital, were especially sensitive to inhibition by zinc ions, and did not show any modulation by diazepam. Subsequent studies have further examined the contribution of the delta subunit to zinc sensitivity (*170, 171*), the greater sensitivity to (and efficacy of) potentiation by many common $GABA_A$ potentiators (*34*), particularly by tracazolate (*145, 172*) and neurosteroids such as 3α, 21-dihydroxy-5α-pregnan-20-one

(THDOC) (*6, 145*). In addition, studies have shown that δ subunit-containing receptors have greater sensitivity to agonist concentrations of gaboxadol (4,5,6,7-tetrahydroisoxazolo[5,4-c]pyridin-3-ol or THIP) (*171, 173, 174*) and GABA than all other receptor subtypes (*174*). The *in vitro* studies of δ subunit pharmacology appear to be physiologically relevant, as observations from hippocampal neurons demonstrate there are tonic conducting channels insensitive to benzodiazepines but sensitive to neurosteroids (*175*). Only a few molecules have been reported to act selectively on δ subunit-containing receptor isoforms; these include ketamine (*5*), ethanol (*6-8*) and two benzamides (*11*). Ketamine is a positive allosteric modulator as well as a partial agonist of α6β2δ and α6β3δ $GABA_A$ receptors and an inhibitor of *N*-methyl-D-aspartic acid (NMDA) receptors (*5*). While somewhat controversial (*9, 10*), ethanol is reported to potentiate primarily δ subunit-containing receptors at low levels of agonist, concentrations that are similar to what may be found extra-synaptically (*7, 8, 176*). The two reported benzamide compounds, DS1 and DS2, are both allosteric modulators of α4β3δ $GABA_A$ receptors, and DS1 also acts as a partial agonist (*11*).

Receptors containing the δ subunit have several distinct mechanistic properties, the most unique being limited or complete lack of desensitization (*10, 163, 170*), clearly shown in Figure 1.2A. This suggests that receptors containing this subunit lack a desensitization phase in their mechanism of action, have a completely different mechanism than other receptor subtypes, or most likely have altered kinetics using the same mechanistic scheme. The general mechanisms that have been proposed for $GABA_A$ receptors are discussed in more detail in section 1.4. Chapter 3 examines both the

mechanism of action of small molecules on δ-containing receptors as well as observations aiding our understanding of the mechanism of action for δ subunit-containing receptors.

To examine the impact of the δ subunit in the context of behavior and the CNS, a $\delta^{-/-}$ knockout mouse was generated (*177*). Surprisingly, the lack of the δ subunit was not lethal. These mice did, however, show several differences from wild-type mice, including: a decrease in the effects of neurosteroids and small molecule ligands (THIP) on animal behavior (*173, 177-179*); an overall hyper-excitability of the CNS, thus a greater susceptibility to seizures than for wild-type animals (*178*); an increase in γ2 subunits and a decrease in α4 subunits in the forebrain (*166*); and several changes in the CNS signaling (*180*).

The distinct membrane localization, pharmacological and biophysical features of δ subunit-containing receptors, in addition to phenotypes of the $\delta^{-/-}$ mouse model, have supported the general hypothesis that these receptors are critical for establishing tonic currents. As such, δ subunit-containing receptors are an important aspect of regional regulation of signal transmission throughout the CNS.

1.7 Techniques and Tools for Investigating Ligand-gated Ion Channels

Ever since Del Castillo, Katz and Thesleff determined that small molecules induce voltage changes in the neuronal membrane potential (*181*), there has been a constant development of techniques to investigate the rapid reactions of ligand-gated ion channels. While many techniques have been developed for the investigation of ion channels in general, this section is

focused specifically on those techniques that have advanced the ability to investigate ligand-gated ion channels such as the $GABA_A$ receptors.

Voltage-Clamp

Voltage-clamp measurement techniques were developed by Marmont and Cole (*182*) to maintain the electric potential across the membrane of squid axons. The technique was further developed and applied by Hodgkin and Huxley to eventually determine the changes in ion permeability during an action potential in squid axons (*183*). Voltage-clamp methods are still used today, most often with *X. laevis* oocytes.

This technique establishes a constant membrane potential (E_M) by using a total of three electrodes to measure, ground and adjust the current flowing across a cellular membrane. The premise of the voltage-clamp relies fundamentally on the relationship described by the modified version of Ohm's law ($(E_M - E_{CL}) = I/g$), where E_{CL} is the electric potential established by the ion concentration and can be determined using the Nerst equation, I is the current and g is a material's conductance. If E_{CL} is equal to zero, then the equation become the classical Ohm's law ($V = I/g$ or $E_M = I/g$). As ion channels open across the membrane of a cell, the conductance of the membrane increases, and the amount of current injected to maintain the experimentally set E_M is measured. The basic concept of how a voltage clamp operates is the foundation of all electrophysiological methods.

Patch-clamp Methods

The technique of patch-clamping developed by Sakmann and Neher (*184*), while conceptually simple, was a giant technological advance that

spurred immense growth in the research of ion channels. This technique was developed to measure changes in the conductance of a membrane as single ion channels open and close in combination with the voltage-clamp technique. To accomplish this goal, it was necessary to minimize electrical noise by using a fire-polished glass pipette with a ~ 3-5 μm diameter tip opening to reduce the area of a membrane from which current was being recorded. The patch-clamp technique was further developed by Neher and Sigworth (*185*) who implemented using a small amount of suction on the pipette to generate an electrically tight, GΩ, seal between the membrane and pipette tip. These methods not only permitted the visualization of single ion channel currents, but over the years have also made it possible to investigate many aspects of ion channels from all cellular organisms. While many of the patch-clamp techniques have been described in detail (*123, 124, 184, 186-189*), the general process for both single-channel and whole-cell current recording is described here.

Single-channel and whole-cell current measurements are performed largely in the same manner, thus this description of the technique applies to both methods until stated otherwise. The preparation for these techniques requires several reagent and equipment components. Equipment used for all electrophysiological work described can be found in Table 1.2. The most important components are healthy cells (or oocytes, vesicles, spheroplasts, etc.) containing the receptor of interest. Cells used must either be transfected with a plasmid encoding cDNAs for exogenous receptor expression or they must endogenously express these receptors.

An important component of these techniques to consider is the composition of intracellular and extracellular buffers. There are no

Table 1.2 Equipment and reagents that are used for the methods of patch-clamp current recording, laser-pulse (flash-lamp) photolysis and cell-flow solution application.

	Patch-Clamp Recording	**Laser-pulse (Flash) Photolysis**	**Cell Flow**
Equipment	- Pipette puller (HEKA, PIP5) - Microforge (Narishige, MF-830) - Recording electrode - Reference electrode - Inverted microscope - Faraday cage - Anti-vibration, floating table (table or table top) - Micromanipulators (Narishige) - Computer with appropriate sampling/acquisition software (Clampex) - Patch-clamp amplifier (Molecular Devices, Axopatch 200B) - Analog-to-digital converter ('digitizer'; Molecular Devices, Digidata 1322A) - Headstage (Molecular Devices) - Pipette holder and electrode - Oscilloscope (optional) - Syringe with fine point Microfil tip or equivalent	- Laser or flash lamp (rapid light pulses) - Calibrated joulemeter - Optical fiber (quartz if UV light is used) - Optical lenses for focusing light (if needed) - Micromanipulator for laser alignment (if needed)	- Stainless steel U-tube - Solenoid valve (i.e. Lee Control Valve; Lee Co., Essex, CT) - Peristaltic pump - Peristaltic pump tubing - Micro manipulator - Fiberglass U-tube arm with clamp - Stand for manipulator and U-tube arm
Reagents	- 35-mm Cell culture dishes - Cells expressing the receptor of interest - Extracellular buffer - Intracellular buffer - Borosilicate capillary tubes (thick wall for single-channel) - Sylgard, Sigmacote or equivalent (for single-channel)	- Caged compound for pertinent receptor and experiment	- Solutions for application made in extracellular buffer

standardized buffer compositions for electrophysiology, or even for particular receptors (*188*). Buffer compositions have several roles; they must mimic the osmotic composition and pH of the cytosol or extracellular environment, provide the ions needed for studying the receptor of interest (*e.g.* chloride ions in the case of $GABA_A$ receptors) and limit the conductance of other ion channels present in the cell membrane.

Systems for Solution Application

Ligand-gated ion channels of all kinds require a change in the concentration of agonist to open, thus to study these channels various solution application devices have been used (*189-195*). Some studies simply use a perfusion system to exchange solutions in the dish containing the patch or cell (*140, 196*). However, ion channels respond rapidly to ligand, so most systems attempt to exchange the solution surrounding the receptors as fast as possible. Several systems using piezo-electric translators coupled with theta tubes, pipettes or multi-channel microfluidic systems require either the patch-clamped sample or the flow system to move (*191, 193, 195*). While very fast solution exchange times have been measured with such systems, the physical movement inherent with exchanging the solution in these systems is not ideal and may lead to inconsistencies as well as damage to the patch. Additionally, these systems are not ideal for testing multiple solutions on a single cell or patch, because the entire solution within the application system must be exchanged before consecutive measurements can be obtained.

In order to test different solutions during an experiment without any movement of the patch or flow system, an alternative technique can be used called cell-flow (*18, 189, 197*). Cell-flow is a U-tube application system

largely based on the system originally described by Krishtal and Pidoplichko (*190*). A diagram of the cell-flow U-tube device is shown in Figure 1.4A and B. In brief, the system uses a peristaltic pump to push solution into one end of a stainless steel U-tube at a typical rate of ~ 1.5 cm/s and draw solution from the other end at a greater rate. This flow rate differential causes extracellular buffer in the dish to be drawn through the porthole of the U-tube, preventing the leakage of solutions. For solution application to a cell, the solution flowing through the U-tube is forced out of the porthole by using a solenoid valve controlled by a computer to block the flow of solution from the end of the U-tube. After an application period, the solenoid valve is opened and solution from the dish is again drawn into the porthole of the U-tube, rapidly removing the recently applied solution. Solution applications are spaced approximately 2 – 2.5 minutes apart, thus allowing receptors to recover from desensitization.

Laser-pulse and Flash-photolysis

Ligand-gated ion channels rapidly bind an agonist and open in the micro- to low millisecond time region, a time frame faster than the tens of milliseconds that cell-flow and other solution application techniques take to exchange neurotransmitter solutions on a cell surface. Solution application systems limit direct measurement of rapid ion channel kinetics due to the fundamental fluid mechanics principle first discussed by Landau and Lifshitz (*138*). This principle describes how the laminar flow of aqueous solutions over a spherical object creates a thin, but static, layer of solution on its surface. Thus, neurotransmitter concentration changes by solution application systems are limited to the rate at which neurotransmitter diffuses

Figure 1.4 Schematic drawings depicting the arrangement of equipment needed for combining patch-clamp, cell-flow and flash/laser-pulse photolysis techniques. **A.** Components shown include the stainless steel U-tube (1), the fiber optic cable (2), a borosilicate recording pipette containing intracellular buffer and the recording electrode (3), the pipette holder (4), the headstage (5), the suction/vacuum tube (6), the reference electrode (7), the microscope (objective) for viewing cells and aligning the U-tube (8), a cell culture plate containing cells expressing the receptor of interest (9), a three port solenoid valve (10), 4.2 mm inner diameter peristaltic tubing drawing solution away from the U-tube (11), and 0.5 mm inner diameter peristaltic tubing with solution flowing towards the U-tube (12). The cell-flow technique requires all of the same components, omitting only the optical fiber. **B.** A larger-scale diagram depicting the alignment of components needed for the flash/laser-pulse photolysis technique. While the solenoid valve is open, solution is actively being drawn away from the U-tube at a higher rate than solution flowing to the U-tube. The U-tube draws extracellular buffer in through the porthole, preventing any leakage or diffusion of testing solutions from flowing over the cell. When the solenoid valve closes, solution being pumped to the U-tube is forced out of the U-tube port hole and over the surface of the cell. Linear flow rates of 1-5 cm/s are typically used.

A

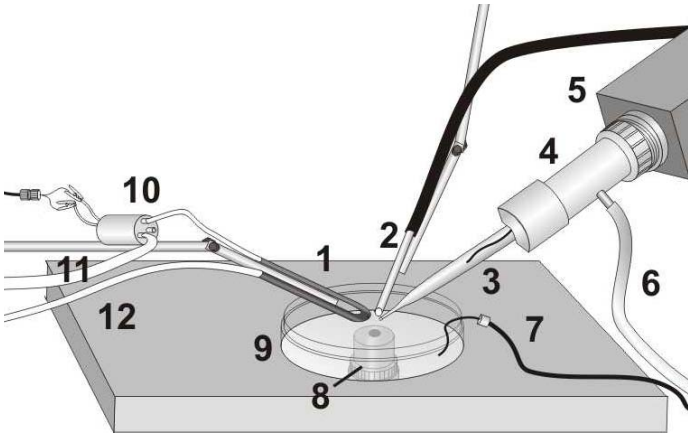
10
11
12
1
2
3
4
5
6
7
8
9

B

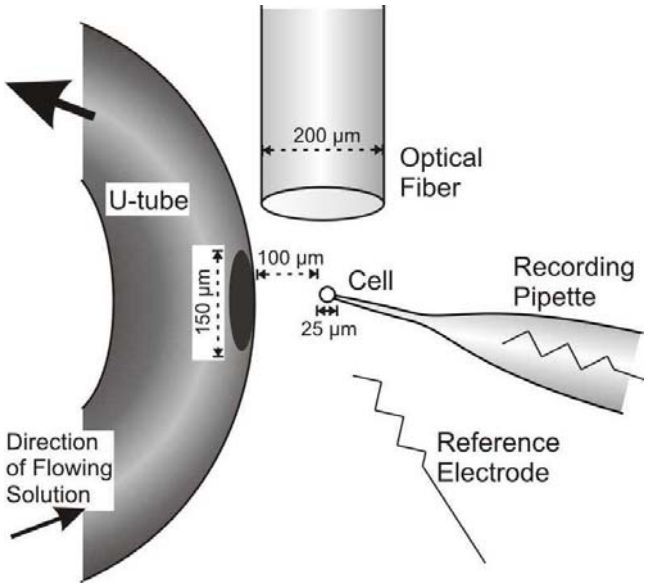
200 µm
Optical
Fiber
U-tube
100 µm
150 µm
Cell
Recording
Pipette
25 µm
Direction
of Flowing
Solution
Reference
Electrode

through this solution barrier. However, direct measurements of these rapid reactions are needed to fully understand the mechanism of ligand-gated ion channels.

Biologically inert photolabile derivatives of neurotransmitters, called 'caged' neurotransmitters, permit measurements to be made in the upper micro- to low millisecond time region (*198*) by allowing a rapid increase in neurotransmitter concentration upon illumination with a pulse of light of the appropriate energy and wavelength. By equilibrating the receptors on the cell surface with the caged neurotransmitter before photolysis, this technique avoids complications that arise from methods involving the application of neurotransmitter solutions. Caged neurotransmitters can be photolytically cleaved in the microsecond time region (*134, 198, 199*), making the application of neurotransmitter fast enough to directly measure the rate constant for opening of the ligand-gated ion channels. Thus, caged compounds are particularly important tools for investigating ligand-gated ion channels and other fast biological reactions that are regulated by small molecules (*198, 200-204*).

Caged neurotransmitters also offer spatial control of neurotransmitter application, as photolytic release is limited to the area illuminated by the pulse of light (*205, 206*). When caged neurotransmitters are combined with two-photon microscopy, a technique permitting the excitation of chromophores with high 3-dimensional spatial control (*207*), neurotransmitter can be applied with subcellular spatial resolution (*208-210*).

Many photolabile protecting groups have been developed and their chemical and physical properties studied (*211*), several of which are commonly used to study biological systems (*206*). These include:

2-methoxy-5-nitrophenyl (MNP) esters (*212, 213*), *p*-hydroxyphenacyl derivatives (*214*), desyl-based compounds (*215*), coumarin esters (*216, 217*) and ruthenium complexes (*218*). The basic structure of several of these caging groups can be found in Figure 1.5.

Caged neurotransmitters offer many advantages for temporal and spatial resolution for the study of ligand-gated ion channels, but these compounds must be carefully evaluated before use. The utility of a caged neurotransmitter for a specific experimental system will be significantly impacted by use of different caging groups, the position on the neurotransmitter at which a caging group is attached, assay conditions, and the photolysis byproducts. So far, attributes of caged neurotransmitters are not predictable and must be determined experimentally. For example, the αCNB-caged GABA is satisfactory for use with α1β2γ2L $GABA_A$ receptors but it inhibits α1β2δ $GABA_A$ receptors under similar concentrations and conditions; currents evoked from α1β2δ $GABA_A$ receptors by 5 μM GABA were inhibited 50% by 50 μM αCNB-caged GABA (Kyle Eagen, unpublished data).

A general, but systematic approach to developing caged neurotransmitters entails the determination of a compound's quantum yield, rate of photolysis, and whether the caged compound prior to photolysis and byproducts after photolysis are biologically inert to the receptor being examined. The rate of photolysis (*i.e.* rate of photolytic cleavage) of the caged neurotransmitter determines the time resolution for any kinetic measurements. The quantum yield is a measure of the number of molecules of neurotransmitter released for each photon of light to which the caged neurotransmitter is exposed. This value will indicate the maximum amount

Figure 1.5 A non-inclusive list of the structures of several generic photolabile leaving groups used to create caged compounds for biological assays. The most commonly used caging group, or derivative thereof, is the 2-nitrobenzyl group, followed by both 7-nitroindoline and coumarin derivates. The coumarin and ruthenium complexes are photolabile groups commonly used to create visible light sensitive caged compounds. LG denotes the leaving group and R denotes an unspecified functional group.

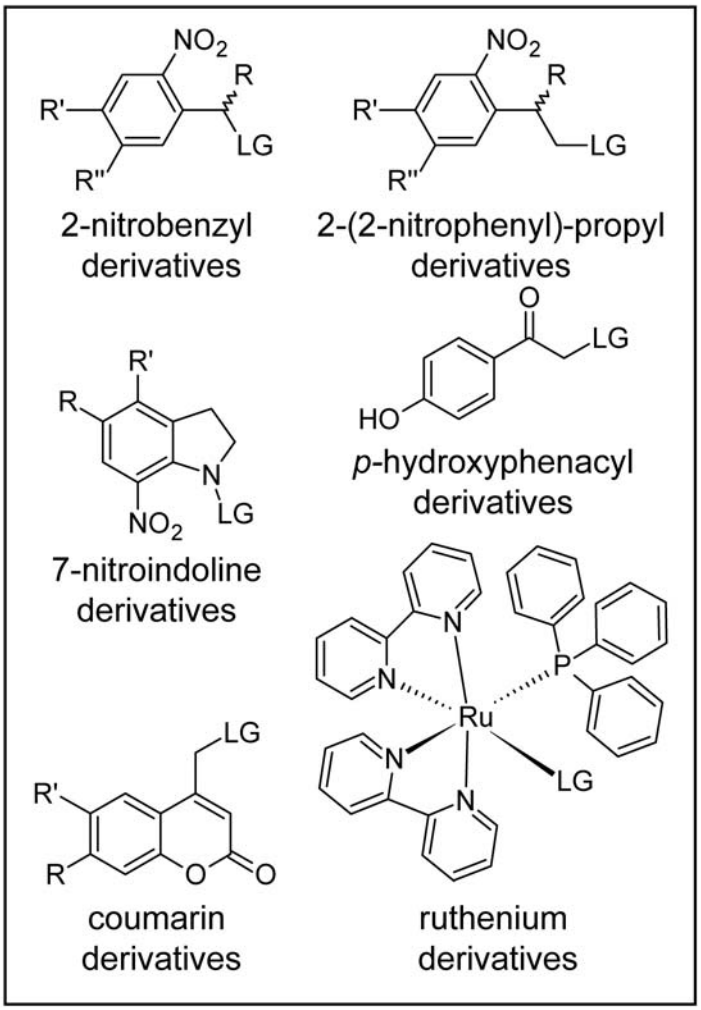
NO2
R
R'
LG
R''
2-nitrobenzyl derivatives
NO2
R
R'
LG
R''
2-(2-nitrophenyl)-propyl derivatives
R'
R
N
LG
NO2
7-nitroindoline derivatives
O
LG
HO
p-hydroxyphenacyl derivatives
LG
R'
R
O
O
coumarin derivatives
N
N
P
Ru
N
N
LG
ruthenium derivatives

of neurotransmitter that can be released upon photolysis. Several other aspects of a caged neurotransmitter should be examined to make sure it is practical for experimentation in a biological system, such as solubility in aqueous solutions, stability at physiological pH, thermal stability at ambient temperature, and photosensitivity at a wavelength greater than 335 nm (to avoid cell damage). The wavelength used for photolysis must not be one at which light is absorbed by the neurotransmitter itself to avoid complications in the characterization and use of the caged compound (*219*).

The quantum yield can be measured with several techniques. One entails monitoring spectroscopic changes in the absorption or fluorescence spectrum of the compound after photolysis of the caged neurotransmitter sample with light pulses of a known energy and length (*198*). [The energy of a light pulse can be determined using standard actinometry methods (*220, 221*), or a calibrated joulemeter.] If no spectroscopic changes occur between the caged neurotransmitter and its photolytic products, an alternative method is analytical separation and quantification of the amount of caged and un-caged species by techniques such as HPLC (*198*). Additionally, it is possible to calculate the quantum yield by performing several laser-pulse measurements on the appropriate ligand-gated ion channel and comparing the current elicited from the photolysis of the cage-compound to a dose response curve of free neurotransmitter. For more details on measuring quantum yield see Chapter 4.

The rate of photolysis can be approximated from the data obtained in a quantum yield determination if the duration of a single light pulse is known. A more physical method of measuring the rate of photolysis is to measure the absorbance of a solution of caged compound during laser or

flash-lamp photolysis and analyze the rate of decay of any observed transient absorption changes that occur during photolysis. These transient absorption changes are due to absorption of light from the formation of a photochromic molecular intermediate of the caged neurotransmitter (*222, 223*). The details of this method are described in the literature (*198, 222, 224*). For more details on measuring the photolysis rate, see Chapter 4.

Caged neurotransmitters permit rapid and spatially controlled concentration increases in neurotransmitter. The rapid change in neurotransmitter concentration upon photolysis of caged neurotransmitters makes these molecules powerful tools in transient kinetic investigations of neurotransmitter receptors, including $GABA_A$ receptors (*1, 2, 225*). Molecules, such as αCNB-caged GABA (*226*), were used to determine changes that occur in the kinetic mechanism of $GABA_A$ receptors due to the epilepsy-associated K289M mutation in the γ2L subunit (*1*). Elucidation of the mechanism of $GABA_A$ receptor modulation by phenobarbital and inhibition by picrotoxin was also made possible using caged GABA (*2, 225*).

CHAPTER 2

DISCOVERY OF DIHYDROPYRIMIDINONE SELECTIVE POTENTIATION OF GABA(A) RECEPTOR CURRENTS

Abstract

Gamma-aminobutyric acid receptors ($GABA_A$ receptors) are ligand-gated chloride channels that play a central role in signal transmission within the mammalian central nervous system. Compounds that modulate specific $GABA_A$ receptor subtypes containing the δ subunit are scarce, but would be valuable research tools and starting points for potential therapeutic agents. Here we report a class of dihydropyrimidinone (DHPM) heterocycles that preferentially potentiate peak currents of recombinant $GABA_A$ receptor subtypes containing the δ subunit expressed in HEK293T cells. Using the three-component Biginelli reaction, thirteen DHPMs with structural features similar to those of the barbiturate phenobarbital were synthesized; one DHPM (monastrol) is commercially available. Up to a ~ 3-fold increase in the current from recombinant α1β2δ receptors was observed with the DHPM compounds JM-II-43A or monastrol when coapplied with saturating GABA concentrations, similar to the current potentiation observed with the nonselective potentiating compounds phenobarbital and tracazolate. No agonist activity was observed for the DHPMs at the concentrations tested. A kinetic model was used in conjunction with dose-dependent measurements to calculate apparent dissociation constant values for JM-II-43A (400 μM) and monastrol (200 μM) at saturating GABA concentrations. Recombinant receptors composed of combinations of α1, α4, α5, α6, β2, β3,

γ2L, and δ subunits were examined with JM-II-43A to demonstrate the preference for potentiation of δ subunit-containing receptors. Lastly, reduced currents from receptors containing the mutated δ(E177A) subunit, described by Dibbens *et al.* (2004) as a heritable susceptibility allele for generalized epilepsy with febrile seizures plus, are also potentiated by these DHPMs.

Introduction

The neurotransmitter γ-aminobutyric acid (GABA) activates a class of ligand-gated chloride ion channels known as $GABA_A$ receptors that are important for regulation of neurotransmission in the central nervous system (CNS) (*19, 20, 227*). Heteropentameric combinations of nineteen different $GABA_A$ receptor subunits (α1-6, β1-3, γ1-3, δ, ε, θ, π, and ρ1-3) (*34*) determine the localization, pharmacology, biophysical properties, and cellular roles of these receptors (*21, 139, 170, 228*). In contrast to $GABA_A$ receptor subtypes that are localized at synapses and have a phasic role in signal transmission, receptors containing the δ subunit are located peri- and/or extra-synaptically and are thought to have an important role in regulating neurotransmission through tonic inhibition (*49, 145, 170*). The importance of the δ subunit for neuronal signaling is exemplified in knockout mice lacking the δ subunit that are more susceptible to seizures and exhibit attenuated responses to neurosteroids compared to normal mice (*177, 178*). In addition, point mutations within several different $GABA_A$ receptor subunits have been genetically associated with various forms of epilepsy and seizures (*76*), such as point mutations E177A (glutamate to alanine), R220H (arginine to histidine), or R220C (arginine to cysteine) in the δ subunit that

are genetically linked to general epilepsy with febrile seizures+ and idiopathic generalized epilepsy (*3, 229*). How these individual mutations within the δ subunit affect the function of $GABA_A$ receptors is not fully understood, but single-channel studies of the α1β2δ receptor indicate that the E177A and R220H mutations alter the equilibrium between the open- and closed-channel states of the receptor toward the closed-channel state (*4*).

Changes in the mechanism of α1β2δ receptors due to the E177A mutation may reduce the channel-opening equilibrium constant (Φ^{-1}) of the receptor, as was determined (*1*) to be the case for the epilepsy-linked γ2L(K289M) mutant subunit originally described by Baulac *et al.* in 2001 (*69*). Based on the proposed mechanism of the $GABA_A$ receptor (*1*) (Figure 2.1A), we hypothesized and determined (*2*) that phenobarbital, a barbiturate anticonvulsant, potentiates $GABA_A$ receptors by binding to the open-channel conformation of the receptor with a higher affinity (K_{app} = 0.23 ± 0.06 mM) than to the closed-channel conformation (K_{app} = 1.08 ± 0.32 mM), stabilizing the open-channel state and thus increasing the channel-opening equilibrium constant.

In an effort to find compounds that potentiate current amplitudes of $GABA_A$ receptors to a greater extent than does phenobarbital, we synthesized (*163*) several dihydropyrimidinones (DHPMs) with structural characteristics similar to phenobarbital and tested them on the epilepsy-linked α1β2γ2L(K289M) and α1β2δ(E177A) receptors as well as their corresponding wild-type α1β2γ2L and α1β2δ receptors. Although DHPMs did not potentiate currents of the γ subunit-containing wild-type α1β2γ2L or mutated α1β2γ2L(K289M) receptors, they did potentiate (~ 3-fold) the δ subunit-containing wild-type α1β2δ and mutated α1β2δ(E177A) receptors.

Figure 2.1 A. The mechanism previously proposed for $\alpha_1\beta_2\gamma_{2L}$ $GABA_A$ receptors (*1, 2*), was originally proposed for the nicotinic acetylcholine receptor by Katz and Thesleff (*12*), with the addition of the desensitized states (DL and DL_2) and the channel-opening equilibrium constant (Φ^{-1}) proposed later (*15*). The mechanism describes the receptor (R) binding two ligand molecules (L) with a dissociation constant K_I. At this stage (RL_2) the receptor is in the closed-channel state, which can change conformation to the open-channel state to allow ion flux across the membrane ($\overline{RL_2}$) and to the subsequent desensitized state (DL_2). DL_2 is a transiently inactive, closed-channel state of the receptor. The equilibrium between the closed- and open-channel states is described by the channel-opening equilibrium constant (Φ^{-1}). **B.** This mechanism describes the binding of a potentiating compound (P) to $\alpha_1\beta_2\gamma_{2L}$ $GABA_A$ receptors as previously reported (*2*). The mechanism here was simplified by omitting the desensitization states of the receptor and combining the two steps of ligand binding. The potentiating compound can bind to either the closed- or open-channel state with the relative binding affinities K_P and $\overline{K_P}$, to yield the respective closed- (RL_2P) and open-channel ($\overline{RL_2P}$) states of the receptor. The channel-opening and -closing rate constants in the presence of the potentiator are shown as k^P_{open} and k^P_{closed} and define the channel-opening equilibrium constant (Φ_P^{-1}) in the presence of a potentiating compound.

A

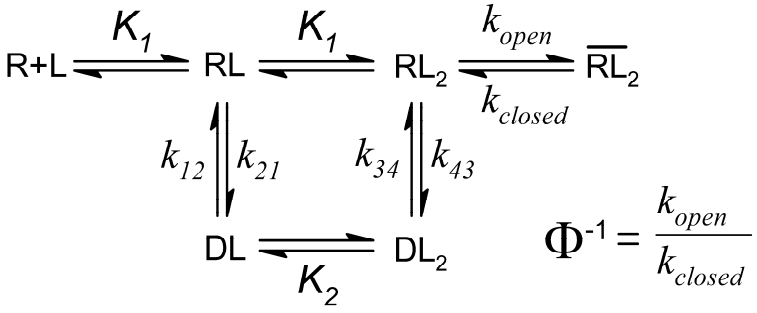

$$\Phi^{-1} = \frac{k_{open}}{k_{closed}}$$

B

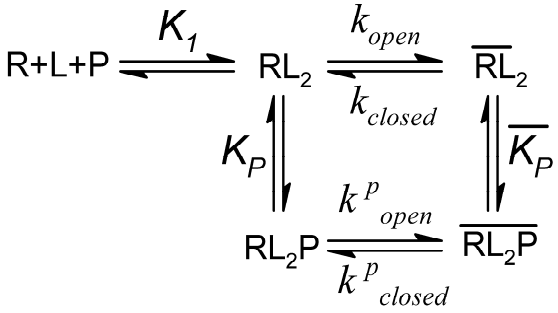

$$\Phi^{p\,-1} = \frac{k^{\,p}_{\,open}}{k^{\,p}_{\,closed}}$$

Thus, these DHPMs selectively modulate $GABA_A$ receptor subtypes.

It is known that $GABA_A$ receptors containing the δ subunit are pharmacologically distinguishable from other receptor subtypes by their higher sensitivity to zinc ion inhibition (*170, 171*), greater sensitivity to (and efficacy of) potentiation by tracazolate (*145, 172*) and neurosteroids such as 3α, 21-dihydroxy-5α-pregnan-20-one (THDOC) (*6, 145*), and a greater sensitivity to the agonist gaboxadol (4,5,6,7-tetrahydroisoxazolo[5,4-c]pyridin-3-ol or THIP) (*171, 173, 174*). However, most of these molecules also act on other $GABA_A$ receptor subtypes. Barbiturates and many other drugs, which have been used for treating epilepsy, depression, anxiety, insomnia and other diseases (*75, 230-232*), also indiscriminately affect various $GABA_A$ receptor isoforms (*34*) including, but not limited to, δ subunit-containing receptors, and often result in undesirable side effects (*147, 232, 233*). Ketamine (*5*), ethanol (*7, 8, 234*) and two benzamides (*11*) have been previously identified as acting selectively on δ subunit-containing receptor isoforms. Ketamine is a positive allosteric modulator as well as a partial agonist of α6β2δ and α6β3δ $GABA_A$ receptors and an inhibitor of *N*-methyl-D-aspartic acid (NMDA) receptors (*5*). While somewhat controversial (*9, 10*), ethanol is reported to primarily potentiate δ subunit-containing receptors at low agonist concentrations that are similar to conditions the receptors may experience extra-synaptically (*7, 8, 234*). The two reported benzamide compounds are allosteric modulators of α4β3δ $GABA_A$ receptors, with one of the two benzamide compounds, DS1, also acting as a partial agonist (*11*).

The family of dihydropyrimidinones reported here allosterically and selectively potentiate currents of several $GABA_A$ receptor subtypes, with a

preference for potentiating receptors containing the δ subunit. Various combinations of the subunits α1, α4, α5, α6, β2, β3, γ2L and δ were transiently expressed in HEK293T cells for a total of twelve subtypes that were electrophysiologically tested with the DHPM JM-II-43A (methyl 6-methyl-2-oxo-4-phenyl-3,4-dihydro-1H-pyrimidine-5-carboxylate). JM-II-43A potentiated currents from δ subunit-containing receptors and the α4β2 receptor subtype but did not change the average peak currents corrected for receptor desensitization (*18*) of the other $GABA_A$ receptor subtypes examined. Currents from α1β2δ receptors over the full dose-dependent range of GABA concentrations (saturating and sub-saturating) were potentiated anywhere from 2.9- to 4-fold by JM-II-43A similar to, or greater than, other reported $GABA_A$ receptor potentiators such as phenobarbital and tracazolate (*2, 145, 172*). Thirteen DHPM compounds were generated through use of a single-step multi-component reaction (*17*) and one, monastrol, was purchased. All fourteen compounds were tested on α1β2δ receptors, yielding a range of potentiation activities. No agonist activity was observed for any of the DHPMs tested. Lastly, these DHPMs potentiated currents of α1β2δ(E177A) mutated receptors genetically linked to epilepsy to a similar extent as those of wild-type α1β2δ receptors.

Methods and Materials

Reagents, Synthesis and Preparation of Dihydropyrimidinones

Monastrol was purchased from Tocris (Ellisville, MO). Other reagents were obtained from Sigma Aldrich, Fisher Scientific, or EM Science. GABA solutions were serially diluted from a frozen stock of 100 mM GABA stored at -20 °C and made weekly. DHPMs were synthesized as

described previously (*17*). Monastrol and DHPMs were dissolved in pure anhydrous DMSO before being diluted 1:200 with extracellular buffer at 65 °C for a final concentration of either 4 mM or 2 mM compound in 0.5 % DMSO. The 0.5 % DMSO aided in compound solubility, with no observed effect on $GABA_A$ receptor currents. The DHPM solutions were cooled to room temperature and serially diluted with extracellular buffer as needed.

Cell Culture and Transient Transfection

HEK293T cells were obtained from the American Type Culture Collection (ATCC) (Manassas, VA) and cultured in Dulbecco's Modified Eagle's Medium (DMEM) supplemented with 10 % fetal bovine serum (FBS), 100 units/mL penicillin and 0.1 mg/mL streptomycin. Cells were maintained at 37 °C with 5 % CO_2. cDNAs encoding the α1, α4, α5, α6, β2, β3 and γ2L subunits of the rat $GABA_A$ receptor in mammalian pRK-5 expression vectors were kindly provided by Professors H. Lüddens (Johannes Gutenberg - Universität, Mainz, Germany) and P. H. Seeburg (Max-Plank-Institut für medizinische Forschung, Heidelberg, Germany). cDNA encoding the δ subunit of the rat $GABA_A$ receptor in the pExpress-1 vector was obtained from ATCC. The pGreen Lantern plasmid (Life Technologies Inc., Gaithersburg, MD) was used as a cell transfection marker. A total of 4 μg of plasmid DNA was transfected, with the plasmid ratios being 1:1:0.1 for α:β:pGreen Lantern and 1:1:10:0.1 for both α:β:γ2L:pGreen Lantern and α:β:δ:pGreen Lantern. These ratios were used to strongly bias the expression of a subunit of interest (i.e. γ2L or δ) relative to the expression levels of α and β subunits to ensure inclusion of the modulatory subunit in the active receptors. For δ subunit-containing

receptors this was clearly identifiable by the characteristic lack of, or limited degree of, receptor desensitization. Currents measured from cells presumed to be expressing αβδ receptors that showed greater degrees of desensitization were very infrequent; but if observed the cell was discarded and the data was not used. PolyFect transfection reagent (Qiagen, Valencia, CA) or polyethylenimine (PEI) (Polysciences Inc. Warrington, PA) was used for transient transfection of cells. The Qiagen protocol for transient transfection with PolyFect was followed with the exception that the DMEM/reagent mixture was replaced after 5-7 hours with fresh DMEM/10 % FBS. PEI was used as reported (*235*) with a PEI:DNA ratio of 4:4 (μg:μg) and replacement of medium with fresh DMEM/10 % FBS after 4-7 hours. When PEI was used the HEK293T cells had greater transfection efficiencies and were healthier; no differences in receptor function were observed.

Molecular Biology

Mutations were introduced to the δ subunit by the QuikChange site-directed mutagenesis technique (Stratagene, La Jolla, CA) and verified by DNA sequencing. The E177A mutation of the δ subunit was introduced through polymerase chain reaction amplification with the primer 5'-GGA CAG GCA GGC GTG CAT GCT GGA CCT GGA GAG C-3' and the reverse complement (Integrated DNA Technologies, Coralville, IA).

Whole-cell Current Recordings

Cells were bathed in an extracellular buffer composed of 145 mM NaCl, 5 mM KCl, 2 mM $CaCl_2$, 1.5 mM $MgCl_2$, and 10 mM HEPES (4-(2-

hydroxyethyl)-1-piperazineethanesulfonic acid) brought to pH 7.4 with 5 N NaOH. Individual cells in a whole-cell patch-clamp configuration, attained as described previously (*125*), were lifted from the dish with a borosilicate glass pipette and suction. Borosilicate glass pipettes were made from capillaries with a 1.5 / 1.12 mm outer / inner diameter (World Precision Instruments Inc., Sarasota, FL) and heat-polished on a microforge to yield pipettes with open-end resistances of 3.0-5.0 MΩ. Pipettes were filled with an intracellular solution composed of 140 mM CsCl, 10 mM tetraethylammonium chloride, 10 mM EGTA (ethylene glycol bis (β-aminoethyl ether)-*N, N, N', N'* tetraacetic acid), 2 mM $MgCl_2$, and 10 mM HEPES brought to pH 7.4 with 5 N CsOH. All measurements were carried out with a constant membrane potential of – 60 mV, at ambient temperature (~ 22 °C). An Axopatch 200B amplifier, Digidata 1322A digitizer and Clampex 9.0 software (Molecular Devices, Sunnyvale, CA) were used for recording whole-cell currents, as previously described by Hamill *et al.* (*186*). Data was filtered with the Axopatch 200B internal Bessel filter at 2 kHz with a digital sampling frequency of 20 kHz.

Rapid Solution Application

Rapid applications of ligands to cells expressing the receptor of interest were performed with the cell-flow technique as previously described by Udgaonkar *et al.* (*18*). Briefly, a cell in the whole-cell current-recording mode in extracellular buffer was suspended from the recording electrode ~ 200 μm in front of the porthole of a stainless steel U-tube. Solution was actively pumped with a peristaltic pump into one end of the U-tube at a typical rate of ~ 1.5 cm/s and drawn from the other end of the U-tube with

the peristaltic pump at a greater rate. This causes extracellular buffer in the dish to be drawn through the porthole of the U-tube, preventing the leakage of solutions in the U-tube on to the cell. The flow of solution out of the porthole is regulated by a solenoid Lee Control Valve (Lee Co., Essex, CT) directed by Clampex software. After an application period, the solution from the dish is again drawn into the porthole of the U-tube, rapidly removing the recently applied solution. Solution applications were spaced a minimum of 2 – 2.5 minutes apart, permitting receptors time to recover from desensitized states before the next measurement.

Current Measurement Analysis and Correction

Many neurotransmitter receptors undergo rapid desensitization, which can have a significant effect on the observed peak current amplitudes but can be corrected for as previously described (*18*). The observed peak amplitudes of non-δ subunit-containing $GABA_A$ receptor currents, in the absence or presence of modulators, were corrected for desensitization by fitting the desensitization phase of each current trace with a three-component exponential function. The time constants obtained from the fit were used for (*i*) comparing how compounds alter the rate of receptor desensitization and (*ii*) estimating the true current amplitudes by accounting for receptor desensitization (*18, 137*) that occurs during the rising phase of the receptor current trace (*236*). Measured currents from $GABA_A$ receptors containing a δ subunit characteristically display limited (if any) desensitization (*237*) and, therefore, were not corrected. To normalize current amplitudes between cells all receptor currents from a single cell were divided by the current amplitude evoked by a control measurement of

current induced by saturating 1 mM GABA (I_A / $I_{Control}$). Dose-dependent data were plotted with their relative standard errors and fitted with either equation [2.1] or equation [2.2] using non-linear least squares regression conducted with Origin V. 3.5 data analysis software (OriginLab Corp., Northampton, MA). All reported values of dissociation constants estimated by non-linear least squares fitting are reported with relative standard errors.

Results

Most $GABA_A$ receptor subtypes are modulated by a variety of small molecules, including barbiturates such as phenobarbital and benzodiazepines such as diazepam, both of which are anticonvulsants that act by positively modulating (potentiating) currents of $GABA_A$ receptors (*139*). Many different molecules have been reported to potentiate $GABA_A$ receptors (several examples are shown in Figure 2.2A). With their structural resemblance to phenobarbital and pentobarbital, DHPMs JM-II-43A (methyl 6-methyl-2-oxo-4-phenyl-3,4-dihydro-1H-pyrimidine-5-carboxylate) and monastrol were considered likely to potentiate $GABA_A$ receptors (Figure 2.2A).

JM-II-43A and the other derivatives (except for monastrol, which is commercially available), shown in Figure 2.2B, were synthesized by Dr. John Mabry and Mr. Jason Polisar using a multi-component Biginelli reaction as previously described (*17*). The DHPMs synthesized were first tested for their solubility at a concentration of 1 to 4 mM in aqueous extracellular buffer with 0.5 % dimethyl sulfoxide (DMSO); most were soluble at concentrations up to 2 mM. To determine whether the DHPM compounds listed (Figure 2.2B) potentiate recombinant $GABA_A$ receptors, the cell-flow

Figure 2.2 A. Structures of several molecules that potentiate various $GABA_A$ receptor subtypes. Of the many compounds known to modulate $GABA_A$ receptors only ketamine (*5*), ethanol (*6-8*) [though ethanol modulation seems somewhat complicated (*9, 10*)] and two benzamide compounds (*11*) have been reported to selectively potentiate δ subunit-containing receptor subtypes. The structural similarities of JM-II-43A (methyl 6-methyl-2-oxo-4-phenyl-3,4-dihydro-1H-pyrimidine-5-carboxylate), monastrol and other DHPMs (Figure 2.2B) to pentobarbital and phenobarbital, suggests that DHPMs may also potentiate whole-cell currents from $GABA_A$ receptors. **B.** A one-step Biginelli reaction (*17*) was used to synthesize derivatives of JM-II-43A. Synthesis of DHPMs was conducted by Dr. J. Mabry and J. Polisar. Each compound was tested for solubility and efficacy to potentiate α1β2δ $GABA_A$ receptor currents at 1 mM compound and 1 mM GABA. Solubility of each DHPM was determined qualitatively in aqueous extracellular buffer containing 0.5 % DMSO, and is described as soluble (Sol), partially soluble (PSol) or not soluble (NSol). The degree of current potentiation (fold potentiation) is described as the current induced by 1 mM GABA and 1 mM of the compound divided by the current induced by 1 mM GABA alone ($I_{1\ mM\ cpd.} / I_{1\ mM\ GABA\ control}$). Activity and solubility were examined by R. Lewis.

A

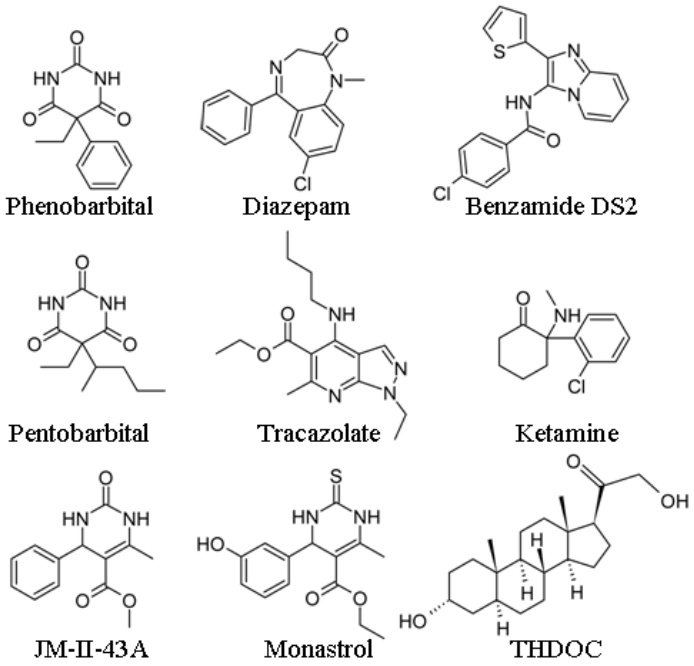

B

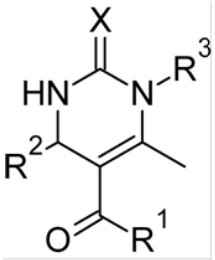

	Compound	R1	R2	R3	X	Fold Potentiation	Solubility*
1	JM-II-43A	OMe	Ph	H	O	2.9	Sol
2	JGP-I-80A	OEt	Ph	H	O	1.2	PSol
3	JM-III-3	Me	Ph	H	O	1.3	Sol
4	JGP-I-142C	OH	Ph	H	O	1	Sol †
5	JGP-II-17F	NH2	Ph	H	O	1	Sol
6	JGP-II-28K	OMe	Ph	Me	O	1	Sol
7	JGP-I-151B	OMePh	Ph	H	O	NA	NSol
8	JM-III-4B	OMe	4-Br-C6H4	H	O	1.3	Sol
9	JM-III-6A	OMe	3-OMe-C6H4	H	O	1.4	Sol
10	JM-III-31	OMe	4-NO2-C6H4	H	O	1.3	Sol
11	JM-III-12A	OMe	3-OMe-4-OH-C6H3	H	O	1.5	Sol
12	JM-III-14A	OMe	C3H7	H	O	2.1	Sol
13	JGP-I-150B	OMe	Ph	H	S	1	Sol
14	monastrol	OEt	3-OH-C6H4	H	S	3.0	Sol

* Compound solubility tested at concentration of 1 mM in extracellular buffer with 0.5% DMSO, pH 7.4

† This compound was not soluble in pure DMSO, but was soluble in extracellular buffer alone, pH 7.4.

technique (*18*) was used to rapidly co-apply 1 mM JM-II-43A and 1 mM GABA to various receptor subtypes transiently expressed in HEK293T cells. Representative current traces evoked by 1 mM GABA alone or co-applied with 1 mM JM-II-43A are shown for α1β2, α1β2γ2L, and α1β2δ receptor subtypes (Figure 2.3A). Currents of specific receptor subtypes, such as α1β2δ, were potentiated, whereas slight increases in the rates of desensitization were observed with currents of α1β2 and α1β2γ2L receptor subtypes (Figure 2.3A). When co-applied with 1 mM JM-II-43A and 1 mM GABA receptor subtypes α1β2δ, α1β3δ, α4β2, α4β2δ, α5β2δ and α6β3δ also demonstrated potentiation anywhere from 1.3- to 3.4-fold the current evoked by 1 mM GABA alone. No changes in corrected peak current amplitudes were observed for currents of receptor subtypes α1β2, α1β2γ2L, α1β3, α4β2, α5β2, α5β3 and α6β3γ2L. However, it was noted that several of these receptor subtypes had small changes in the rates of desensitization. For unknown reasons, limited expression of receptor subtypes α5β3δ, α6β2, and α6β3 was observed when transiently transfected in HEK293T cells, preventing the examination of the effect of JM-II-43A on these receptor subtypes. The observed low expression of the α6β2 receptor subtype agrees with a previous report in which *Xenopus laevis* oocytes were used as an expression system (*238*). However α6β3 receptors have been successfully expressed in *X. laevis* oocytes (*8*) and it is not known why expression of these receptors is limited in HEK293T cells. The potentiation mechanism of $GABA_A$ receptors by JM-II-43A was further investigated with the α1β2δ receptor subtype because of the high degree of potentiation and satisfactory expression level of the subtype in HEK293T cells. With the α1β2δ subtype the mean current measured in the presence of 1 mM JM-II-43A plus 1 mM

Figure 2.3 A. Representative traces showing the effects of 1 mM JM-II-43A on currents evoked by 1 mM GABA with three different receptor isoforms α1β2, α1β2γ2L, and α1β2δ. The current traces for α1β2 and α1β2γ2L receptor subtypes were corrected for receptor desensitization (grey line) (*18*). Current correction for the receptor subtype α1β2δ is not needed because limited to no desensitization is observed. **B.** 1 mM GABA with 1 mM JM-II-43A was applied to various receptor subtypes to test the specificity of JM-II-43A current potentiation. Of the subtypes examined here, only the α4β2 receptor subtype and receptors containing the δ subunit were potentiated by JM-II-43A. Error bars display the standard error, numbers above each bar represent the number of independent cells measured and the asterisk (*) denotes a significant difference ($p \leq 0.01$), as tested by a one-way ANOVA statistical test.

A

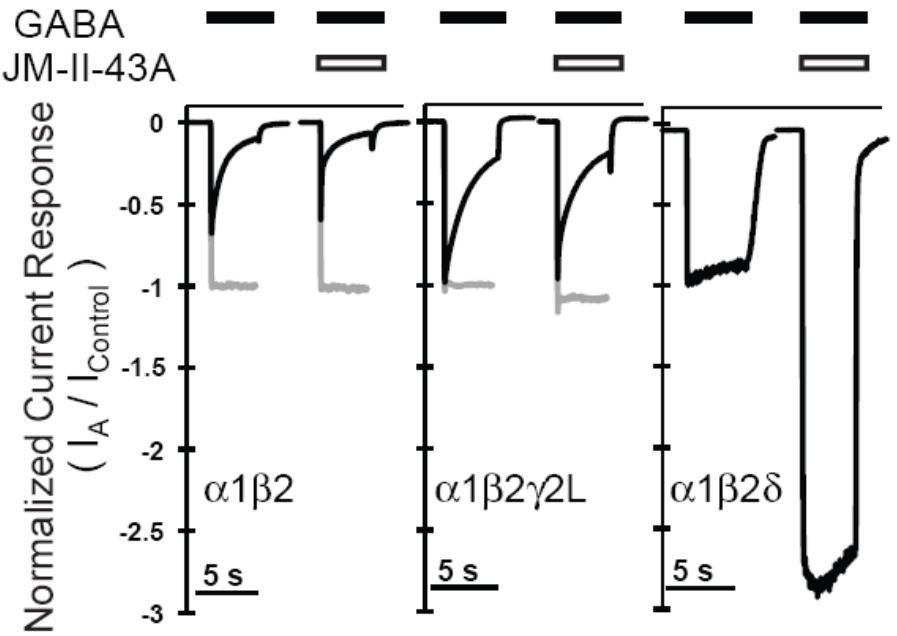
GABA
JM-II-43A
Normalized Current Response
(I_A / $I_{Control}$)
0
-0.5
-1
-1.5
-2
-2.5
-3
α1β2
α1β2γ2L
α1β2δ
5 s
5 s
5 s

B

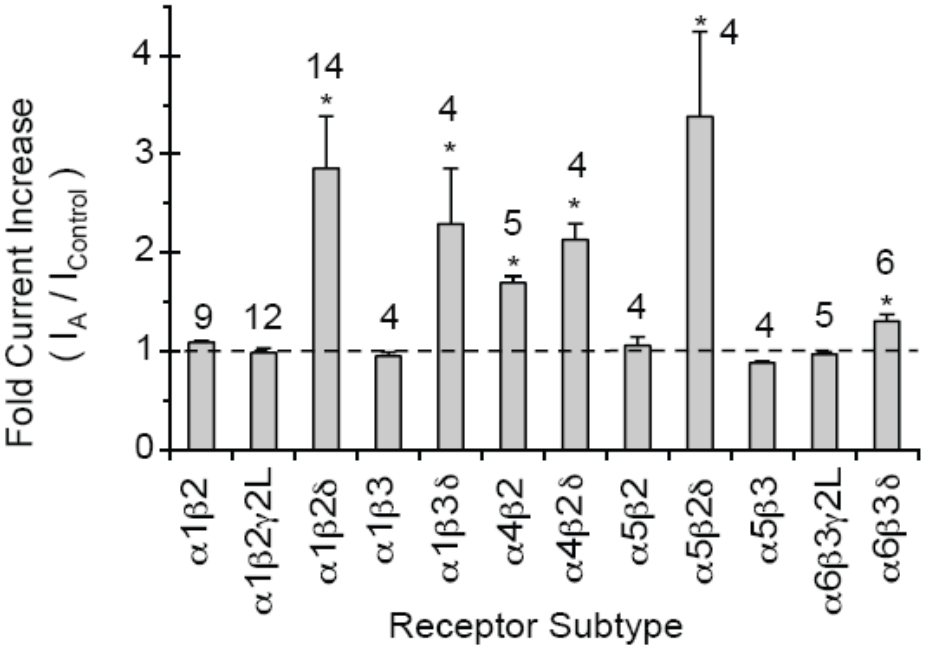
Fold Current Increase
(I_A / $I_{Control}$)
0
1
2
3
4
9
12
14
4
4
5
4
4
4
5
4
6
α1β2
α1β2γ2L
α1β2δ
α1β3
α1β3δ
α4β2
α4β2δ
α5β2
α5β2δ
α5β3
α6β3γ2L
α6β3δ
Receptor Subtype

GABA was 2.9-fold larger than in the presence of 1 mM GABA alone (Figure 2.4A and 2.4B). The maximum (3.5-fold) potentiation of current occurred with 1.5 mM JM-II-43A. In the presence of 3 μM GABA currents observed for the α1β2δ receptor subtype are only 25 % of the maximal current response (EC_{25}), indicating that the receptors are primarily in a closed-channel state. However, upon co-application of 3 μM GABA and 1 mM JM-II-43A, receptor currents are potentiated up to ~ 4-fold compared to those evoked by 3 μM GABA alone (Figure 2.4A). To better describe how JM-II-43A affects the receptors, dose-dependent data (Figure 2.4A) were fitted with equation [2.1] to obtain values for the apparent dissociation constant of JM-II-43A ($*K_{d\,(\text{JM-II-43A})}$).

JM-II-43A may potentiate currents of α1β2δ receptors by preferentially binding to the open-channel form of the receptor, thus shifting the receptor channel-opening equilibrium toward the open-channel state. This mechanism would be similar to that described for the potentiation of the α1β2γ2L(K289M) receptor by phenobarbital (Figure 2.1) (*2, 139*). It would require that JM-II-43A binds with higher affinity to the open-channel state than to the closed-channel state of the receptor. Therefore, the dissociation constant of JM-II-43A was determined in the presence of 1 mM and 3 μM GABA to assess the compound's binding affinity for the α1β2δ receptor in the open- and closed-channel states, respectively (Figure 2.4A). Various concentrations of JM-II-43A were co-applied with either 1 mM or 3 μM GABA, and equation [2.1] (*155*) was used to evaluate the JM-II-43A dissociation constant, K_d.

$$I_P/I_o = I_o + (R_{MAX})(1+(K_d/[\text{Cpd}])^h)^{-1} \qquad [2.1]$$

Equation [2.1], which has been used previously to measure barbiturate

Figure 2.4 A. JM-II-43A dose-dependent curves (0.01 to 2 mM) were obtained from α1β2δ receptors for the compound alone (gray squares), in the presence of 1 mM GABA (saturating concentration, ▲) and in the presence of 3 μM GABA (effective concentration for 25 % of maximal current response, EC_{25}, O). Curves were fitted with equation [2.1] and gave an apparent dissociation constant for JM-II-43A ($*K_{d\,(\text{JM-II-43A})}$) of 410 ± 74 μM at 1 mM GABA and 810 ± 32 μM at 3 μM GABA, with Hill coefficients of 2.1 and 2.2 respectively. The difference between the apparent dissociation constants is statistically significant with a p-value less than 0.0001 as tested by a Welch's two way t-test, assuming unequal variance, using an $\alpha=0.05$ and data analysis having 79 degrees of freedom (d.f.). The inset shows two representative current traces evoked by 1 mM GABA and 1 mM GABA with 1 mM JM-II-43A. Current amplitudes are normalized to the peak of the 1 mM GABA current response. **B.** A monastrol dose-dependent curve was obtained with α1β2δ receptors in the presence of 1 mM GABA and fitted with equation [2.1] to calculate an apparent dissociation constant for monastrol ($*K_{d\,(\text{monastrol})}$) of 190 ± 28 μM. Potentiation at concentrations of monastrol above 1 mM decreased, likely due to solubility limitations of the compound and/or possible receptor inhibition. The inset shows two representative current traces evoked by 1 mM GABA and 1 mM GABA with 1 mM monastrol. Current amplitudes are normalized to the peak of the 1 mM GABA current response. **C.** GABA dose-dependent curves obtained with α1β2δ receptors in the absence (◇) or presence (■) of 1 mM JM-II-43A were fitted with equation [2.2] and gave a value for the dissociation constant for GABA (K_I) of 9.9 ± 1.1 μM and 7.0 ± 1.5 μM respectively, values were not statistically different ($p=0.12$, Welch's two way t-test, $\alpha=0.05$, d.f.=104).

All currents were recorded at ambient temperature (~ 22 °C), – 60 mV membrane potential and pH 7.4. Measurements from a single cell are normalized by dividing the current amplitude evoked in the presence of an experimental compound by a 1 mM GABA control current measurement (I_A / $I_{Control}$). The value of each data point shown in C, E and F is the mean of four to fourteen measurements from independent cells and is plotted on a logarithmic scale with error bars representing the standard error.

A

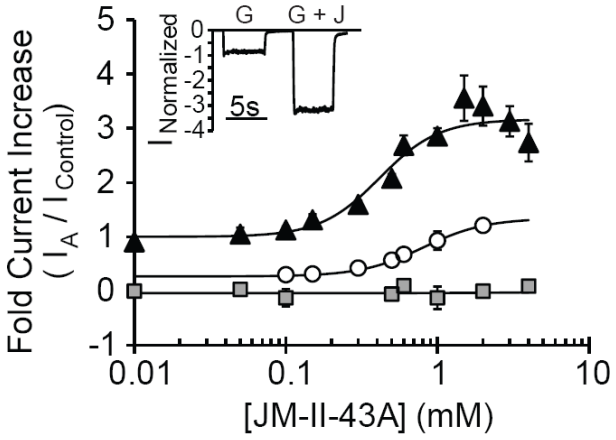
G
G + J
5s
I Normalized
Fold Current Increase
(I A / I Control)
[JM-II-43A] (mM)

B

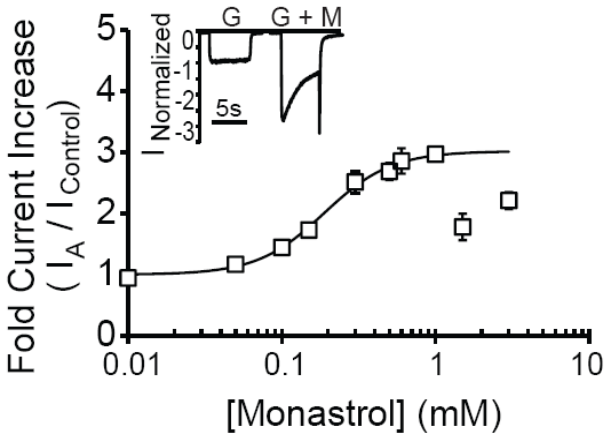
G
G + M
5s
I Normalized
Fold Current Increase
(I A / I Control)
[Monastrol] (mM)

C

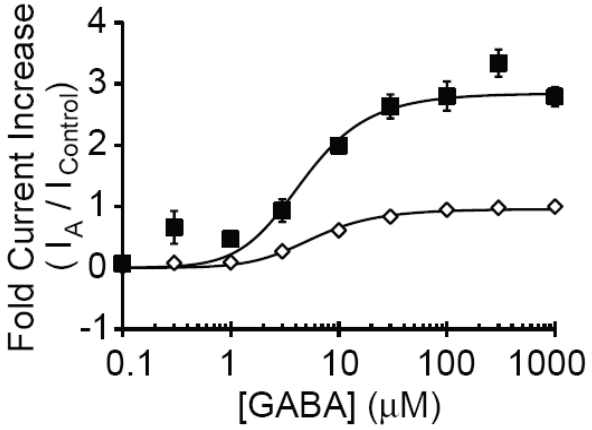
Fold Current Increase
(I A / I Control)
[GABA] (μM)

interactions with $GABA_A$ receptors (*2, 155*), relates the ratio of measured current amplitudes (I_P/I_o) induced by a constant GABA concentration in the presence (I_P) or absence (I_o) of the compound of interest ([Cpd]), JM-II-43A. R_{MAX} is the maximum I_P/I_o ratio observed when the potentiating compound is co-applied with GABA. The empirical parameter h is equivalent to the Hill coefficient. Because 1 mM JM-II-43A does not saturate α1β2δ receptors at either 1 mM or 3 μM GABA, and is not easily soluble at higher concentrations, fitting the dose-dependent data in Figure 2.4A afforded only the apparent value of its dissociation constant ($*K_{d\,(JM\text{-}II\text{-}43A)}$) (The $*K_d$ is approximately equal to the EC_{50}). For the α1β2δ receptor the values of $*K_{d\,(JM\text{-}II\text{-}43A)}$ were estimated to be 410 ± 74 μM and 810 ± 32 μM in the presence of 1 mM and 3 μM GABA, respectively, These values are statistically different $p<0.0001$ as tested with a Welch's two way t-test, assuming unequal variance using an $\alpha=0.05$ and with the data analysis having 79 degrees of freedom (d.f.). (The measured constants for various receptors and conditions can be found in Table 2.1.) Hill coefficients of 2.1 and 2.2 were obtained for these two fittings, values similar to 2.2 (*239*), 1.5 (*155*), and 1.5-1.9 (*2*) previously observed for phenobarbital modulation of $GABA_A$ receptors.

The apparent dissociation constants of these compounds are relatively large, so it was of interest to investigate if these compounds rapidly or slowly associate with the receptors. To address this question we designed an experiment similar to that described by Wallner et al. (*8*), in which whole-cell currents were recorded upon application of the modulating compound at various concentrations while the receptors are continually in the presence of 2 μM GABA. A perfusion system was used to exchange the buffer bathing

Table 2.1: Apparent dissociation constants obtained for the $GABA_A$ receptor α1β2δ subtype and the α1β2δ(E177A) variant.

Receptor subunit composition	$K_{I\ (GABA)}$ (μM)	$K_{I\ (GABA)}$ with 1 mM JM-II-43A (μM)	$K_{d\ (JM\text{-}II\text{-}43A)}$ with 1 mM GABA (μM)	$K_{d\ (JM\text{-}II\text{-}43A)}$ with 3 μM GABA (μM)	$K_{d\ (monastrol)}$ with 1 mM GABA (μM)
α1β2δ	9.9 ± 1.1	7.0 ± 1.5	410 ± 74	810 ± 32	190 ± 28
α1β2δ(E177A)	5.7 ± 0.26	8.6 ± 2.0	620 ± 120	1140 ± 390	-

the cell with buffer containing 2 μM GABA (EC_{15}), followed by increasing concentrations of JM-II-43A co-applied with 2 μM GABA using a U-tube. Not only does this data (Figure 2.5) clearly display the dose-dependent effect of JM-II-43A on the receptor, but the rapid change in the current amplitude upon application demonstrates that JM-II-43A is associating and dissociating with the receptor on a relatively fast time scale. In the current trace the 10% to 90 % response times for the 1 mM and 2 mM JM-II-43A applications were 155 ms and 123 ms, respectively.

Monastrol and other DHPMs also potentiated α1β2δ receptors, as shown in Figure 2.1B. Because monastrol had one of the largest potentiating efficacies at 1 mM in the presence of 1 mM GABA, a full dose-dependent response for this compound was measured (Figure 2.4B). Fitting of the dose-dependent curve for monastrol yielded a value for the apparent dissociation constant ($*K_{d\,(\text{monastrol})}$) of 190 ± 28 μM, indicating that α1β2δ receptors have a statistically higher binding affinity for monastrol than they do for JM-II-43A ($*K_{d\,(\text{JM-II-43A})}$ = 410 ± 74 μM) (p=0.0056 by a Welch's two way t-test, α=0.05 and d.f.=75). Potentiation of the α1β2δ receptor currents by monastrol declined above 1 mM, which may be due to solubility limitations of monastrol and/or inhibitory activity at higher concentrations. It is interesting to note that while JM-II-43A had no observed effect on receptor desensitization, monastrol dramatically increases the desensitization rate of α1β2δ receptors and causes a large rebound current at the end of ligand application (inset, Figure 2.4B).

No agonist activity on α1β2δ receptors in the absence of GABA was observed for any of the DHPMs tested. However, it is possible that JM-II-43A and the other DHPMs tested potentiate α1β2δ receptor currents by

Figure 2.5 A current trace from α1β2δ recombinant receptors in a single cell was used to demonstrate the current response upon application of 2 μM GABA and increasing concentrations of JM-II-43A during the 2 μM GABA application. 1 mM GABA in the absence of JM-II-43A was applied at the beginning and end of the current trace. This trace displays the dose-dependent modulation of the receptor by JM-II-43A, the increase in amplitude of the current by JM-II-43A, and the rapid association and dissociation of the compound with the receptor during a JM-II-43A application period. All currents were recorded at ambient temperature (~ 22 °C), – 60 mV membrane potential and pH 7.4.

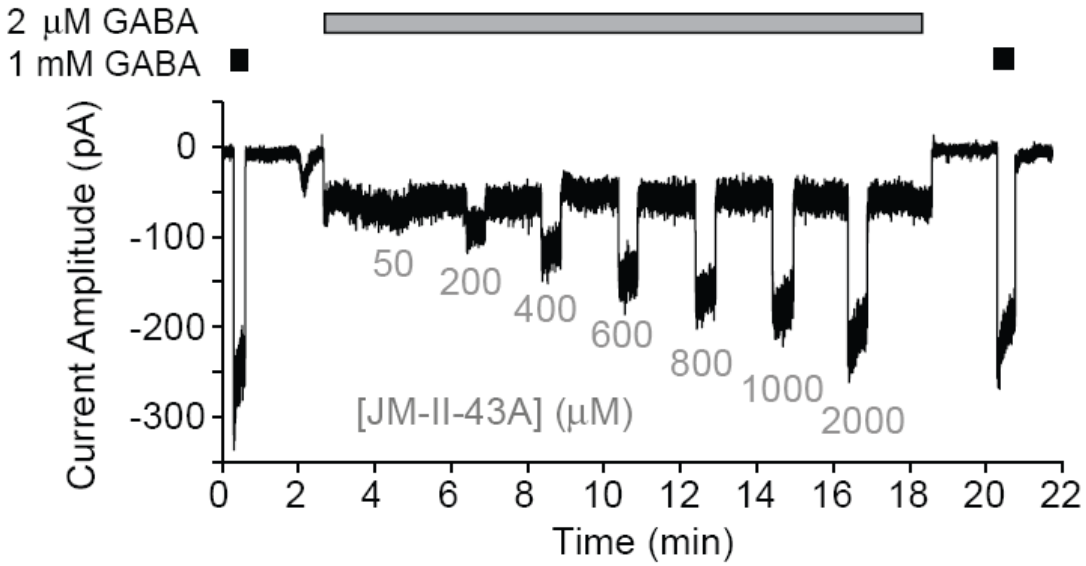
2 μM GABA
1 mM GABA
Current Amplitude (pA)
0
-100
-200
-300
50
200
400
600
800
1000
2000
[JM-II-43A] (μM)
0
2
4
6
8
10
12
14
16
18
20
22
Time (min)

changing the receptor affinity for GABA or by acting in cooperation with GABA as an agonist or partial agonist. To test these possibilities, we examined the dose-dependence of GABA on receptor currents in the presence and absence of JM-II-43A (Figure 2.4C). If the mechanism for α1β2δ receptors is similar to that proposed for the α1β2γ2L receptor (Figure 2.1A), it is possible to estimate the GABA dissociation constant ($K_{I\,(GABA)}$) by fitting the data with equation [2.2] (*18*).

$$I_A = I_M R_M L^2 (L^2 + \Phi(L + K_1)^2)^{-1} \qquad [2.2]$$

This equation describes the expected current amplitude (I_A) evoked by a known agonist concentration (L). I_M represents the current from one mole of receptors in the open-channel state and R_M the number of moles of receptors on the cell surface. Experimentally, we used the current amplitude at a saturating concentration of the activating ligand (GABA) as the $I_M R_M$ value and the observed current amplitude as I_A. Φ is the channel-closing equilibrium constant (the reciprocal of the channel-opening equilibrium constant), defined in Figure 2.1A. Fitting the GABA dose-dependent response data from α1β2δ receptors with equation [2.2] gave values for K_I (GABA) of 9.9 ± 1.1 μM and 7.0 ± 1.5 μM in the absence and presence of 1 mM JM-II-43A, respectively, which was not statistically different ($p=0.12$ by a Welch's two way t-test, $\alpha=0.05$ and d.f.=104). These K_1 values agree well with the previously reported dose-dependent curve of the α1β2δ receptor subtype (*145*). Compounds were also tested, up to concentrations of 4 mM, in the absence of GABA and no induced currents were observed. Data for JM-II-43A in the absence of GABA is shown in Figure 2.4A.

$GABA_A$ receptors containing the δ subunit typically exhibit limited desensitization and α1β2δ receptor desensitization was not altered by JM-II-

43A. However, JM-II-43A did alter the desensitization phase of current recorded from α1β2 (Figure 2.3A), α1β2γ2L (Figure 2.3A), α1β3, α4β2, α5β2, α5β3 and α6β3γ2L receptor subtypes. The rate at which ligand-gated ion channels, such as $GABA_A$ receptors α1β2 and α1β2γ2L, pass into a desensitized state and how modulating compounds change the rate of desensitization can be described by time constants (τ_x). The values of the time constants were obtained from fitting the desensitization phase of each current trace with an exponential function (*240*), shown below:

$$I = A_1(e^{t/\tau 1}) + A_2(e^{t/\tau 2}) + A_3(e^{t/\tau 3}) + C \qquad [2.3]$$

Equation [2.3] describes the desensitization of current traces where t is time, A_x represents the relative amplitude of component x and C the current remaining at the end of the GABA application period. In previous studies, ligand-gated ion channels currents are typically fitted with a two-component exponential function to describe the fast and slow desensitization rates observed (*137, 240*), but in the presence of DHPMs a third component was needed for appropriate fitting. Therefore, all traces analyzed for desensitization were fitted with a three-component exponential function so that comparisons could be made between the presence and absence of modulating compounds. The values obtained for τ_x were also used to determine desensitization-corrected amplitudes of peak currents, as previously described (*18*). JM-II-43A changed the desensitization rate of both α1β2 and α1β2γ2L receptors but did not affect the desensitization-corrected current amplitudes (Figure 2.3A, Table 2.2). In Table 2.2 the resulting time constants and relative amplitudes are listed for α1β2 receptors (9 independent cells) and α1β2γ2L receptors (12 independent cells) when 1 mM GABA or 1 mM JM-II-43A with 1 mM GABA was applied to them.

Table 2.2: Parameters obtained from fitting equation [2.3] to the desensitization phase of α1β2 and α1β2γ2L $GABA_A$ receptor currents in the presence and absence of JM-II-43A.

receptor subtype	no. of cells	conditions	mean corrected peak current	A_1 (pA)	τ_1 (ms)	A_2 (pA)	τ_2 (ms)	A_3 (pA)	τ_3 (ms)	C (pA)
α1β2	9	1 mM GABA	-4680 ± 930	-1480 ± 410	650 ± 150	-1370 ± 270	1270 ± 210	-1150 ± 210	1590 ± 220	760 ± 200
		1 mM GABA with 1 mM JM-II-43A	-5050 ± 990	-2290 ± 450	68 ± 15	-1170 ± 330	600 ± 180	-1190 ± 240	1900 ± 360	590 ± 170
α1β2γ2L	12	1 mM GABA	-6210 ± 630	-1490 ± 200	970 ± 270	-1880 ± 310	2090 ± 200	-1710 ± 210	2130 ± 150	1150 ± 160
		1 mM GABA with 1 mM JM-II-43A	-6250 ± 930	-2440 ± 780	460 ± 200	-1500 ± 210	1510 ± 320	-1660 ± 180	2090 ± 240	830 ± 110

[a]Paired current traces from a single cell were obtained by application of 1 mM GABA with and without 1 mM JM-II-43A. The desensitization phase of each current trace was fitted with a three-component exponential equation [3] and using non-linear least-squares regression. The mean values for the parameters are shown above. A_x and τ_x represent the current amplitude and time constant associated with the 'x' exponential component, respectively. C is the current amplitude at the end of the fit region.

Since JM-II-43A and monastrol potentiated the α1β2δ subtype, these compounds were also tested on receptors that contained the single amino-acid mutation E177A within the δ subunit, a mutation that was determined to be a heritable susceptibility allele (*3*). $GABA_A$ receptors α1β2δ(E177A) [as well as α4β2δ(E177A)] are reported to have significantly reduced currents (*3, 4*) due to a decrease in the channel mean-open time of the receptor as measured with single-channel recording (*4*). The extent of the decrease in whole-cell currents for these mutations varied. The reported amplitudes of averaged whole-cell currents from receptors containing the δ(E177A) subunit range from ~ 12 % (α1β2δ E177A) (*3*) and ~ 33 % (α4β2δ E177A) (*4*) to ~ 53 % (α1β2δ E177A) (Figure 2.6A) of that of the maximum wild-type currents measured at the same concentrations of GABA. The degree of current reduction due to the mutations varied when maximum currents recorded from independent cells were measured, because whole-cell currents depend on the number of moles of receptors on the cell surface, R_M, (Equation [2.2]), which depends on transfection efficiencies for each cell. As a result, a large standard error was observed in the averaged maximum current amplitudes evoked by 1 mM GABA from 34 cells expressing α1β2δ receptors and 19 cells expressing α1β2δ(E177A) receptors (Figure 2.6A), but the difference was statistically significant ($p<0.003$). The dose-response curve of α1β2δ(E177A) receptors for JM-II-43A with saturating 1 mM GABA afforded a value of 0.624 ± 0.116 mM for $*K_{d\,(\text{JM-II-43A})}$ with a Hill coefficient of 1.7 ± 0.3 (Figure 2.6B). The value of $*K_{d\,(\text{JM-II-43A})}$ at low (3 μM) concentrations of GABA changed to 1.14 ± 0.39 mM with a Hill coefficient of 1.5 ± 0.3. However, these binding affinity constants were not statistically different ($p=0.21$, Welch's two way t-test, $\alpha=0.05$ and d.f.=56).

Figure 2.6 Mutated α1β2δ(E177A) $GABA_A$ receptors, which give lower average current responses to GABA than do the wild-type receptor (*3, 4*), were potentiated by JM-II-43A. **A.** Mean current amplitudes evoked by 1 mM GABA from 34 independent cells for wild-type α1β2δ and 19 independent cells for mutant α1β2δ(E177A) receptors demonstrate a 47% reduction in current amplitude and are shown with relative standard errors. The difference is statistically significant ($p<0.003$) using a Welch's two-tailed t-test assuming unequal variance and an $\alpha = 0.05$. The somewhat large standard errors, despite 34 and 19 independent measurements, are likely due to large variations in the number of receptors expressed on the surface of each cell. **B.** Fitting equation [1] to the dose-dependent response data from α1β2δ(E177A) receptors in the presence of 0.01 to 2 mM JM-II-43A and 1 mM GABA (▲), gave a value for the apparent dissociation constant for JM-II-43A ($*K_{d\,(\text{JM-II-43A})\,(\text{E177A})}$) of 0.62 ± 12 mM, with a Hill coefficient of 1.7 ± 0.3. In the presence of 3 μM GABA (EC_{25}) (O) the value for $*K_{d\,(\text{JM-II-43A})\,(\text{E177A})}$ was 1.1 ± 0.39 mM, with a Hill coefficient of 1.5 ± 0.3. Apparent dissociation constants were not statistically different, with $p=0.21$ by a Welch's two way t-test ($\alpha=0.05$ and d.f.=56) **C.** Fitting the GABA dose-dependent data with equation [2] gave values for the dissociation constant (K_I) for GABA from α1β2δ(E177A) receptors of 5.68 ± 0.26 μM (◇) and 8.64 ± 1.98 μM (■) in the absence and presence of JM-II-43A respectively. K_1 values for mutant receptors were not statistically different ($p=0.20$ by a Welch's two way t-test, $\alpha=0.05$ and d.f.=54). Independent measurements from 3-6 cells were made for every concentration shown in B and C and plotted on a logarithmic scale. **D**. Comparison of the potentiation due to saturating concentrations of JM-II-43A, monastrol, phenobarbital or tracazolate coapplied with 1 mM GABA shows that DHPMs positively modulate both α1β2δ and α1β2δ(E177A) $GABA_A$ receptors to a similar or greater extent than do phenobarbital and tracazolate. The means and relative standard errors shown are calculated from 12 independent cells for JM-II-43A and 3-9 independent cells for monastrol, phenobarbital and tracazolate, normalized to the current response evoked by 1 mM GABA. (Tracazolate measurements were conducted by K. Eagen. All other measurements were made by R. Lewis.) All current measurements were made at ambient temperature (~ 22 °C), –60 mV membrane potential and pH 7.4.

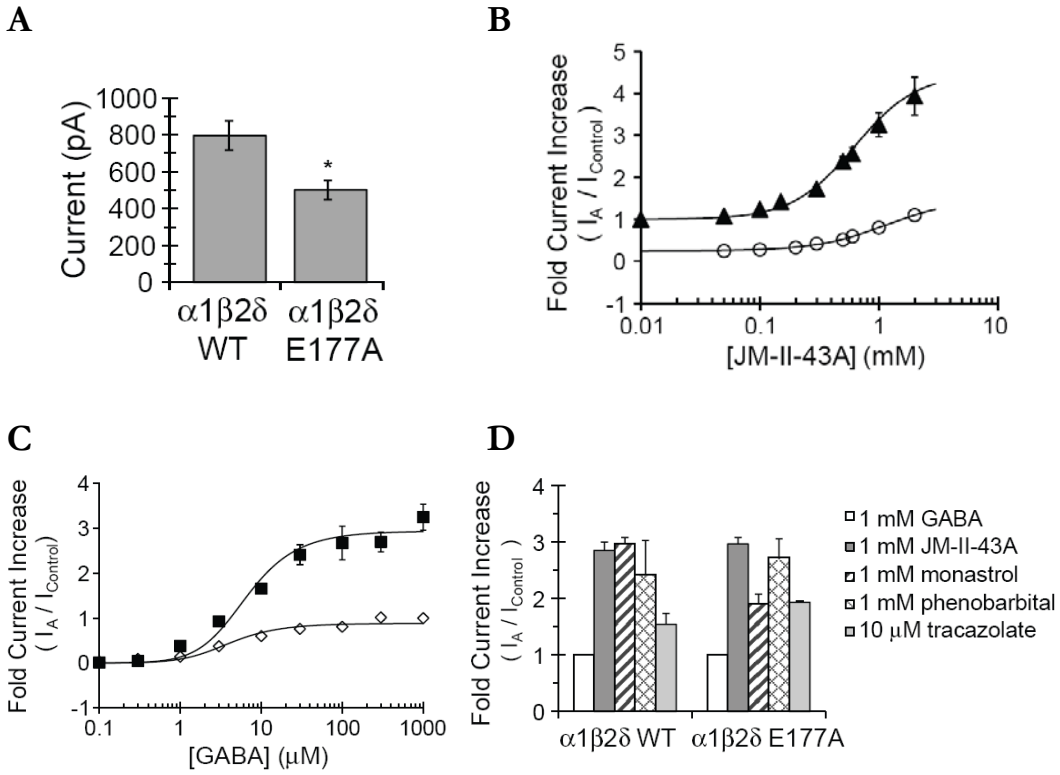
A
Current (pA)
1000
800
600
400
200
0
*
α1β2δ WT
α1β2δ E177A
B
Fold Current Increase (I_A / I_Control)
5
4
3
2
1
0
-1
0.01
0.1
1
10
[JM-II-43A] (mM)
C
Fold Current Increase (I_A / I_Control)
4
3
2
1
0
-1
0.1
1
10
100
1000
[GABA] (μM)
D
Fold Current Increase (I_A / I_Control)
4
3
2
1
0
α1β2δ WT
α1β2δ E177A
1 mM GABA
1 mM JM-II-43A
1 mM monastrol
1 mM phenobarbital
10 μM tracazolate

Additionally, no statistical difference was observed in the affinity of α1β2δ(E177A) receptors for GABA in the absence (K_I = 5.68 ± 0.26 μM) or presence (K_I = 8.64 ± 1.98 μM) of 1 mM JM-II-43A (p=0.20, Welch's two way t-test, α=0.05 and d.f.=54) (Figure 2.6C). Both 1 mM JM-II-43A and 1 mM monastrol potentiated currents from receptors containing the mutant δ(E177A) subunit, by 3.2-fold and 2.0-fold respectively (Figure 2.6D). These values were directly compared to the approximate ~ 3-fold potentiation of wild-type α1β2δ $GABA_A$ receptors by 1 mM JM-II-43A or monastrol in the presence of 1 mM GABA, as well as to potentiation by 1 mM phenobarbital and 10 μM tracazolate (Figure 2.6D).

Discussion

Many neurological pathologies, including schizophrenia, depression, anxiety, insomnia and epilepsy, are linked to $GABA_A$ receptor dysregulation of signal transmission in the mammalian CNS (*35*). Understanding how $GABA_A$ receptors work in the CNS, what molecules modulate these receptors, and how various compounds affect their functions is critical information to aid in the treatment of diseases, such as epilepsy, which affects ~ 50 million people world wide (*101*). Compounds that target subsets or specific $GABA_A$ receptor isoforms allow for more detailed and precise studies and potentially more specific treatment of $GABA_A$ receptor-related disorders. However, the repertoire of known compounds that preferentially potentiate currents from $GABA_A$ receptor isoforms containing the δ subunit was limited to ketamine (*5*), two benzamide molecules (*11*), and ethanol (*7, 8*). Here we have established that a family of dihydropyrimidinones also has this selective property. Ketamine, a well

characterized allosteric inhibitor of NMDA receptors, was recently reported (*5*) to selectively potentiate currents of recombinant α6β2δ and α6β3δ receptors that were expressed in *X. laevis* oocytes. The degree of potentiation reported for ketamine was largest when it was tested with GABA concentrations that evoke 1 % of maximal current (EC_1) and declined with increasing GABA concentrations. The two benzamide molecules described (*11*) potentiated currents evoked by low (EC_{20}) GABA concentrations when applied to recombinant α4β3δ receptors expressed in cells from an L(tk^-) cell line. The effects of the benzamides when co-applied with higher concentrations of GABA were not reported. Potentiation of δ subunit-containing receptors by ethanol has been reported at both low and high agonist concentrations (*7, 8*). However, this observed response seems to be a complicated relationship and necessitates further investigation (*9, 10*).

The structural similarity of DHPMs to the barbiturates pentobarbital and phenobarbital led us to hypothesize that these molecules may similarly potentiate $GABA_A$ receptor currents, but the DHPMs presented in our study have several novel characteristics. These compounds contrast to other compounds such as ketamine and benzamides, which were reported to specifically potentiate one or two receptor subtypes selectively, whereas DHPMs are somewhat selective for potentiation of a subgroup of receptors containing the δ subunit, with α4β2 receptors being the exception. In addition, the potentiation of $GABA_A$ receptor currents by DHPMs occurs over the entire effective range of GABA concentrations, without the DHPMs alone showing any agonist activity at concentrations up to 4 mM (Figure 2.4A). It is possible that these DHPMs may act as agonists at higher concentrations than those tested, however their solubility prevented

examination of this possibility. This finding also contrasts with barbiturates, such as pentobarbital and phenobarbital, which modulate most $GABA_A$ receptor subtypes and display partial agonist activity at high concentrations (*155, 156*). The observation that DHPMs do not change the affinity of the α1β2δ receptor for GABA suggest that DHPMs interact with $GABA_A$ receptors at an allosteric binding site; however, it is not known if the binding site is novel or the same one to which barbiturates bind. The binding site for DHPMs is evidently not specific to the presence of the δ subunit as α4β2 receptors were potentiated by DHPMs and these compounds increase desensitization rates of receptor subtypes lacking the δ subunit. These results, and observations previously reported (*144*) for the potentiation of both α4β3 and α4β3δ receptor subtypes by etomidate, propofol and the neurosteroid THDOC, indicate that the delta subunit is not essential for binding and potentiation, but likely assists in facilitating potentiation of several receptor subtypes.

The general mechanism for $GABA_A$ receptors presented here (Figure 2.1) was originally proposed by Katz and Thesleff for the nicotinic acetylcholine receptor (*12*), with the later addition of the desensitized states (DL and DL_2) and channel-opening equilibrium constant (Φ^{-1}) (*15*). This mechanism indicates that observed currents will be affected by any changes in the channel-opening equilibrium caused by receptor mutations or ligands that stabilize either the open-channel or closed-channel receptor state. While the measurement of several kinetic constants, such as k_{open} and k_{close} rate constants, for the specific α1β2δ receptor mechanism must await the development of appropriate reagents, results reported here support the hypothesis that potentiation of α1β2δ receptors and other receptor subtypes

by JM-II-43A may be due to the compound preferentially binding to and stabilizing the open-channel state. JM-II-43A has a higher affinity for the wild-type receptor ($^*K_{d\,(\text{JM-II-43A})}$ = 410 ± 74 μM) at a saturating concentration (1 mM) of GABA (receptor predominantly in the open-channel state) than at a low (3 μM) concentration of GABA (receptor predominantly in the closed-channel state) ($^*K_{d\,(\text{JM-II-43A})}$ = 810 ± 32 μM). It is also possible that DHPMs increase the desensitization rates of α1β2 and α1β2γ2L receptor isoforms due to preferential binding to and stabilization of the desensitized receptor state.

Previous chemical kinetic investigations of the α1β2γ2L(K289M) receptor genetically linked to epilepsy (*69*) used the mechanism proposed in Figure 2.1A to explain how the mutation decreases the channel-opening equilibrium constant (Φ^{-1}) 5-fold by reducing the channel-opening rate constant (k_{open}) (*1*). Moreover, the anticonvulsant phenobarbital was found to bind with higher affinity to the open-channel state of the mutated α1β2γ2L(K289M) receptor than to the closed-channel state, shifting the channel-opening equilibrium of the receptor towards the open-channel state (*2*), reaffirming the receptor mechanism. As with the α1β2γ2L(K289M) isoform, $GABA_A$ receptors containing the mutated δ(E177A) subunit together with the α1 and β2 subunits have reduced current amplitudes in whole-cell current recordings (Figure 2.6A) (*3, 4*). The decrease in whole-cell currents of receptors containing the δ(E177A) subunit is due to a decrease in the mean-open time (τ_{open}) of the receptor (the average period of time that the receptor occupies the state able to conduct current before closing), as measured in single-channel current recordings (*4*). The approximate 3-fold increase in current of α1β2δ(E177A) receptors when in

the presence of 1 mM JM-II-43A is consistent with the compound causing a shift of the channel-opening equilibrium towards the open-channel receptor state. While these observations do not establish that JM-II-43A alters the channel-opening equilibrium constant of the receptor, they are consistent with this hypothesis. Once appropriate reagents are developed, it will be of interest to determine if changes in the channel-opening (k_{open}) or channel-closing (k_{close}) rate constants confirm this hypothesis.

In addition to suggesting that DHPMs potentiate $GABA_A$ receptors by shifting the channel-opening equilibrium to increase receptor currents, our data also supports the increasing amount of literature describing GABA as a partial agonist for δ subunit-containing $GABA_A$ receptors (*6, 8, 143-145*). DHPMs seem to increase the efficacy of GABA to open $GABA_A$ receptor channels while not changing receptor affinity for GABA. As previously suggested (*143*), the modulation of GABA efficacy on δ subunit-containing $GABA_A$ receptors may be an important attribute of tonic currents used to regulate neuronal excitation. Taking this one step further, selective modulation of $GABA_A$ receptor subtypes involved with tonic inhibition may yield additional levels of regulation and control. It is interesting that of the receptor subtypes potentiated by DHPMs (α1β2δ, α1β3δ, α4β2, α4β2δ, α5β2δ and α6β3δ), the α4- and α6 subunit-containing receptors are modulated to a lesser extent than other subtypes, even though α4 and α6 are currently thought to be the predominant partnering subunits of the δ subunit in the CNS (*6*). These results, in addition to the colocalization of various GABA subunits with the δ subunit in immunocytochemical distributions in the rat brain (*48*), support the idea that less abundant minor receptor subtypes may still be functionally relevant. In fact, the α1β2δ

receptor subtype, while not a predominant subtype in much of the CNS, has been reported as a significant subtype in specific hippocampal interneurons (*6*) and was described as a silent receptor unless in the presence of modulators such as the neurosteroid THDOC (*6*). The increased efficacy of GABA on minor receptor subtypes in the presence of DHPMs and other potentiating compounds suggests that less abundant endogenous receptor subtypes in the nervous system may be selectively modulated to play a significant role in regulating tonic conductance of neurons.

The potentiation efficacy of JM-II-43A and monastrol on α1β2δ receptor currents is comparable to that of phenobarbital and tracazolate (Figure 2.6D). Phenobarbital, which was reported to potentiate α1β2γ2L receptors ~ 1.5-fold (*2*), has higher efficacy on α1β2δ receptors, increasing maximum currents by 2.5-fold. Although tracazolate was reported to potentiate α1β2δ currents by ~ 23-fold when co-applied with 100 μM GABA to *X. laevis* oocytes (*145*), it increased by only ~ 1.5-fold the whole-cell currents evoked by 1 mM GABA from α1β2δ receptors expressed in HEK293T cells reported here. At saturating GABA concentrations 10 μM tracazolate was reported to potentiate α2β3δ receptors expressed in HEK293 cells by approximately 2.7-fold (*241*) and α1β1δ receptors expressed in *X. laevis* oocytes by 2-fold (*172*), which both more closely resemble the results reported here for α1β2δ receptors. These reported differences in the degree of potentiation by tracazolate support previous suggestions that the expression system may affect the degree of potentiation observed for $GABA_A$ receptor currents (*144*). However, the direct comparison of potentiation efficacy of JM-II-43A, monastrol, tracazolate and phenobarbital with saturating GABA concentrations in HEK293T cells

(Figure 2.6D) demonstrates that these molecules all increase the efficacy of GABA on α1β2δ receptors to a similar extent.

JM-II-43A seems to only increase α1β2δ receptor currents without changing the other properties of the observed current. However, the effects of monastrol on α1β2δ receptors are clearly more complex as the application of 1 mM monastrol causes not only an increase in the overall current amplitude but also the appearance of both a desensitizing phase in the current response and a large rebound current at the end of the application period (inset, Figure 2.4B). It is not clear how this compound may be causing these features other than to suggest that the compound stabilizes both a conducting and a non-conducting state.

Monastrol was originally identified as a kinesin inhibitor (*242*) and because of this the activity of monastrol on $GABA_A$ receptors may raise questions as to the specificity of DHPMs and their future as a potential therapeutics. Monastrol itself is a very specific inhibitor of kinesin Eg5, with a subsequent report showing that the single change of its sulfur atom to an oxygen atom results in the loss of kinesin inhibition (*243*). Various DHPMs have biological activity in several other contexts as well, including modulation and inhibition of calcium channels (*244*). DHPMs that modulate calcium channels were discovered in the process of making derivatives and compounds structurally related to nifedipine and nifedipine-like dihydropyridines (*245, 246*), compounds that are therapeutically used as vasodilators, antianginals and antihypertensives. In this report JM-II-43A was primarily examined for modulation of specific GABA receptor subtypes. However, we have also tested this DHPM on recombinant GluN1N2A NMDA receptors and recombinant α4β2 nicotinic acetylcholine receptors

(nAChRs) separately and transiently expressed in HEK293T cells. It was also tested on endogenous muscle-type nACh receptors of the BC_3H1 cell line. At 1 mM concentrations of JM-II-43A coapplied with 10 μM glycine/100 μM glutamate there was no observed effect of the compound on the NMDA receptor currents. In contrast, both α4β2 and muscle-type nAChRs were inhibited ~ 90% when 1 mM of JM-II-43A was coapplied with 100 μM carbamoylcholine. These results were not entirely unexpected as many barbiturates are known antagonists of nAChRs (*247, 248*), including pentobarbital (one of the barbiturates this class of DHPMs was modeled after, Figure 2.2A), which has a reported EC_{50} of 32 μM using the endogenous receptors of BC_3H1 cells (*248*). With all this in mind, monastrol and the other DHPMs presented in this report may not be directly relevant for therapeutic use. However, they do display $GABA_A$ receptor subtype specificity that will make them good tools for the study of $GABA_A$ receptors. Furthermore, modifications of these compounds may yield molecules that retain the ability to modulate specific $GABA_A$ receptor subtypes while making the molecules more selective for $GABA_A$ receptors than the DHPMs examined here. Such molecules would undoubtedly be desirable developments for therapeutic purposes.

Chemical libraries of DHPMs are readily synthesized through a multi-component Biginelli reaction (*17*) and afford access to a range of molecules having promising biological applications (*244, 249*). The accessibility of DHPM derivatives and our results showing selectivity for potentiation of α1β2δ $GABA_A$ receptors, suggest that DHPM derivatives should be useful as biological tools and may be helpful for developing future therapeutic agents to target $GABA_A$ receptor isoforms containing the δ subunit.

CHAPTER 3

DETERMINING THE MECHANISM OF DIHYDROPYRIMIDINONE POTENTIATION OF δ SUBUNIT-CONTAINING $GABA_A$ RECEPTORS

Abstract

Neuronal signaling within the mammalian central nervous system is regulated and repressed primarily by gamma-aminobutyric acid receptor ($GABA_A$ receptors) ligand-gated chloride channels (*19, 20, 227*). Understanding how small molecules, such as endogenous neurosteroids and therapeutic compounds, modulate these receptors on a mechanistic level reveals how these receptors function and leads to new approaches for the design and discovery of new therapeutic compounds. Recently, a small family of dihydropyrimidinones (DHPMs) were discovered that modulate $GABA_A$ receptor subtypes containing the δ subunit (*163*). The DHPM JM-II-43A showed a ~ 3-fold increase in GABA-activated whole-cell current measurements obtained from recombinant α1β2δ receptors expressed in HEK289T cells. Based on the structural resemblance of DHPMs to barbiturates, it was speculated that these compounds modulate α1β2δ $GABA_A$ receptors in a similar fashion by altering k_{open} and/or k_{close}. However, we report here evidence that suggests an alternate and novel mechanism of action. Single-channel current measurements were employed to examine the mean open-channel time of the receptor to estimate the rate of channel closing (k_{close}) and the channel conductance, but no changes in these parameters were observed in the presence of JM-II-43A. The flash-

photolysis technique was use with photolabile RuBi-caged GABA to measure the rate constant of channel opening (k_{open}) and the rate constant of channel closing, but no change in the rate constants in the presence of JM-II-43A and GABA as compared to GABA alone was indicated. Instead, multi-channel patch clamp experiments strongly suggest that these compounds potentiate whole-cell receptor currents by increasing the population of $GABA_A$ receptors that are sensitive to the presence of GABA. In the presence of 1 mM JM-II-43A, large membrane patches containing a population of channels show a 2.5 to 5 -fold increase in currents and result in an increased frequency of channel stacking. These studies have led to a new general mechanism for $GABA_A$ receptors that includes an equilibrium between an active and inactive receptor state before agonist binds to the receptor.

Introduction

The super family of cys-loop ligand-gated ion channel receptors are critical for the transmission of signals between neurons within the central nervous system (CNS) (*19, 20, 53, 250*). These receptors stimulate or repress neuronal signaling depending upon the ions they permit to flux across the neuronal plasma membrane. The most well characterized of the cys-loop receptor super family are nicotinic acetylcholine receptors (nAChRs), which have been studied since the discovery in 1957 that acetylcholine can stimulate neuronal and muscle excitation (*12, 22*). The binding of acetylcholine to nAChRs induces a conformational change in the receptor structure that opens a cation-selective channel, facilitating the flux of sodium and calcium into a neuron. This cation flux depolarizes the

neuron membrane potential to stimulate an excitatory response known as an action potential. Another family of cys-loop receptors is γ-aminobutyric acid GABA type-A ($GABA_A$) receptors, which operate in a similar manner when binding the ligand γ-aminobutyric acid (GABA). However, these receptors open a chloride and bicarbonate selective channel, which represses action potentials in the neuron by hyperpolarizing the membrane potential. $GABA_A$ receptors, in particular, are thought to be the primary ion channels that regulate and repress signal transmission in the CNS.

$GABA_A$ receptors, nAChRs, serotonin receptors ($5\text{-}HT_3$, cation selective) and glycine receptors (GlyRs, anion selective) have originated from a distant ancestral ligand-gated ion channel (*52, 53*). Thus, these receptors have many similarities in their structure and function in spite of their different agonists and their opposing effects on neuronal excitation. Cys-loop receptors are pentameric and are composed of a variety of different subunits, which allow for a large diversity of receptor subtypes. The $GABA_A$ receptor specifically can form pentamers composed of combinations of 19 subunits in the human genome (α1-6, β1-3, γ1-3, δ, ε, θ, π, and ρ1-3) (*20, 43*). Even though these receptors are typically composed of at least two α and two β subunits, there exist a large number of possible receptor subtypes.

The various subunits incorporated into a $GABA_A$ receptor determine the receptor localization, pharmacology, biophysical properties, and cellular roles in the CNS (*21, 139, 170, 228*). In contrast to $GABA_A$ receptor subtypes containing γ subunits that are localized at synapses and have a phasic role in signal transmission, receptors containing the δ subunit are located peri- and/or extra-synaptically and are thought to have an important

role in regulating neurotransmission through tonic inhibition (*49, 145, 170*). In addition, $GABA_A$Rs containing the δ subunit have much shorter mean-open times, lower whole-cell current amplitudes when expressed *in vitro*, a higher affinity for GABA, a greater response to receptor modulators such as THDOC and other progesterone derivatives, and do not desensitize. It is thought that these properties play an important role in neuronal modulation by generating extra-synaptic tonic chloride conductances that arise from extra-synaptic $GABA_A$ receptors responding to low levels of environmental GABA. The mechanism of $GABA_A$ receptors containing the δ subunit has been investigated and the lack of receptor desensitization observed for these receptors is thought to contribute to their function as extrasynaptic tonic conducting receptors. In addition it has been shown that residues in the second transmembrane region within the δ subunit are responsible for this lack of desensitization and lower observed current (*251*). However, it has not been revealed mechanistically how this region alters the mechanism to result in a lack of desensitization.

A significant amount of literature has suggested that GABA acts as only a partial agonist of δ subunit-containing $GABA_A$ receptors of various subtypes (*6, 8, 143-145, 163, 176*) and that small molecules are likely important for the modulation of receptor function *in vivo*. However, the mechanism for how δ subunit-containing $GABA_A$ receptor currents are modulated has not been established.

Recently we reported the discovery of a family of dihydropyrimidinone small molecules that preferentially increase whole-cell currents of δ subunit-containing $GABA_A$Rs recombinantly expressed in HEK293T cells. It was proposed that these small molecules preferentially

bind to and stabilize the open-channel state of the receptors to alter the rate constants of channel-opening or channel-closing, a mechanism similar to modulation by the structurally similar barbiturate phenobarbital. There are, however, several alternative ways that DHPMs may alter the mechanism of α1β2δ receptors to potentiate whole-cell currents: by increasing the binding affinity of the receptor for GABA, altering the conductance of the ion channels, increasing the number of receptors responding to GABA, or changing the rate of receptor desensitization. The last possibility is unlikely, as receptors containing the δ subunit characteristically have little or no desensitization (*145, 170, 175*). Additionally, it was previously determined that the affinity of the receptor for GABA (K_1) is not altered (*163*).

Here we examine each of three remaining possible mechanisms that may explain how DHPMs yield an observed ~ 3-fold increase in whole-cell current conductance, using single-channel, multi-channel (large- or macro-patch) measurements, and flash-photolysis studies. Surprisingly, these studies demonstrate that the mechanism of action for DHPMs is different than that of barbiturates. Our results strongly suggest that DHPMs act by increasing the number of receptors that are in an active or 'ready' state to respond to the presence of GABA, as the number of receptors responding to GABA is greater in the presence of JM-II-43A than in the presence of saturating GABA concentrations alone. Not only does this mechanism describe the ability of modulators like DHPMs to potentiate whole-cell currents, but it also explains why δ subunit-containing receptors have several of their characteristic features, such as a lack of desensitization. In addition, this new perspective on the $GABA_A$ receptor mechanism may generally apply to all $GABA_A$ receptor subtypes.

Methods and Materials

Reagents, Synthesis and Preparation of Dihydropyrimidinones

JM-II-43A was synthesized as previously described (*17*) and Ruthenium-bipyridine-triphenylphosphine (RuBi) caged GABA was purchased from Tocris (Ellisville, MO). All other reagents were obtained from Sigma Aldrich, Fisher Scientific, or EM Sciences. JM-II-43A was dissolved in pure anhydrous DMSO (to aid compound solubility in buffer), then diluted 1:200 with extracellular buffer at a temperature of 65 °C to make a solution of 2 mM JM-II-43A in 0.5 % DMSO. A concentration of 0.5% DMSO had no observed effect on $GABA_A$ receptors. Room temperature solutions of 2 mM JM-II-43A were diluted and used as needed. Serial dilutions of a frozen (-20 °C) 100 mM GABA stock were used to make all GABA solutions.

Cell Culture and Transient Transfection

HEK293T cells, obtained from the American Type Culture Collection (ATCC) (Manassas, VA), were grown at 37 °C with 5 % CO_2 in Dulbecco's Modified Eagle's Medium (DMEM) containing 10 % fetal bovine serum (FBS), 100 units/mL penicillin and 0.1 mg/mL streptomycin. Professors H. Lüddens (Johannes Gutenberg - Universität, Mainz, Germany) and P. H. Seeburg (Max-Plank-Institut für medizinische Forschung, Heidelberg, Germany) kindly provided the cDNAs encoding the rat $GABA_A$ receptor α1, β2, and γ2L subunits in the mammalian pRK-5 expression vector. The rat $GABA_A$ receptor cDNA for the δ subunit in a pExpress-1 mammalian expression vector was obtained from ATCC. A plasmid containing cDNA for pGreen Lantern (Life Technologies Inc., Gaithersburg, MD) was used as

a marker for transfected cells. Cells were transfected with 4 μg total of plasmid DNA, with plasmid ratios of 1:1:10:0.1 for α:β:δ:pGreen Lantern cDNAs to bias the expression of the δ subunit relative to α and β subunits. For whole-cell current recordings, δ subunit-containing receptors were clearly identifiable by a characteristic lack of receptor desensitization. Polyethylenimine (PEI) (Polysciences Inc. Warrington, PA) was used for transient transfection of cells as reported (*235*) with a PEI:DNA ratio of 4:4 (μg:μg) with medium being replaced after 4-7 hours with fresh DMEM/10 % FBS. Cells were used 24 to 48 hrs. after transfection.

Rapid Solution Application

The previously described cell-flow technique(*18*) was used for the rapid application of solutions to membrane patches or cells used in electrophysiological measurements.

Electrophysiology Measurements.

Whole-cell current recordings were obtained from individual cells in a whole-cell configuration lifted from the bottom of a 35 mm cell culture dish with a borosilicate glass pipette and suspended in extracellular buffer composed of 145 mM NaCl, 5 mM KCl, 2 mM $CaCl_2$, 1.5 mM $MgCl_2$, and 10 mM HEPES (4-(2-hydroxyethyl)-1-piperazineethanesulfonic acid) at pH 7.4 attained with 5 N NaOH. Borosilicate glass capillaries with a 1.5 / 1.12 mm outer / inner diameter (World Precision Instruments Inc., Sarasota, FL) were pulled with a vertical pipette puller and heat-polished on a microforge to make recording pipettes with open-end resistances of 3.0-5.0 MΩ. Intracellular solution backfilled into the pipettes was composed of 140 mM

CsCl, 10 mM tetraethylammonium chloride, 10 mM EGTA (ethylene glycol bis (β-aminoethyl ether)-*N, N, N', N'* tetraacetic acid), 2 mM $MgCl_2$, and 10 mM HEPES brought to pH 7.4 with 5 N CsOH. Whole-cell patches were voltage clamped at – 60 mV. An Axopatch 200B amplifier, Digidata 1322A digitizer and Clampex 9.0 software (Molecular Devices, Sunnyvale, CA) were used for recording whole-cell currents at a sampling frequency of 50 kHz with Bessel filtering at 5 kHz as previously described by Hamill *et al.* (*186*).

Single-channel and multi-channel outside-out patches were obtained largely as described above with a few alterations. The borosilicate glass pipettes with open tip resistances of 5-10 MΩ were made from capillaries with a 1.5 / 0.84 mm outer / inner diameter. Single-channel and multi-channel membrane patches were voltage clamped at -80 mV, sampled at 250 kHz and Bessel filtered at 10 kHz. Signals were later digitally low-pass filtered at 1.5 kHz.

Flash-photolysis Measurements

Current measurements for flash-photolysis were carried out using Ruthenium-bipyridine-triphenylphosphine (RuBi) caged GABA, a photolabile caged GABA derivative, and cells expressing α1β2δ $GABA_A$ receptors in a whole-cell patch-clamp configuration, voltage clamped at -60 mV as previously described (*252*). Briefly, solutions of 20 μM RuBi caged GABA with or without 1 mM JM-II-43A were applied to a cell using the cell-flow technique. An optical fiber with an internal diameter of 600 μm directed a flash of light generated by a Rapp xenon flash lamp (SP-20) (Rapp OptoElectronic GmbH, Wedel, Germany) onto the cell in a whole-cell configuration. The flash of light was filtered with a 385-450 nm band-pass

filter. The flash of visible light causes the photolytic cleavage of the RuBi caged GABA to rapidly release free GABA neurotransmitter. Because RuBi caged GABA is visible light-sensitive, all experiments were conducted under dark room red lights. A saturating 1 mM GABA solution applied with the standard cell-flow method was used as a control for normalization of all current amplitudes from cell-flow and flash-photolysis measurements obtained with a single cell.

Data Analysis

Current amplitudes from various whole-cell patches were normalized by dividing all measurements by the current amplitude evoked by a 1 mM GABA control measurement (I_A / $I_{Control}$). A single exponential equation

$$I(t) = \sum A_1 e^{-t/\tau_1} \qquad [3.1]$$

was fit to the current rising-phase of all flash-photolysis measurements using non-linear regression, conducted with Origin V. 3.5 data analysis software (OriginLab Corp., Northampton, MA). The observed current rise rate constant (k_{obs}) is equal to $1/\tau_1$. Because k_{obs} can be described as

$$k_{obs} = k_{close} + k_{open}([L]/([L]+K_1))^2 \qquad [3.2]$$

as previously reported (*199*), a linear regression is used to fit the values of k_{obs} *versus* $([L]/([L]+K_1))^2$ to obtain values for k_{open} and k_{close}. The values are reported with relative standard errors. The values of [L] were obtained by comparing the peak current evoked by photolysis of RuBi caged GABA to a dose-dependent curve of GABA applied to α1β2δ $GABA_A$ receptors using the cell-flow method previously reported (*163*), in Chapter 2. The value for K_1 also comes from the dose-dependent curve of GABA previously reported (*163*), in Chapter 2.

Single-channel events were identified individually with the assistance of Clampex 9.0 software (Molecular Devices, Sunnyvale, CA) and used to generate histograms of the dwell-times (channel open time) and current amplitudes of the events. Following standard methods (*13, 14*), the square root of the number of events per bin was used to generate a dwell-time histogram. These histograms were fit with a two component, logarithmic exponential function (*13, 14*) using non-linear regression. The fit required two exponential components, one of which fit greater than 85% of the area of the histogram. The value of the tau time constant for this component was used for computing k_{close}, by the relationship ($1/\tau = k_{close}$).

Results

As was previously reported, JM-II-43A and the other DHPMs tested potentiate α1β2δ receptor currents up to ~ 3 fold that of currents evoked by saturating concentrations (1 mM) of GABA alone (*163*). While the mechanism of action was not known, dose-dependent measurements were made at high (1 mM) and low (3 μM) GABA concentrations to obtain apparent dissociation constants for JM-II-43A (${}^{*}K_{JM\text{-}II\text{-}43A}$) for the open-channel state and closed-channel state of the receptor, respectively. This data yielded ${}^{*}K_{JM\text{-}II\text{-}43A}$ values of 400 μM for the open-channel state and 800 μM for the closed-channel state, suggesting that these molecules may act by binding to and stabilizing the open-channel state of the receptor. This would result in changes to the rate constants of channel-opening (k_{open}) and channel-closing (k_{close}), therefore directly affecting the open-channel equilibrium constant (Φ^{-1}). To investigate this possibility, both flash-photolysis (laser-pulse photolysis) and single-channel current measurements

were made and analyzed from α1β2δ $GABA_A$ receptors in the absence and presence of JM-II-43A.

Flash-photolysis Data Shows JM-II-43A Does Not Change $GABA_A$ Receptor Rate Constants of Channel Opening and Closing

Current measurements of HEK293T cells transiently expressing recombinant α1β2δ $GABA_A$ receptors were made for current responses evoked by 1 mM saturating GABA concentration using whole-cell patch clamping and the cell-flow solution application technique. These measurements were used for current normalization between cells. These control measurements were followed by flash-photolysis measurements. αCNB caged GABA (*226*), which has been used previously with α1β2γ2L $GABA_A$ receptors (*1, 2, 225, 253*), was found to significantly inhibit α1β2δ $GABA_A$ receptor subtypes at concentrations needed for flash-photolysis (data not shown). Instead, the visible-light-sensitive RuBi caged GABA was utilized for flash-photolysis measurements. The RuBi caged GABA was used at a maximum concentration of 20 μM, as photolysis of RuBi caged GABA solutions at higher concentrations resulted in an observed inverse-agonist modulation (or inhibition) of the receptor current, likely due to photolytic byproducts, in agreement with previous reports (*218, 254*). The amount of free GABA released from the RuBi-GABA was controlled by changing the intensity of the pulse of light from the Rapp flash-lamp. By varying the amount of GABA released, different concentrations of GABA could be used to observe different current amplitudes and observed rate constants (k_{obs}) for the current rising phase. The peak amplitudes of the evoked current were compared to a GABA dose-response curve to estimate

the concentration of GABA photolytically released. Values for k_{obs} were obtained by fitting the current rising phase with the standard single exponential function, equation [3.1], as shown in Figure 3.1. The concentration of GABA released and the values of k_{obs} were used to determine the rate constants of channel opening (k_{open}) and closing (k_{close}) by plotting k_{obs} *versus* $([L]/([L]+K_1))^2$ and fitting the data with the linear relationship described by equation [3.2], as shown in Figure 3.1C. The data demonstrates no significant change in k_{open} and k_{close}. Values for k_{open} and k_{close} are 150±5.0 and 16±0.45 in the absence of 1 mM JM-II-43A and 110±4.6 and 15±0.51 in the presence of 1 mM JM-II-43A. While the values for k_{open} are statistically different ($p<0.001$ as evaluated by a Welch's two way t-test assuming unequal variance, using an $\alpha=0.05$ and with 47 degrees of freedom (d.f.) in the analysis), the difference is only a 1.3 fold change in the rate of receptor opening, not enough to account for the 3 fold increase in current observed in whole-cell measurements. The values of k_{close} were statistically not different ($p=0.10$, Welch's two way t-test, $\alpha=0.05$, d.f.=47).

Single-channel Data Reveals no Change in Rate Constants of Channel Closing or Channel Conductance

Patches containing single α1β2δ $GABA_A$ receptors were voltage clamped at -80 mV and monitored for 30+ minutes while in the presence of 3 μM GABA with or without 1 mM JM-II-43A, Figure 3.2. These concentrations of GABA were chosen, because a greater degree of current potentiation (~ 4.5 fold) was previously observed for channels in the presence of low 3 μM GABA with 1 mM JM-II-43A compared to saturating 1 mM GABA with JM-II-43A (~ 3 fold) (*163*). Thus, changes in receptor

Figure 3.1 Flash-photolysis methods indicate no apparent change in the rate constants of opening (k_{open}) or closing (k_{close}) for α1β2δ receptors. Whole-cell patched HEK293T cells transiently expressing recombinant receptors were used for flash-photolysis measurements using solutions containing 20 μM RuBi caged GABA with or without 1 mM JM-II-43A. **A.** Shown is the first 100 ms of the rising-phase from a current evoked by the photolysis of 20 μM RuBi caged GABA from a whole cell patch (green line). **B.** Shown here is the first 100 ms of the rising-phase from a current evoked by the photolysis of 20 μM RuBi caged GABA in the presence of JM-II-43A (red line) using the same flash intensity and from the same whole cell patch as in **A**. Equation 3.1 was fitted to the rising phase of the current trace of all flash-photolysis currents (black lines in **A** and **B**) to obtain the first-order rate constant (k_{obs}) for the current rising phase. The observed rate constant is defined as $k_{obs} = k_{close} + k_{open}([L]/([L]+K_1))^2$, thus by plotting k_{obs} against $([L]/([L]+K_1))^2$ the values for k_{open} and k_{close} are the slope and y-intercept, respectively. **C.** The values of k_{obs} are plotted against $([L]/([L]+K_1))^2$, resulting in k_{open} values of 150±5.0 s^{-1} and 110±4.6 s^{-1} in the absence and presence of JM-II-43A, respectively, and k_{close} values of 15.6±0.45 s^{-1} and 14.4±0.51 s^{-1} in the absence and presence of JM-II-43A, respectively. k_{open} values were statistically different ($p<0.001$, Welch's two way t-test, $\alpha=0.05$, d.f.=47), but the values of k_{close} were not statistically different ($p=0.10$, Welch's two way t-test, $\alpha=0.05$, d.f.=47). Twenty five measurements were obtained for both the presence and absence of 1 mM JM-II-43A using 7 independent cells. Measurements were made at ambient temperature (~ 22 °C) with extracellular and intracellular buffers of pH 7.4. Currents were sampled at 50 kHz and low-pass filtered at 5 kHz.

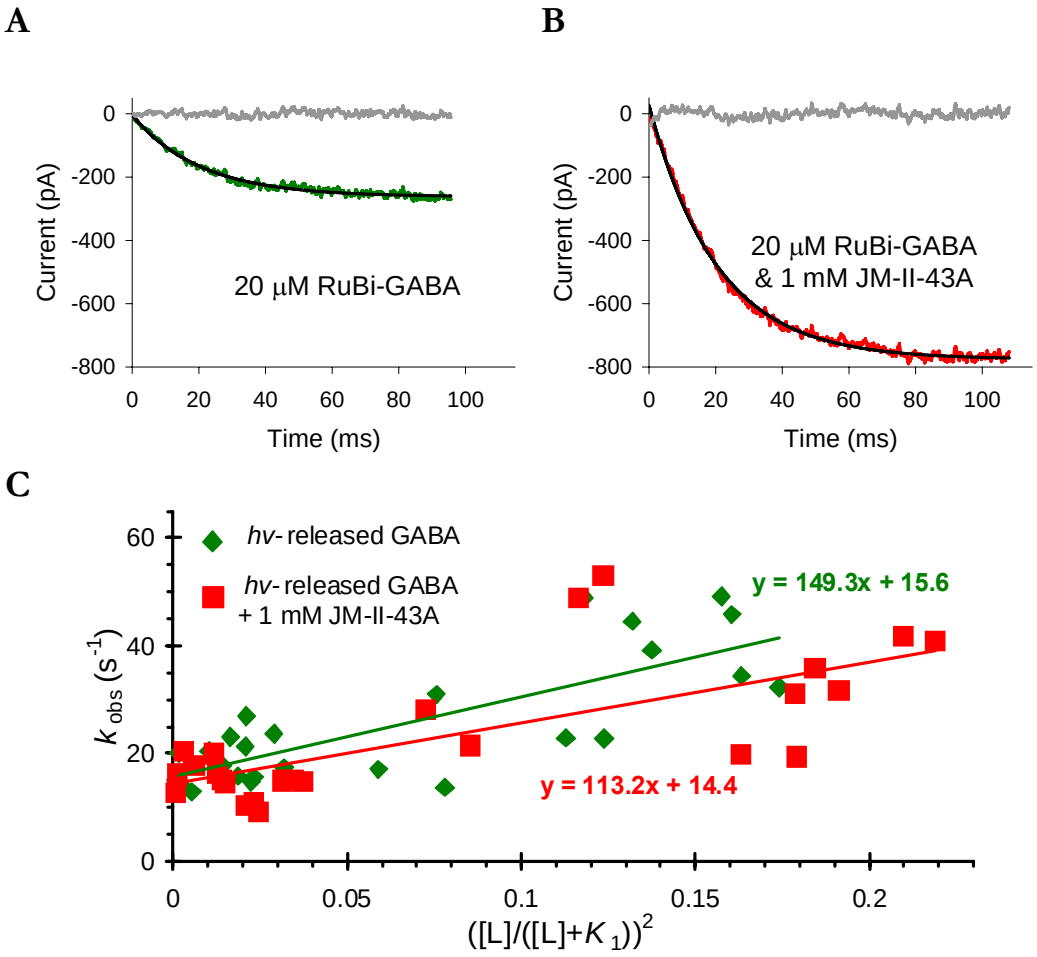
A
B
C
Current (pA)
Time (ms)
20 μM RuBi-GABA
20 μM RuBi-GABA
& 1 mM JM-II-43A
hv-released GABA
hv-released GABA
+ 1 mM JM-II-43A
y = 149.3x + 15.6
y = 113.2x + 14.4
k obs (s-1)
([L]/([L]+K 1))2

Figure 3.2 Single-channel measurements of α1β2δ $GABA_A$ receptors obtained from two separate single-channel patches show no change in channel conductance or mean-open time in the presence of 1 mM JM-II-43A. **A.** A single-channel patch from an HEK293T cell expressing α1β2δ $GABA_A$ receptors measured in the presence of 3 μM GABA. **B.** A single-channel patch from an HEK293T cell expressing α1β2δ $GABA_A$ receptors α1β2δ $GABA_A$ receptors measured in the presence of 3 μM GABA with 1 mM JM-II-43A. The patches were recorded for 30+ minutes. A total of 18673 channel-opening events were counted for **A** and 8965 events for **B**. The regions of the current traces have been selected to show events that contain longer than average open-channel dwell times to better display the amplitude of current. Measurements were made from patches pulled from HEK293T cells transiently expressing recombinant receptors voltage clamped at -80 mV and measured at ambient temperature (~ 22 °C) with extracellular and intracellular buffers of pH 7.4. **C**. A histogram of the dwell-time (the period of time the receptor is in the open-channel state) for all events from patches in **A** (red) and **B** (blue). The mean open-time for channels was ~ $10^{-3.4}$s (~ 0.4 ms), for both patches with no statistical difference (p=0.79, Welch's two way t-test, α=0.05, d.f.=167). The histograms were normalized by their total area, transformed by taking the square root of the frequency density, and fit with a two component logarithmic probability function (black lines) to obtain values for time constants (τ) of the fit, as previously described (*13, 14*). A single component was able to fit > 85% of the area for both histograms and thus the value of tau for that component is used to estimate the value for k_{close}.

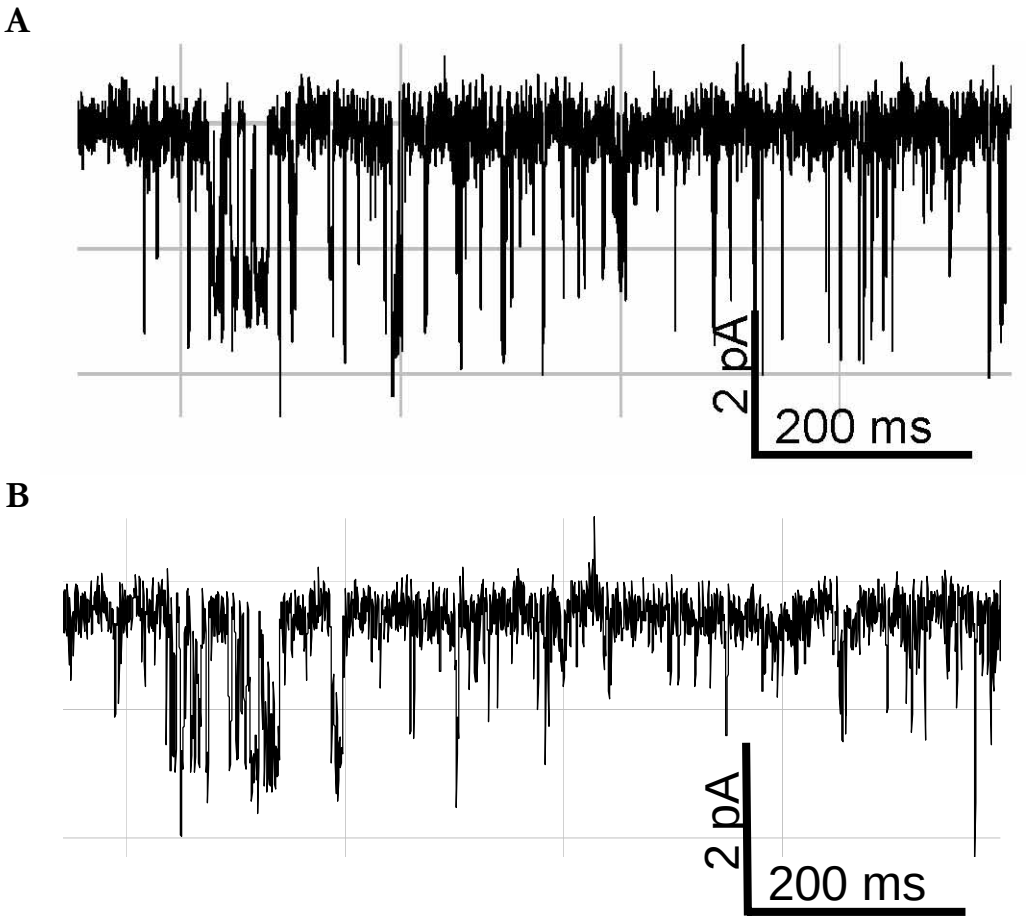
A
2 pA
200 ms
B
2 pA
200 ms
C
Sq. Rt. of Events ((N)^0.5)
30
20
10
0
-4
-3
-2
Log of Dwell Time (Log (s))
τGABA
0.57 ± 0.22 ms
kclose GABA
1750 ± 680 s-1
τGABA+JMII43A
0.48 ± 0.25 ms
kclose GABA +JMII43A
2083 ± 910 s-1

kinetics were expected to be greatest at 3 μM GABA. The channel-opening events obtained during the current traces shown were individually measured, binned into histograms and analyzed to determine channel conduction states and the average amount of time the channel was in an open-channel state (the receptor mean-open time). The regions of the current traces shown contain longer than average open-channel events to better demonstrate the channel conductances observed. In the histogram of current amplitudes generated from single-channel events, two current amplitudes of ~ 1 and 2 pA were observed in the presence and absence of 1 mM JM-II-43A, translating to channel conductances of ~ 12 and 25 pSiemens, comparable in value to those previously reported for similar δ subunit-containing receptor subtypes (*4, 170*). (These current amplitudes are also observed in the multichannel-patches discussed and shown later, in Figure 3.3 and 3.4.). The presence of JM-II-43A does not change these values, demonstrating that this DHPM does not alter channel conductance.

The histogram of open-channel dwell-times obtained (Figure 3.2C) shows mean-open times of ~ $10^{-3.4}$s or (~ 0.4 ms) for receptors in the presence or absence of 1 mM JM-II-43A. Fitting the histogram of open-channel dwell times with a logarithmic probability function (*13, 14*) was performed to determine time constants for how rapidly these channels close. The histograms shown were best fit with two exponential components, one component encompassed greater than 85% of the area of each histogram. The time constant from this predominant exponential component was used to estimate a rate constant for channel closing (k_{close}) in the presence or absence of 1 mM JM-II-43A ($k_{close\ GABA}$ =1800 ± 700 s^{-1} and $k_{close\ GABA\ +\ JM\_II\_43A}$ =2080 ± 900 s^{-1}) but showed no statistical difference

(p=0.79, Welch's two way t-test, α=0.05, d.f.=167) (Figure 3.2C) Additionally, all parameter values can be found in Table 3.1.

Multichannel Measurements Reveal the Activation of More Channels in the Presence of JM-II-43A

To determine if JM-II-43A increases the number of α1β2δ $GABA_A$ receptors that respond to GABA, a large patch (or multi-channel patch) method was used to examine a small population of α1β2δ receptors. This method is a modified version of single-channel current recording, the only difference being the use of slightly larger membrane patches to examine the behavior of several channels at a time. Figure 3.3 shows currents from three patches applied with 1 mM GABA in the absence or presence of 1 mM JM-II-43A using the cell-flow technique. The current traces from Patch I in the presence of 1 mM GABA or 1 mM GABA with 1 mM JM-II-43A from Figure 3.3 are also shown with expanded time scales to display single-channel events in Figure 3.4. As previously observed with single-channel measurements and evident here by the brief spikes in amplitude, the channel-opening events are short-lived. The potentiation of the current by JM-II-43A is clearly displayed by the large amount of current observed in the current traces. The current potentiation for each patch was quantified and is shown in the bar graphs. The potentiation was determined from a mean current amplitude during GABA or GABA and JM-II-43A application for each patch by averaging 1.5 s worth of a current trace from three separate measurements under each condition.

If more channels are responding to GABA, yet no change in kinetic parameters is observed, then it is predicted that there must be an increased

Table 3.1 Table of all parameters measured with whole-cell and single channel patch-clamping as well as flash-photolysis methods. Whole-cell data is from Chapter 2.

conditions	technique	K_1 (pA)	Φ^{-1}	k_{open} (s^{-1})	k_{close} (s^{-1})	g (pSiemens)
α1β2δ	whole-cell	7.0 ± 1.5	4.3 ± 0.8	-	-	-
	single-channel	-	-	-	1750 ± 680	~12 and 25
	flash photolysis	-	9.6 ± 5.0	150 ± 5.0	16 ± 0.45	-
α1β2δ with JM-II-43A	whole-cell	9.9 ± 1.1	5.4 ± 0.6	-	-	-
	single-channel	-	-	-	2080 ± 910	~12 and 25
	flash photolysis	-	7.8 ± 4.6	110 ± 4.6	15 ± 0.51	-

Figure 3.3 JM-II-43A increases the current amplitude of a small population of $GABA_A$ receptors in a large outside-out membrane patch. Shown are current traces evoked from three large outside-out patches containing multiple α1β2δ $GABA_A$ receptors by application of 1 mM GABA or 1 mM GABA with 1 mM JM-II-43A. The mean current amplitude evoked by coapplication of 1 mM GABA with 1 mM JM-II-43A from these patches was 2.6- to 5.2-fold those of the currents evoked by 1 mM GABA on the same membrane patches (bar graphs). Mean current amplitudes shown in the bar graphs were obtained by averaging the current amplitude over 1.5 s for three independent current traces under both conditions from the same membrane patch. All mean currents measured in the presence of 1 mM JM-II-43A were significantly increased (*) with p-values <0.001 using Welch's two way t-test with an α=0.05. Solutions were applied to the patch using the cell-flow technique. The current traces from Patch I in this figure are also shown in Figure 3.4 with an expanded time scale to show single-channel events. Measurements were made from patches pulled from HEK293T cells transiently expressing recombinant receptors, at ambient temperature (~ 22 °C) with extracellular and intracellular buffers of pH 7.4. Currents were sampled at 250 kHz and digitally filtered at 1.5 kHz.

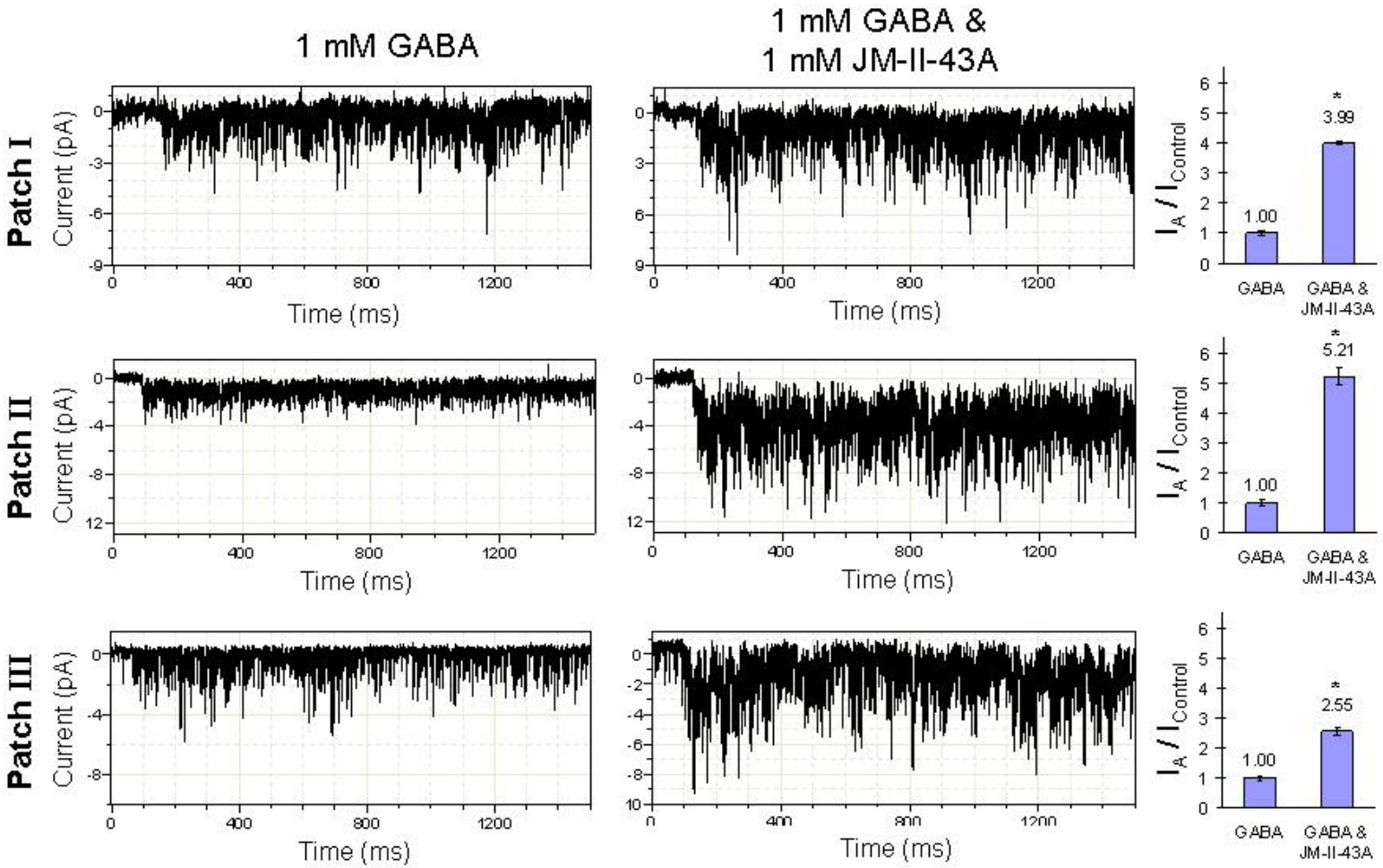
1 mM GABA
1 mM GABA &
1 mM JM-II-43A
Patch I
Patch II
Patch III
Current (pA)
Time (ms)
I_A / I_Control
1.00
3.99
5.21
2.55
GABA
GABA & JM-II-43A

Figure 3.4 JM-II-43A increases the number of α1β2δ channels in a population of receptors that open at the same time. **A.** The current traces from Patch I in the presence of 1 mM GABA from Figure 3.2 are shown with an expanded time scale to display channel-opening events. As discussed in the text, these channel-opening events are short-lived as evident here by the brief spikes in amplitude. To examine the frequency of event stacking, amplitudes of the channel-opening events in three current traces from the same conditions were measured and binned to compile the histograms shown. The histogram displays events binned according to current amplitudes, showing densities of events roughly every 1 pA (arrows). Events with amplitudes greater than 1 or 2 pA are likely from channel 'current stacking', *i.e.* channels opening at the same time. **B.** The current trace from Patch I in the presence of 1 mM GABA with 1 mM JM-II-43A is shown with an expanded time scale. The event amplitudes were measured and binned in the same manner as in **A** from three current measurements under the same conditions. The observed increase in events with larger amplitudes in the presence of 1 mM GABA with 1 mM JM-II-43A, suggest a greater degree of 'current stacking'. Measurements were made from patches pulled from HEK293T cells transiently expressing recombinant receptors at ambient temperature (~ 22 °C) with extracellular and intracellular buffers of pH 7.4. Currents were sampled at 250 kHz and digitally filtered at 1.5 kHz.

A

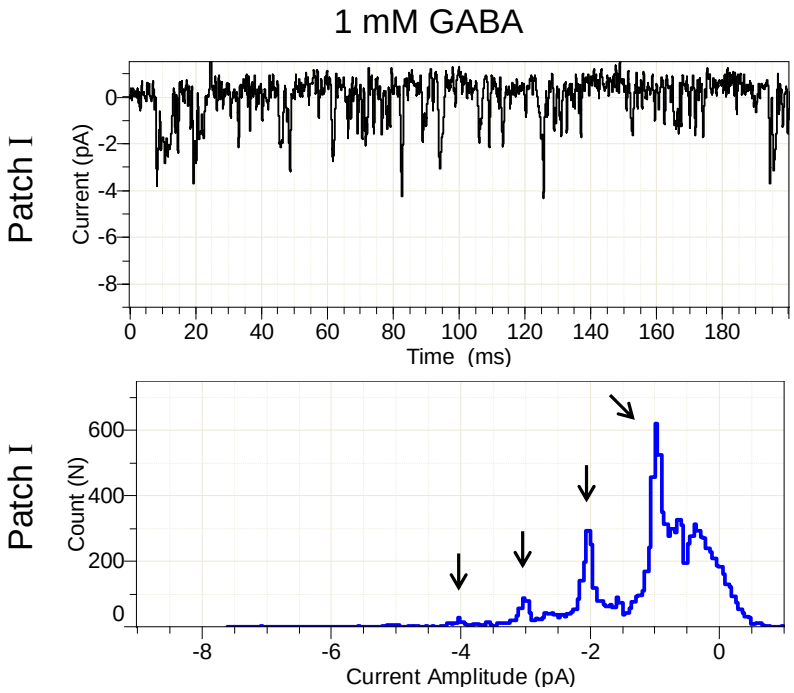
1 mM GABA
Patch I
Current (pA)
0
-2
-4
-6
-8
0
20
40
60
80
100
120
140
160
180
Time (ms)
Patch I
Count (N)
600
400
200
0
-8
-6
-4
-2
0
Current Amplitude (pA)

B

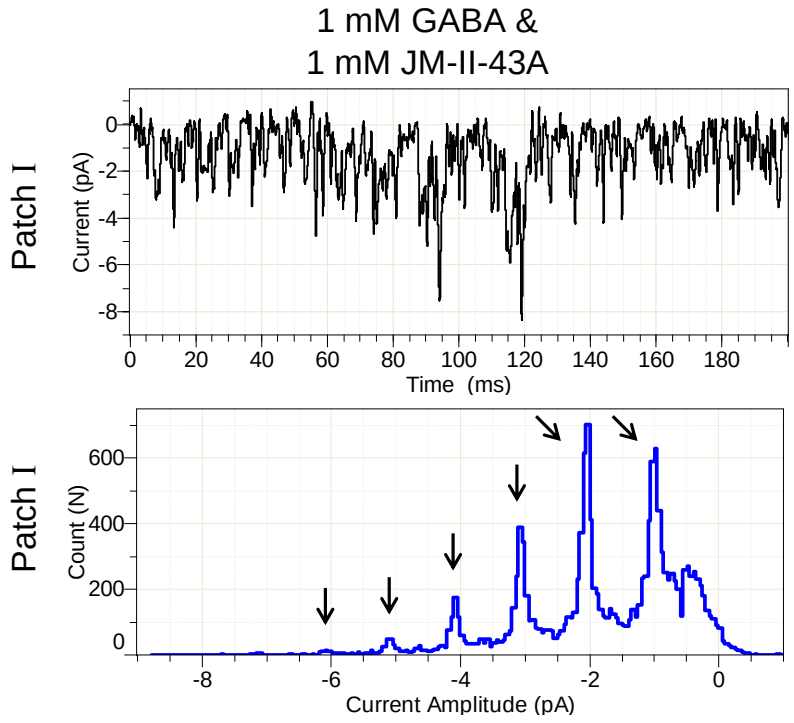
1 mM GABA &
1 mM JM-II-43A
Patch I
Current (pA)
0
-2
-4
-6
-8
0
20
40
60
80
100
120
140
160
180
Time (ms)
Patch I
Count (N)
600
400
200
0
-8
-6
-4
-2
0
Current Amplitude (pA)

frequency of current stacking (i.e. events where two or more receptors open at the same time). In the expanded current trace from Patch I, this is visible as spikes in current of greater amplitude in the presence of JM-II-43A compared to GABA alone (Figure 3.4). To quantify the frequency of current stacking observed, all event amplitudes were measured and events were binned into an amplitude histogram for traces obtained in the absence and presence of JM-II-43A, shown in Figure 3.4. The histograms display current amplitudes incremented roughly every 1 pA (arrows), which agrees with the two different current conductances observed in single-channel measurements of α1β2δ receptors, as previously discussed (Figure 3.1). Amplitudes greater than 1 or 2 pA are likely from channel current stacking. The increase in amplitudes observed in the presence of 1 mM GABA and 1 mM JM-II-43A suggests a greater degree of current stacking.

Discussion

Multi-channel patch-clamp recording methods used here demonstrate that JM-II-43A increases channel activity and increases the frequency that channels open simultaneously. However, single-channel measurements and flash-photolysis methods show that JM-II-43A increases channel activity and potentiates $GABA_A$ receptor currents without altering the rate constants of channel closing, the open-channel equilibrium constant or the channel conductance. It was previously demonstrated that JM-II-43A does not alter the receptor affinity for GABA (*163*). Together, these results suggest that JM-II-43A must potentiate $GABA_A$ receptor currents through an alternative mechanism. One explanation that satisfies all observed results thus far is that δ subunit-containing $GABA_A$ receptors may primarily reside in an

inactive state prior to the receptor binding agonist. The presence of this inactive receptor state can account for the large degree of receptor current potentiation typical of δ subunit-containing receptors as well as the lack of desensitization observed from these receptor subtypes. Additionally, this explains how JM-II-43A and other DHPMs may selectively increase currents from receptors containing the δ subunit.

Various techniques and methods have been used to investigate the mechanism of the super-family of cys-loop ligand-gated ion channels and have resulted in an equally diverse number of proposed mechanisms for $GABA_A$ receptors and other cys-loop receptors (*15, 27, 28, 31, 126-128*). However, underlying all these mechanisms are the fundamental features of the receptor binding agonist, undergoing a conformational change to open a channel, and desensitization; processes all described in the first cys-loop receptor mechanism proposed by Del Castillo and Katz (*22*). The Cash and Hess mechanism, Figure 3.5A (*15*), was originally proposed to describe nAChRs. Later this mechanism was shown to apply to α1β2γ2L $GABA_A$ receptors and was used to investigate picrotoxin inhibition (*225*), neurosteroid and barbiturate modulation (*2, 253*), as well as changes in the receptor function due to the K289M point mutation within the γ2 subunit linked to a heritable form of epilepsy (*1, 69*). While this mechanism excludes some aspects of receptor function, such as the different channel conduction states, its simplicity has permitted predictions regarding receptor behavior that have fit well with electrophysiological data on α1β2γ2L receptors (*1, 2, 225*)and focuses attention on the major features contributing to receptor function.

The mechanism of $GABA_A$ receptors is modulated to increase GABA

Figure 3.5 Proposed mechanisms for the function of $GABA_A$ receptors. **A.** The Cash and Hess mechanism (*15*) has been proposed based on research primarily carried out with nAChRs, and then applied to $GABA_A$ receptors. The receptors start in a non-conducting state (R) in the absence of GABA (L). Upon application of GABA, the receptors rapidly bind a first (RL) and second (RL_2) molecule of GABA and enter a rapid equilibrium with the open-channel state ($\overline{RL_2}$). The receptors in the RL_2 state slowly enter a non-conducting desensitized state (DL_2). **B.** This mechanism is largely based on the Cash and Hess mechanism with the addition of a D state that is free from bound ligand. The addition of this single state eliminates the assumption that the population of receptors starts in a 'ready' state and suggests that the population of receptors can be distributed between an inactive (GABA insensitive) state prior to the presence of GABA and a state ready to bind GABA and rapidly proceed to an open-channel state.

A

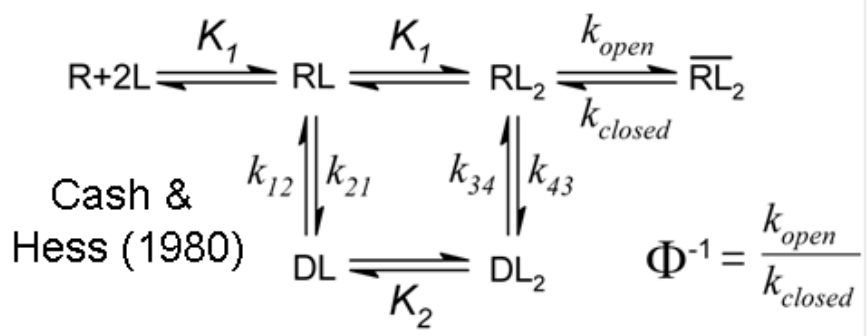
R+2L
RL
RL2
RL2
K1
K1
kopen
kclosed
k12
k21
k34
k43
Cash &
Hess (1980)
DL
DL2
K2
Φ-1 = kopen / kclosed

B

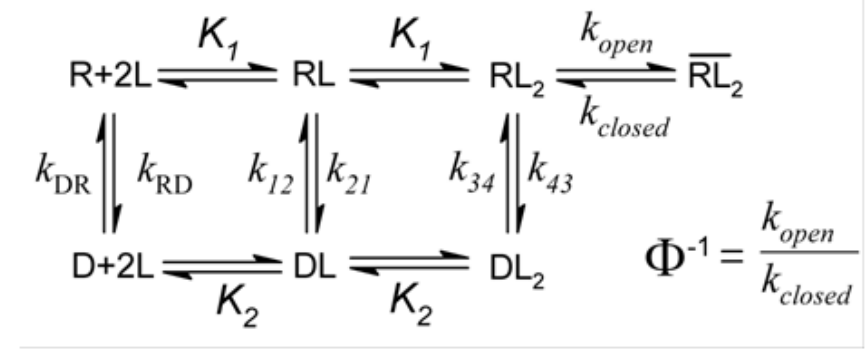
R+2L
RL
RL2
RL2
K1
K1
kopen
kclosed
kDR
kRD
k12
k21
k34
k43
D+2L
DL
DL2
K2
K2
Φ-1 = kopen / kclosed

evoked currents by a wide array of small molecules, including benzodiazepines, barbiturates, endogenous neurosteroids and many other compounds (*20, 21, 33, 139*). Several hypotheses exist as to how these compounds alter the receptor mechanism to potentiate receptor currents. Work using the Cash and Hess mechanism suggests that current inhibition and potentiation may occur through the preferential binding of compounds to the closed-channel state (inhibition) or open-channel state (potentiation) of the receptor. This preferential binding alters the open-channel equilibrium constant to increase or decrease the time that the receptor is in the open-channel state, thus changing the current amplitudes observed in whole-cell current measurements. However, compounds may also alter the receptor mechanism in different ways, such as affecting the receptor affinity for GABA, the channel conductance, or receptor desensitization. Another hypothesis, supported by an increasing amount of literature, suggests that GABA is a full agonist only on some receptor subtypes and acts as a partial agonist on others, such as δ subunit-containing receptors (*6, 8, 143-145, 163, 176*). It has been proposed that this partial agonist activity may be because GABA can readily bind to the receptor but requires the aid of additional potentiating ligands binding to the receptor to overcome the activation energy barrier to form an open-channel state, also referred to as the channel gating efficacy (*143, 144*). This mechanism in many ways is similar to that described by the research mentioned here demonstrating a shift in the open-channel equilibrium constant in the presence of modulators.

The work described here investigates the mechanism of JM-II-43A potentiation of currents from δ subunit-containing $GABA_A$ receptors, and how it does this preferentially for these specific receptor subtypes. Because

JM-II-43A has many structural similarities to the barbiturate phenobarbital, it was thought that this molecule may act on the $GABA_A$ receptor in a similar manner, *i.e.* altering the open-channel equilibrium constant (*163*). Surprisingly, single-channel current recording (Figure 3.2) and flash-photolysis (Figure 3.1) methods demonstrated that neither the receptor rate constants of opening and closing nor the receptor conductance were altered by the presence of JM-II-43A. As was previously determined, the binding affinity of the receptor for GABA was also not changed (*163*). Increases in observed whole-cell currents cannot be due to changes in receptor desensitization, as these receptors show little to no receptor desensitization. These results indicate that the increase in current observed with JM-II-43A must be due to an increase in the total number of receptors that are entering the open-channel state. This could be attained through the recruitment of more receptors to the cell surface or the presence of receptors that do not enter an open-channel state even with saturating concentrations of GABA present. Since the current potentiation induced by JM-II-43A occurs within tens of milliseconds and is rapidly reversible (*163*), the trafficking of receptors to and from the cell surface is not likely. Additionally, the potentiation by JM-II-43A observed in multi-channel patches removed from cells (Figures 3.3 and 3.4) would be impossible if receptor trafficking to the plasma membrane was the mechanism of action. However, the Cash and Hess mechanism does not account for receptors that do not respond to GABA.

The Cash and Hess mechanism makes an assumption that all receptors start in the R state, ready to bind GABA and rapidly enter into an open-channel state (Figure 3.5A). Receptors in this mechanism enter an

inactive D state (desensitized state) only after GABA is bound. This assumption may not apply to all receptors. The inclusion of an additional D state to the Cash and Hess mechanism, results in a mechanism (Figure 3.5B) that eliminates this assumption and permits a population of receptors to distribute between the active R and inactive D states before the presence of agonist. Depending upon the equilibrium between the D and R states it would be possible for the majority of receptors to start in the inactive D state ($k_{DR} > k_{RD}$). This mechanism is consistent with the current potentiation of receptors by JM-II-43A and the characteristic lack of desensitization observed in δ subunit-containing $GABA_A$ receptor currents (*145, 170, 175*).

The mechanism proposed explains how receptors containing the δ subunit can be preferentially and significantly modulated by JM-II-43A and likely other modulatory compounds (*6, 8, 145, 174, 255-257*). JM-II-43A may act by preferentially binding to and stabilizing the active R state of α1β2δ receptors. If the rate of transition between the R and D states of the receptor is faster than the rate of channel opening and closing, then preferential binding of JM-II-43A to the R state would not lead to any observed changes in the open-channel equilibrium constant (Φ^{-1}) or the channel-closing rate constant (k_{close}). Additionally, because increasing GABA concentrations lead to a greater number of receptors in an R state (this state is required for the channel to open), a binding preference of JM-II-43A for the R state *versus* the D state, should be visible by an apparent increase in binding affinity of the receptor for JM-II-43A in the presence of high GABA concentrations. All these predictions based on the new mechanism have been observed: no change in the open-channel equilibrium constant (Φ^{-1}) (Figure 3.1) or the channel-closing rate constant (k_{close})

(Figures 3.1 and 3.2) was measured with flash-photolysis and single-channel patch-clamp measurements, and a higher apparent binding affinity of recombinant α1β2δ $GABA_A$ receptors for JM-II-43A was previously observed (*163*).

This mechanism is also consistent with the lack of desensitization characteristic of δ subunit-containing receptors (*145, 170, 175*). If receptors in the absence of GABA primarily reside in an inactive D state, then these receptors must both bind GABA and become an active R state before they can become an open-channel state. If the equilibrium between the R and D states is strongly in favor of the D state ($k_{DR} > k_{RD}$), the presence of GABA will result in only a fraction of receptors reaching an open-channel conformation. Such a mechanism would result in whole-cell currents without significant desensitization, as most receptors are already inactivated. Additionally, this would yield lower overall current amplitudes relative to the total number of receptors being expressed. Both of these attributes are commonly observed in electrophysiological studies of recombinant δ subunit-containing $GABA_A$ receptors (*10, 21, 145, 170, 175*).

It must be noted that if receptors start primarily in a D state, whole-cell currents observed in flash-photolysis methods will not directly measure k_{open} and k_{close} of the $GABA_A$ receptors. Rather this technique would measure a combination of multiple parameters that dictate the fraction of receptors in the RL_2 state in the presence of GABA and the rate constants of receptor opening and closing. If the equilibrium between R and D states strongly favors the D state, only a small fraction of receptors will rapidly enter a conducting state. Thus, the k_{close} rate constant obtained with flash-photolysis would likely be inconsistent with the k_{close} obtained with single-

channel current recording methods, as is observed Table 3.1. Because the value obtained for k_{close} using single-channel measurements is based on direct observation of the receptor mean open time, it will be a more accurate measure of k_{close}. The value obtained for k_{close} of ~ 2000 s^{-1} with single-channel analysis as opposed to 16 s^{-1} with flash-photolysis (Table 3.1) is more consistent with the very short (~ 0.4 ms) open-channel dwell times observed for α1β2δ $GABA_A$ receptors (Figure 3.2) and relates well to open-channel dwell times of other δ subunit-containing receptors previously reported (*4, 126*).

This new mechanism also suggests that molecules increasing the number of receptors in R states will increase the total number of receptors that enter into an open-channel state, thus leading to larger observed whole-cell currents. Such an increase in the population of open channels should be observable as an increase in channel activity without any observed changes in the time that the receptor is open. This increase in channel activity would yield a greater frequency of receptors channels randomly opening at the same time creating currents of higher amplitudes due to current stacking. This is precisely what was observed in the multi-channel patches shown and examined in Figures 3.3 and 3.4. This multi-channel data does not directly measure the equilibrium of receptors in R states *versus* D states, but it does clearly demonstrate that more receptors are opening their channels simultaneously in the presence of JM-II-43A compared to GABA alone, strongly supporting the mechanism proposed here for δ subunit-containing $GABA_A$ receptors.

The preferential selectivity of molecules like JM-II-43A for $GABA_A$ receptors containing δ subunits may be simply due to the state that the

particular receptor subtype resides in at rest. In other words, depending on what state the receptor starts in (R *versus* D), even if the compound binds with equal affinity to both states, the modulation by this compound could appear as current potentiation or more rapid current desensitization / inhibition. For example, it was noted in the previous report that JM-II-43A and other DHPMs increased the rate of desensitization of receptors that did not contain the δ subunit, indicating that DHPMs bind to and modulate other receptor subtypes (*163*). It may be that these compounds are binding to both the R and D states for these other receptors, but because the receptors are starting primarily in the R state the modulation appears as increasing the receptor desensitization rate.

The experimental results presented here suggest that an additional state must be considered in the Cash and Hess mechanism. It is clear that δ subunit-containing $GABA_A$ receptors have several unique attributes from many other $GABA_A$ receptor subtypes, such as their lack of desensitization (*145, 170, 175*), and their ability to be modulated to a larger degree by potentiators, such as JM-II-43A (*163*), neurosteroids (*145, 174, 255*) and other small molecules (*6, 8, 256, 257*). The inclusion of the equilibrium between an unbound inactive receptor D state with an unbound 'ready' R state to the Cash and Hess mechanism can explain the observed characteristics of δ subunit-containing $GABA_A$ receptors. Although the mechanism presented here is largely focused on explaining the function of $GABA_A$ receptors containing the δ subunit, it is possible that this model has implications for other $GABA_A$ receptors and cys-loop receptors.

CHAPTER 4

CHARACTERIZATION OF VISIBLE-LIGHT-SENSITIVE PHOTOLABILE CAGED GABA COMPOUNDS

Introduction

Precise spatial and temporal resolution is often difficult to obtain in studies of *in vivo* enzyme kinetics, functions of proteins that are membrane bound, subcellular protein responses, cellular functions within tissues and other common biological processes. A problem for investigating such experiments is the ability to rapidly change concentrations of ligands or substrates involved with these process due to limited control over diffusion and mixing of solutions as well as invasive methods to make measurements (*258*). One method to overcome these impediments is the use of biologically inert photolabile compounds. Upon illumination, these molecules undergo photolytic cleavage to produce a biologically active molecule or ion and an inert caging group byproduct. Because light can readily pass through cellular membranes, these compounds permit excellent temporal (*201, 252*) and spatial resolution (*259*) that can be employed for the study of biological processes within cells. These photolabile compounds are commonly called caged compounds and have greatly aided investigations in a number different fields of research, particularly the neurosciences (*260*).

The first biologically relevant caged compounds were developed by Engels and Schlaeger (*261*) for cyclic adenosine 3',5'-phosphate (cAMP). Caged adenosine 5'triphosphate was later developed and used for biological research by Kaplan et al. (*200*) and McCray and Trentham (*262*). Since these

initial studies, many photolabile protecting groups have been identified (*211*), several of which have become commonly used for investigating biological systems (*206*). These protecting groups have been used to make photolabile small molecules, Ca^{2+}, phospholipids, steroids, hormones, specific residues of peptides and proteins, enzyme substrates and cofactors, neurotransmitters, nucleic acids, oligonucleotides such as aptamers and siRNAs, and others (reviewed by Mayer and Heckel (*206*)).

The most commonly used caging group for biological studies is the 2-nitrobenzyl group with various substituents (*263, 264*). Several other common caging groups that are used in biological assays include coumarin esters (*216, 217*), *p*-hydroxyphenacyl derivatives (*214*), 2-methoxy-5-nitrophenyl (MNP) esters (*212, 213*), desyl-based compounds(*215*)and ruthenium complexes (*218*).

Numerous caged GABA derivatives have been reported (*218, 226, 254, 265-269*), yet caged GABA compounds continue to be developed, because no single caged molecule seems to be suitable for all research applications. Many factors contribute to whether a caged molecule is appropriate for a system: the caging group, the functional group on the neurotransmitter to which it is attached, the photolysis characteristics, and the byproducts of photolysis. Each of these factors must be examined before the use of a caged compound, as the effects are so far not predictable. For example, the UV sensitive αCNB-caged GABA has been successfully used for transient kinetic measurements of the α1β2γ2L receptor subtype (*1, 2, 226*); however, it acts as a competitive inhibitor of the α1β2δ receptor subtype (K. Eagen, unpublished work, 2007). Similarly, the visible-light-sensitive RuBi-caged GABA, which photolyzes rapidly with an

excellent quantum yield, has a concentration limitation of 20 μM for some $GABA_A$ receptor subtypes because at higher concentrations photolysis byproducts of the caging group act as inverse agonists (*218, 254*).

Through collaboration with Professor Bruce Ganem and Dr. Lijun Fan, a variety of visible-light-sensitive caged GABA molecules were designed and then synthesized by Lijun Fan. The synthesis of these compounds can be briefly described as a Passerini 3-component condensation reaction, shown in Figure 4.1, of a coumarin aldehyde **1** with BOC-protected GABA **2** and different molecules containing a cyano-group **3**, **4**, and **5**. This reaction yielded the three compounds **6**, **7**, and **8**, Figure 4.1 (*265*). These resulting products were confirmed by C^{13} and H^1 NMR as well as infrared spectroscopic methods (*265*). For further details regarding the synthesis of these compounds please refer to Lijun Fan's dissertation and Fan et al., 2009(*265*).

Discussed here is the purification and characterization of caged compounds **6**, **7**, and **8**. Characterization included determination of the quantum yield, rate of photolysis, thermal stability, and biological activity of these compounds. Also examined was the ability of these compounds to be photolyzed in the visible spectrum and for their application to transient kinetic techniques for the investigation of $GABA_A$ receptor kinetics. Techniques used to measure these properties included whole-cell current recordings, flash-photolysis, actinometric methods, analytical high pressure liquid chromatography (HPLC), transient-absorption, absorption and fluorescent techniques, and thin layer chromatography. The wide array of methods employed was due to difficulties in measuring the uncaging of compound **6** (Figure 4.1). It was ultimately determined that **6** would be

Figure 4.1 Synthetic scheme for the synthesis of three different coumarin caged GABA derivatives. Methyl coumarin **1** is converted to the coumarin aldehyde **2** through the use of a selenium oxide reaction (**a**). The resulting aldehyde is combined with three different cyano-compounds and BOC-protected GABA in a Passerini 3-component condensation reaction (**b**) to generate **3**, **4** and **5**. The removal of the BOC protecting group (**c**) generates the coumarin caged GABA molecules **6**, **7** and **8**. The synthesis of **6**, **7** and **8** was designed and carried out by Dr. L. Fan.

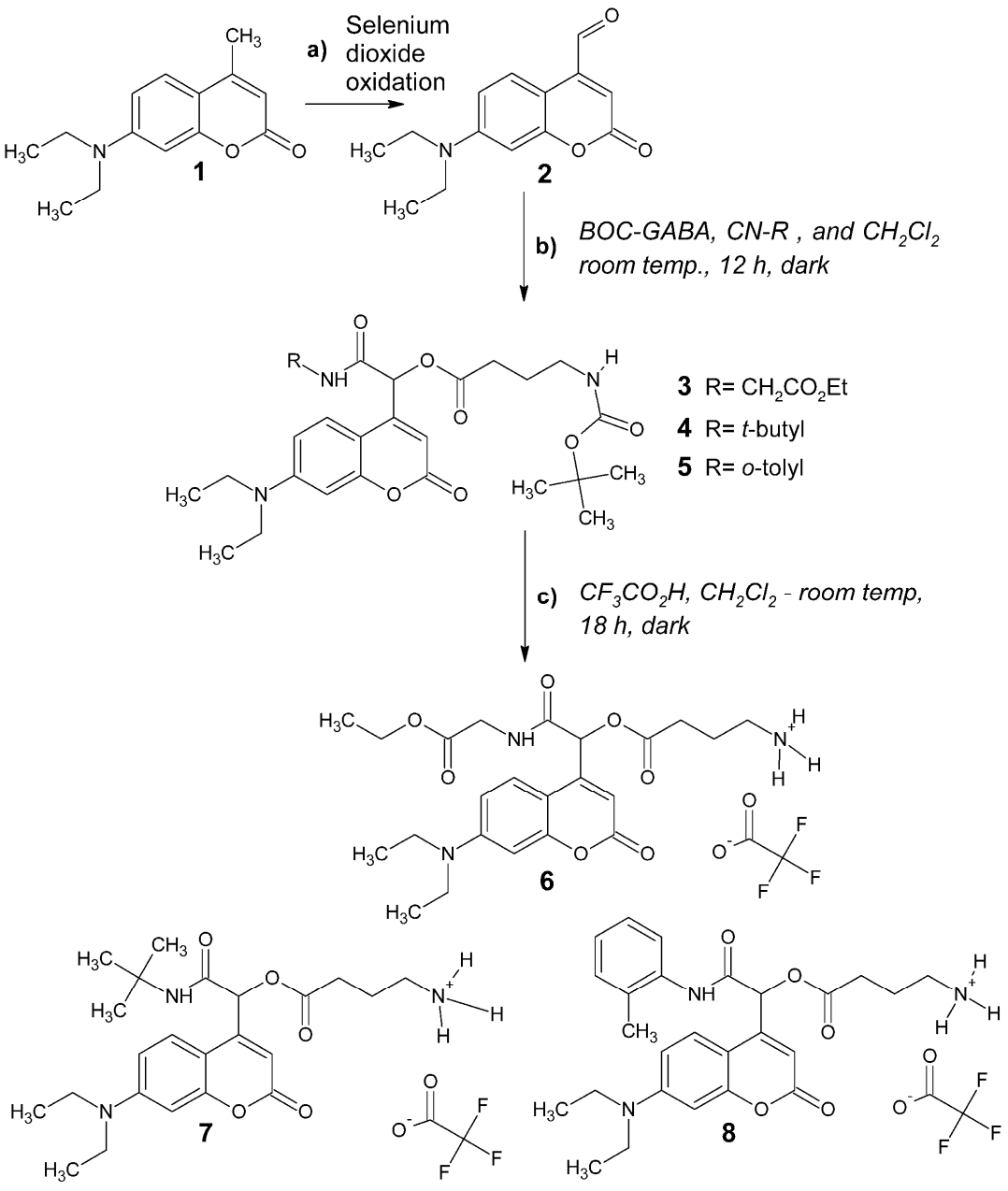
a) Selenium dioxide oxidation
1
2
b) BOC-GABA, CN-R , and CH_2Cl_2 room temp., 12 h, dark
3 R= CH_2CO_2Et
4 R= t-butyl
5 R= o-tolyl
c) CF_3CO_2H, CH_2Cl_2 - room temp, 18 h, dark
6
7
8

useful for biological investigations, however the rate of photolytic cleavage is too slow for kinetic measurements. These different approaches and their results are briefly presented and discussed.

Methods and Materials

Reagents, Synthesis and Preparation of Dihydropyrimidinones

Reagents were obtained from Sigma Aldrich, Fisher Scientific, or EM Science. GABA solutions were serially diluted from a frozen stock of 100 mM GABA stored at -20 ºC and made weekly. Caged compounds were synthesized as described previously (*265*). Solvents used for HPLC analysis were HPLC grade.

Solid-phase Extraction for Compound Purification

The purification of the caged compounds was carried out under a red light (darkroom light) to avoid photolytic cleavage of the compounds. Chloroform present from the compound synthesis was removed with a rotary evaporator. The dried compound was then resuspended in double distilled H_2O (ddH_2O) and loaded onto a silica column prewashed with ddH_2O. The compound on the column was washed with two column volumes worth of ddH_2O to remove polar molecules (*e.g.* free GABA), followed by a wash of two volumes of pure acetonitrile to remove non-polar byproducts and residual coumarin. The caged compound was eluted off the silica column with three volumes acetonitrile containing 0.5% TFA. The eluent was then rotationally evaporated to concentrate the compound, aliquoted into micro-centrifuge tubes and lyophilized for 24 hours in the dark at room temperature. The tubes were stored after lyophilization in an

opaque container, in the dark at -80°C. The individual tubes/aliquots permit easy quantification of the mass of compound, avoid potential exposure to light, and avoids problems from repeated thawing and refreezing.

Actinometry

Actinometric methods were used to measure the energy of light emitted from both a Rapp xenon flash lamp (SP-20) (Rapp OptoElectronic GmbH, Wedel, Germany) and a Compex 102 excimer laser (Lambda Physik), as well as to calibrate a Molectron joule meter. After calibration, the joule meter was primarily used for measurement of energy from light sources. The method used is described by Hatchard and Parker (*221*) with the modifications suggested by Murov (*220*). Potassium ferrous oxalate ($K_3Fe(C_2O_4)_3$) was made in the dark, under a red light, by adding 16 mL of 2.5 M $FeCl_3$ to 40 mL of a continuously stirred, hot solution of 3.3 M $K_2C_2O_4$. After mixing for 10 minutes, the resulting solution was chilled on ice to ~ 0°C without stirring to cause the $K_3Fe(C_2O_4)_3$ crystallize. The mother liquor was removed and the crystals were dissolved into 20 mL of 80°C ddH_2O and recrystallized twice more. The final crystals were sucked dry on a filter and then dried in a 45°C oven in the dark for 24 hrs. 1 mL of a 12 mM solution of the fresh $K_3Fe(C_2O_4)_3$ was pipetted into a cuvette and placed in front of a fiber optic cable used to transmit pulses of laser light. The solution was then irradiated with a variable number of pulses of light from the laser. The solution was then mixed with 2 mL of a 0.2% solution of triply recrystalized 1,10-phenanthroline solution and 1 mL of a buffer solution of 1 M sodium acetate and 1.8 M H_2SO_4 in a 10 mL volumetric flask. Water was immediately added up to the 10 mL mark, the solution

mixed, and then incubated at room temperature for 15-20 minutes before absorbance measurement at 510 nm. The energy emitted was calculated as described by Murov (*220*).

Transient Absorption Measurements

Transient absorption measurements are methods which entail monitoring the formation and decay of a photochromic transition state upon excitation by a high energy light pulse. These methods have been described in detail (*223, 270*). The absorbance of a low energy beam of light by a caged compound solution is monitored while being photolytically excited by pulses of high energy light perpendicular to the monitoring beam. The monitoring light beam was filtered light of 450+ nm to avoid excitation of the caged compound. The absorption was detected using a monochromater and a photomultiplier tube. The signal of the photomultiplier tube was monitored with an oscilloscope measuring at a frequency of 2 MHz. The high energy light pulses were generated by a Compex 102 Lambda Physik laser source, and the energy of the light pulses was measured using both actinometry and a calibrated joule meter. The cuvette holding the compound had a 1 cm path-length in both directions.

High Pressure Liquid Chromatography (HPLC)

Standard HPLC methods were used to separate compounds after varying degrees of photolysis using a Waters 600E pump and system controller with a Waters Nova-Pak C18 column (3.9 x 150 mm), an ISCO FL-2 fluorescence detector, and a LDC/Milton Roy absorption detector. The three liquid phases individually used were acetonitrile containing 0.1%

trifluoroacetic acid (TFA), 45% acetonitrile/ 55% water containing 0.1% TFA, and pure ddH_2O.

The photolysis of **6** was carried out in a cuvette with a photolyzable window volume of 250 μL. Triplicate solutions of 80 μM of **6** and 10 μM of methyl coumarin **1** (used as an internal control) were photolyzed using a Rapp xenon flash lamp with 0, 1, 2, 4, 6, 10, 25, 50, 100, 150 and 200 pulses of light. A calibrated joule meter was used to measure the energy of light absorbed by the samples of **6**. Samples were loaded onto a Waters 717plus, temperature controlled HPLC auto-sampler and triplicate injections of 5 μL per sample were run under the isocratic conditions stated above. Sample temperature during photolysis and in the HPLC auto sampler was kept at ~ 4°C.

Thin Layer Chromatography

Caged compounds were evaluated for purity and integrity using thin layer chromatography. The mobile phase used was a solution of 3:1:1 of n-butanol, acetic acid and water. The plates used were silica gel matrix plates. GABA and caged GABA compounds were detected using a 0.4% ninhydrin solution in mobile phase and heat treatment. Caged GABA and free coumarin caging group could be detected with UV light.

Rapid Solution Application

Rapid applications of ligands to HEK293T cells expressing the receptor of interest were performed with the cell-flow technique as previously described by Udgaonkar *et al.* (*18*), also see Chapters 1 and 2.

Electrophysiology Measurements

Whole-cell current recordings were obtained from individual cells in a whole-cell configuration lifted from the bottom of a 35 mm cell culture dish with a borosilicate glass pipette and suspended in extracellular buffer composed of 145 mM NaCl, 5 mM KCl, 2 mM $CaCl_2$, 1.5 mM $MgCl_2$, and 10 mM HEPES (4-(2-hydroxyethyl)-1-piperazineethanesulfonic acid) at pH 7.4 attained with 5 N NaOH. Borosilicate glass capillaries with a 1.5 / 1.12 mm outer / inner diameter (World Precision Instruments Inc., Sarasota, FL) were pulled with a vertical pipette puller and heat-polished on a microforge to make recording pipettes with open-end resistances of 3.0-5.0 MΩ. Intracellular solution backfilled into the pipettes was composed of 140 mM CsCl, 10 mM tetraethylammonium chloride, 10 mM EGTA (ethylene glycol bis (β-aminoethyl ether)-*N, N, N', N'* tetraacetic acid), 2 mM $MgCl_2$, and 10 mM HEPES brought to pH 7.4 with 5 N CsOH. Whole-cell patches were voltage clamped at – 60 mV. An Axopatch 200B amplifier, Digidata 1322A digitizer and Clampex 9.0 software (Molecular Devices, Sunnyvale, CA) were used for recording whole-cell currents at a sampling frequency of 50 kHz with Bessel filtering at 5 kHz as previously described by Hamill *et al.* (*186*).

Flash-photolysis Measurements

Current measurements for flash-photolysis were carried out using the visible-light-sensitive compounds **6**, **7**, and **8** (Figure 4.1) with cells expressing α1β2δ $GABA_A$ receptors in a whole-cell patch-clamp configuration that were voltage clamped at -60 mV, as previously described (*252*). Solutions of 100 μM of the three coumarin caged GABA molecules were applied to a cell using the cell-flow technique. An optical fiber with an

internal diameter of 600 μm directed a flash of light generated by a Rapp xenon flash lamp (SP-20) (Rapp OptoElectronic GmbH, Wedel, Germany) onto the cell in a whole-cell configuration. The flash of light was filtered with a 385-450 nm band-pass filter. All experiments were conducted under dark room red lights. A saturating 1 mM GABA solution applied with the standard cell-flow method, was used as a control for normalization of all current amplitudes from cell-flow and flash-photolysis measurements obtained with a single cell.

Results and Discussion

The compounds **6**, **7**, and **8** (Figure 4.1) synthesized by Lijun Fan were purified using a method similar to solid-state extraction (see methods for details). This purification process was important for two reasons: i) to remove residual GABA that may be in the sample, and ii) to remove excess TFA that may be in the sample. While it is evident that free GABA is not desirable, the removal of TFA is also critical as $GABA_A$ receptors and many other ion channels are pH sensitive (*271*). We found that solutions of unpurified material tended to both evoke current and cause inhibition of the receptor (data not shown). Both of these attributes were not observed with the purified caged GABA molecules.

The purity and thermal stability of these compounds was most accurately evaluated using the cell-flow and whole-cell patch-clamp techniques with cells transiently expressing recombinant α1β2δ $GABA_A$ receptors. This is because $GABA_A$ receptors respond to concentrations of GABA well below the detection limit of most other detection methods that are available. The current trace shown in Figure 4.2A demonstrates that no

Figure 4.2 Electrophysiological measurements of coumarin caged GABA **6** conducted with recombinant α1β2δ $GABA_A$ receptors expressed in HEK293T cells demonstrate that **6** is biologically inert before photolysis. **A.** A solution of 100 μM of **6** was applied using the cell-flow method to a cell containing α1β2δ $GABA_A$ receptors and was then photolyzed at time = 0 with a flash of 385-450 nm light from a Rapp xenon flash-lamp. Before illumination there is no current evoked, indicating that **6** does not act as a receptor agonist. Upon illumination there is an increase in current observed indicating photolysis of **6** to release free GABA. **B.** The large amount of overlap between the application of 10 μM GABA (Trace 1), and co-application of 10 μM GABA with 100 μM of **6** (Trace 2) demonstrates that **6** does not act as an inhibitor of the receptor. All currents were recorded at ambient temperature (~ 22 °C), – 60 mV membrane potential and in extracellular buffer pH 7.4.

A

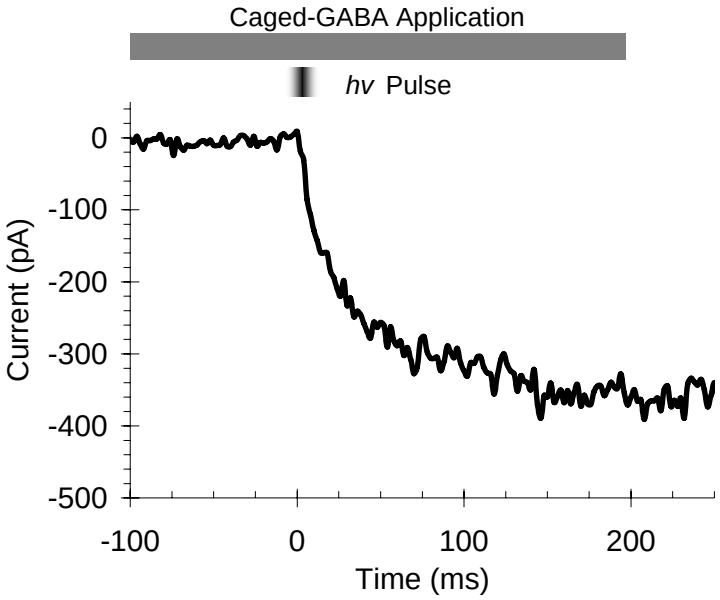
Caged-GABA Application
hv Pulse
0
-100
-200
-300
-400
-500
Current (pA)
-100
0
100
200
Time (ms)

B

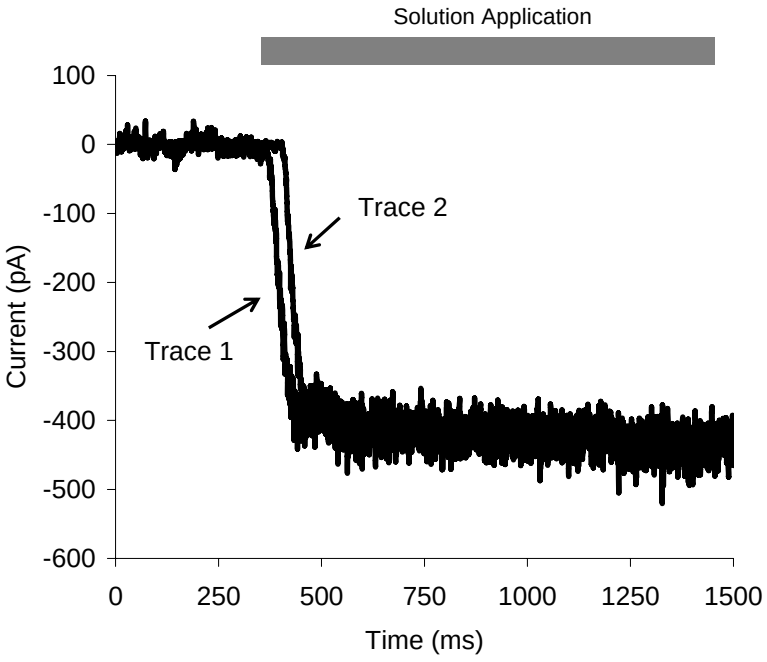
Solution Application
100
0
-100
-200
-300
-400
-500
-600
Current (pA)
Trace 2
Trace 1
0
250
500
750
1000
1250
1500
Time (ms)

current is evoked by compound **6** until photolysis is initiated with a pulse of light, which causes an increase in current over several hundred milliseconds. This indicated that the compound was both photolabile and does not activate the receptor until photolysis. In contrast, photolysis of a solution of 100 μM of **7** only evoked a few pA of current, indicating that this compound is not significantly photolabile (data not shown).

Thermal stability was also monitored by using the cell-flow and whole-cell patch-clamp techniques to measure any currents evoked by caged GABA derivatives without photolysis after incubating at room temperature or on ice. Solutions of **6** kept on ice were stable for 5-6 hours or more, whereas solutions of **6** at room temperature for 2+ hours caused currents to appear upon application showing that **6** is not thermally stable in aqueous solution at room temperature.. It should be noted that compound 6 is thermally stable enough for flash photolysis measurements using whole-cell current measurements and the cell-flow application system as solutions can easily be kept on ice and will warm to room temperature before being applied to the cell. This same approach was used to test the thermal stability of compound **8** and it was determined that **8** seemed to gradually uncage (hydrolytically cleave) over 1-2 hours while in aqueous solution, even when kept on ice.

To test whether these compounds inhibit the receptor and are biologically inert prior to photolysis, 100 μM of compound **6** was co-applied with various concentrations of free GABA. No change in the current amplitude evoked by GABA was observed (Figure 4.2B) indicating that **6** does not inhibit the receptor.

Once it was established that **6** is pure, stable for measurements and

biologically inert, an effort to determine the quantum yield was initiated. Because no absorption changes were observed after **6** was exposed to two hours of high intensity light, Figure 4.3, techniques for quantifying the quantum yield using spectral changes after photolysis (*198, 219, 272*) could not be used. Thus, molecular separation using HPLC methods with detection by fluorescence and absorption was attempted. Isocratic pumping of a 45% to 55% acetonitrile and water liquid phase with 0.1% TFA was found to yield well-separated peaks of the caged compound **6** from several presumably coumarin-caging group byproducts and methyl coumarin **1**, which was used as an internal standard. However, increasing numbers of pulses of light from the Rapp flash lamp to solutions of compound **6** did not result in any visible change in the detected compound peak amplitudes or peak areas under these conditions, even after maximizing the sample volume exposed to light, increasing compound concentrations loaded onto the HPLC, and decreasing loading volumes (Figure 4.4A). Only after hour-long exposure times to a halogen light source were amplitude changes in the molecular peak heights visible (Figure 4.4B). The same situation was observed when the caged compound solutions subjected to flashes of light or long-term light exposure were run using TLC methods. Caged compounds, free GABA and coumarin caging groups could all be detected on TLC, however the detection limit of free GABA was limited to ~ 0.5 nmoles and release of GABA from photolysis is expected to be much lower than this. The caged compound ran with slightly different retention factors (Rf) with values around 0.52, free GABA had an Rf value of 0.23 and free coumarin caging-groups had Rf values of 0.92+. However, changes in the ratios of these compounds could not be observed until subjected to long

Figure 4.3 Three different absorption scans of 1 mL of 100 μM compound **6** before illumination (Scan 1), after 250 pulses of light (~ 0.1 mJ each) from the Rapp flash lamp (Scan 2), and after leaving a sample on ice and under an intense halogen lamp for 2 hours (Scan 3). No differences were observed. Solutions of **6** were made in extracellular buffer pH 7.4 at ambient temperature (~ 22 °C).

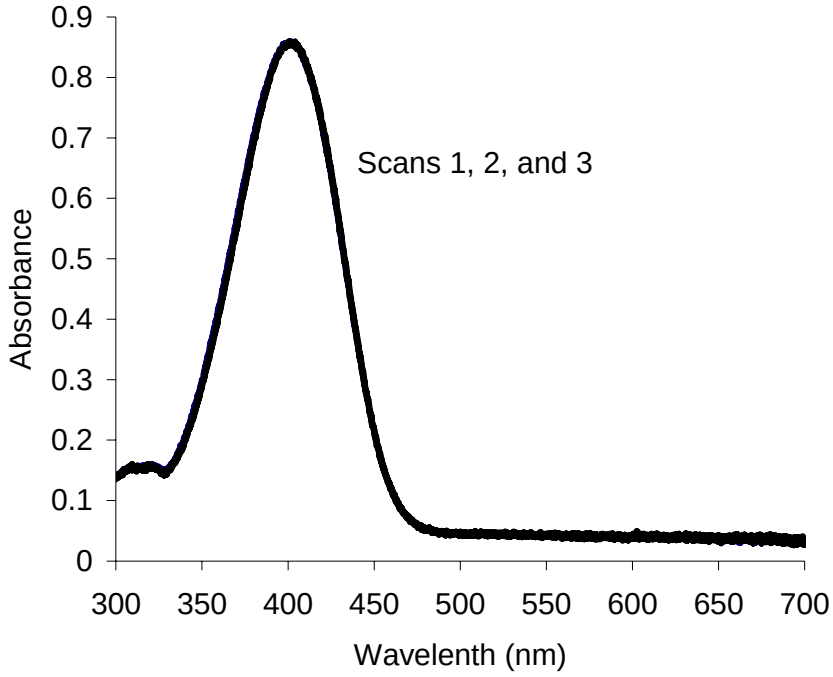
0.9
0.8
0.7
0.6
0.5
0.4
0.3
0.2
0.1
0
Absorbance
Scans 1, 2, and 3
300
350
400
450
500
550
600
650
700
Wavelenth (nm)

Figure 4.4 HPLC separation of **6** from coumarin caging group byproducts and an internal standard of methyl coumarin **1** did not demonstrate any changes in peak amplitude after variable extent of photolysis. **A.** Triplicate samples of 80 μM of **6** were photolyzed with a Rapp flash lamp. Three 5 μL injections of each sample were separated on a HPLC C18 column at a flow rate of 0.2 mL/min and detected by fluorescence. Samples contained 10 μM of **1** as an internal standard. All triplicate of triplicate sample traces are shown. **B.** A fresh solution of 10 μM of **6** and 10 μM of **1** was divided into two tubes: one kept on ice in the dark (thin trace), the other kept on ice under a halogen bulb for 2 hours (thick trace). 5 μL from each tube were separated on a HPLC C18 column at a flow rate of 0.4 mL/min and detected by fluorescence. **C.** No changes in peak amplitudes or area could be observed for caged GABA **6** (■), or the coumarin cage byproducts (◆). The peak area of methyl coumarin **1** (▲) was used to normalize the areas of all peaks to account for variation in volumes injected. Error bars representing standard error of the triplicate measurements of triplicate samples are shown. Solutions of **6** were made in extracellular buffer pH 7.4 at a temperature of 4°C.

A

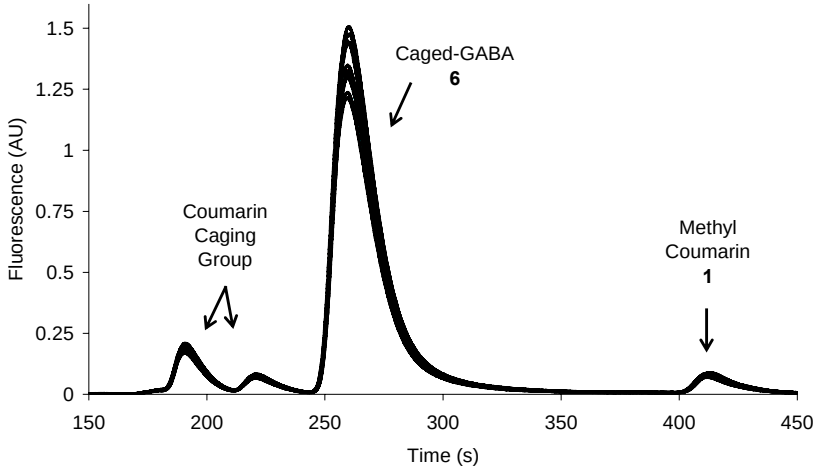
Fluorescence (AU)
1.5
1.25
1
0.75
0.5
0.25
0
150
200
250
300
350
400
450
Time (s)
Caged-GABA
6
Coumarin
Caging
Group
Methyl
Coumarin
1

B

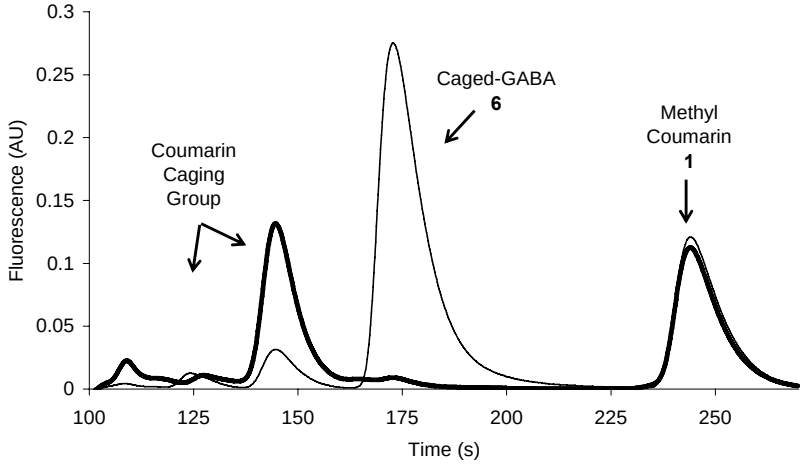
Fluorescence (AU)
0.3
0.25
0.2
0.15
0.1
0.05
0
100
125
150
175
200
225
250
Time (s)
Caged-GABA
6
Coumarin
Caging
Group
Methyl
Coumarin
1

C

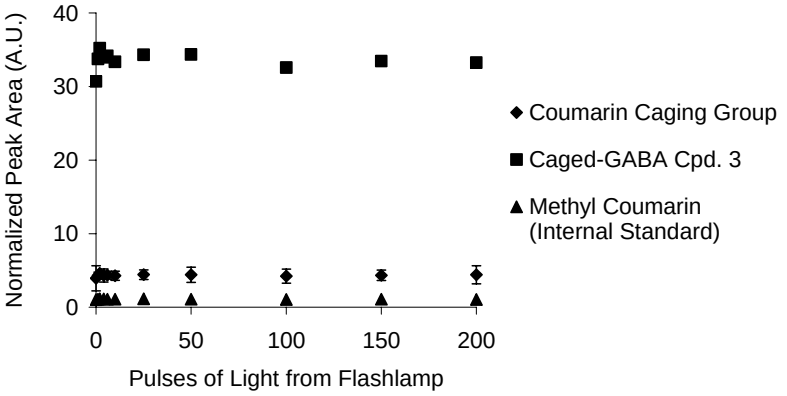
Normalized Peak Area (A.U.)
40
30
20
10
0
0
50
100
150
200
Pulses of Light from Flashlamp
Coumarin Caging Group
Caged-GABA Cpd. 3
Methyl Coumarin
(Internal Standard)

light exposure times.

Ultimately the quantum yield of 0.1 ± 0.04 molecules photolyzed per photon absorbed was estimated based off flash-photolysis data using recombinant α1β2δ $GABA_A$ receptors expressed in HEK293T cells. The estimate is based on the apparent concentration of GABA released upon photolysis of compound **6** with a single flash from the Rapp flash-lamp, the number of photons that are absorbed by the caged compound and the period of time that the compound is exposed to light. The apparent concentration of GABA released was estimated based on a GABA dose-response curve of free GABA with α1β2δ $GABA_A$ receptors, as shown and described in Figure 4.5. Actinometric and absorption data was used to determine the molar absorption of photons for compound **6**. For details on this and the calculation of quantum yields see Murov, 1993 (*220*).

The rate of photolysis was ultimately not possible to measure. Transient absorption measurements have been previously used as described in the methods section to determine the rate of photolysis, but compound **6** did not display any observable transient absorption above 450 nm. The reason only wavelengths above 450 nm were considered is because compound **6** absorbs light at these wavelengths prior to photolysis and light absorption likely translates into photo excitation and photolytic cleavage. Since no transient absorption was visible, and other methods used to calculate the rate of photolysis rely on spectroscopic changes in the final products or HPLC analysis, this value could not be determined.

However, when compound **6** was tested on α1β2γ2L receptors using flash-photolysis, a significantly lower open-channel equilibrium constant was obtained than the value previously reported (*1*). This suggests that the rate-

Figure 4.5 Comparison of the current response evoked by photolyzed caged GABA to a dose-response curve of free GABA to estimate a quantum yield. Shown is a dose-response curve of currents evoked by application of GABA (●) to recombinant α1β2δ $GABA_A$ receptors expressed in HEK293T cells obtained using the cell-flow and whole-cell patch-clamp techniques. A quantum yield of 0.1 ± 0.04 molecules photolyzed per photon was determined for compound **6** (■) based on the concentration of GABA released upon photolysis as detected by α1β2δ $GABA_A$ receptor response. Currents from recombinant α1β2δ $GABA_A$ receptors were measured as solutions of 100 μM caged GABA **6** were photolyzed by single flashes of 350-450 nm of light (~ 0.1 mJ / flash) in flash-photolysis experiments. The concentration of GABA released from the photolytic cleavage of **6** was estimated by averaging the peak current amplitudes of three measurements on 4 separate cells (12 measurements total). This concentration was estimated at 5.3 ± 1.0 μM GABA and was used to estimate a molar fraction of caged GABA that underwent photolysis (0.053 ± 0.01) during a single flash (0.11 ms). This fraction was then divided by the molar absorption of photons per second by compound **6** (0.52 ± 0.02 photons/mole·s, which was estimated by actinometry and absorption measurements) to give the quantum yield. All currents were recorded at ambient temperature (~ 22 °C), – 60 mV membrane potential and in extracellular buffer pH 7.4. Error bars represent the standard error.

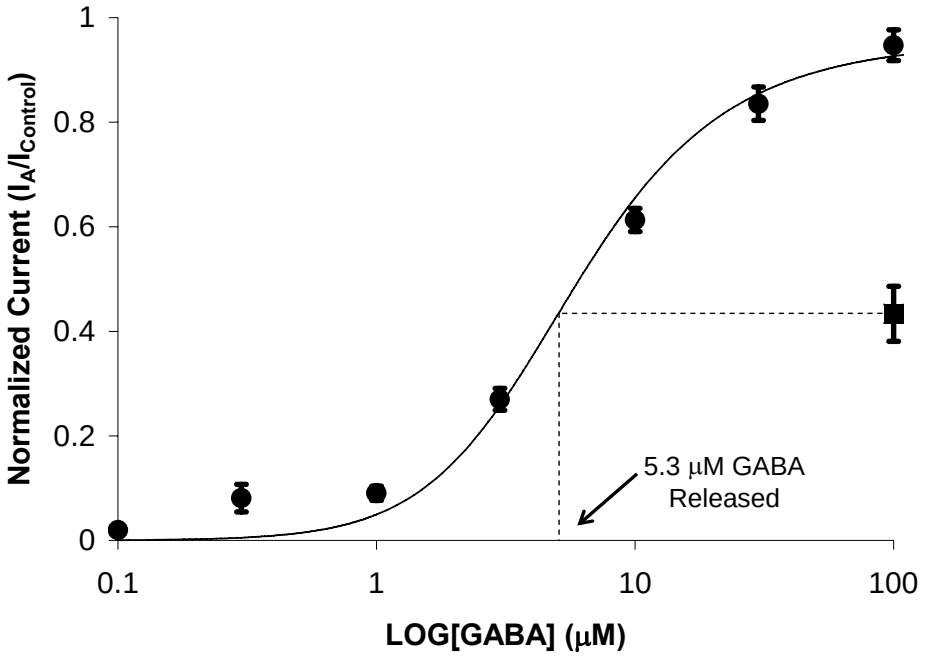
Normalized Current ($I_A/I_{Control}$)
1
0.8
0.6
0.4
0.2
0
0.1
1
10
100
LOG[GABA] (μM)
5.3 μM GABA
Released

limiting step of the flash-photolysis measurements was the photolytic cleavage of the caged compound.

Thus the visible-light-sensitive caged GABA, compound **6**, generated and examined here is useful for biological assays requiring spatial resolution and can tolerate a temporal resolution in the upper millisecond range. The quantum yield of 0.1 corresponds to a modest amount of release that has been reported for other caged compounds (*198, 219, 252*). This compound does have some limitation, such as its stability at room temperature and higher temperatures. Initially, we were hopeful that the biological measurements needed for Chapters 2 and 3 of this dissertation could be achieved with these new compounds, but for better temporal resolution another caged GABA (RuBi caged GABA) was utilized. Additionally these compounds exemplify the numerous difficulties that can arise during the development of caged compounds and emphasize the importance of characterizing caged compounds before application to biological studies.

APPENDIX

A.1 Equations and Derivations

This section is included to aid the reader by grouping all equations used in this dissertation in one location. A few of these equations are derived so that the reader can better understand how the equation relates to the system it describes.

Equation [1.1]

$$E_S = (RT/zF)\ln([S]_{out}/[S]_{in})$$

This equation is known as the Nernst equation after the individual who first related the electric potential generated by a difference in ion concentration (*24*). E_S is the energy potential in units of volts generated by the concentration difference of the ion S, R is the universal gas constant, T is the temperature in Kelvin, z is the charge of the ion being investigated, F is Faraday's constant.

Equation [1.2]

$$E_M = (RT/F)\ln((\sum P_C[C]_{out} + \sum P_A[A]_{in})/(\sum P_C[C]_{in} + \sum P_A[A]_{out}))$$

This equation is known as the Goldmann/Hodgkin/Katz equation after the individuals that contributed to adapting the Nernst equation [1.1] to determine the electric potential that exists across the membrane of a cell (membrane potential, E_M) when multiple cations (C) and anions (A) with different permeabilities (P_C or P_A) and concentration difference are present (*25, 26*). This equation is limited to the investigation of monovalent anions and cations, but can be expanded to include ions of other valences (*273,*

274). The form of this equation shown here does not specify the anions involved, but Na^+, K^+ and Cl^- are commonly considered to yield the equation

$$E_M = (RT/F)\ln((P_{Na^+}[Na^+]_{out} + P_{K^+}[K^+]_{out} + P_{Cl^-}[Cl^-]_{in})/ (P_{Na^+}[Na^+]_{in} + P_{K^+}[K^+]_{in} + P_{Cl^-}[Cl^-]_{out})) \quad [1.2B]$$

Equation [1.3]

$$F_{open\ t=0} = [\overline{RL_2}]_{t=0}/[R_M] = ([L])/([L]^2 + \Phi([L] + K_1)^2)$$

This equation is used to estimate the fraction of receptors that are in the open-channel state $\overline{RL_2}$ at time=0, or immediately after GABA (the receptor ligand, L) becomes present. The equation is derived from the Cash and Hess mechanism (*15*) as shown below. Parameters include $[R_M]$, which is the molar concentration of all functional $GABA_A$ receptors, and K_1, which is the binding affinity of the receptor for GABA ($K_1 = k_{off}/k_{on}$). Derivation of [1.3] comes from the concentrations predicted from the Cash and Hess mechanism as follows:

$$[RL] = 2[R][L]/K_1 \quad [1.3A]$$

Note that [R][L] is multiplied by 2 because these receptors contain two binding sites.

$$[RL_2] = [RL][L]/2K_1 = [R][L]^2/K_1^2 \quad [1.3B]$$

$$[\overline{RL_2}] = [RL_2]/\Phi = [R][L]^2/\Phi K_1^2 \quad [1.3C]$$

These relationships can then be inserted into the following description of the fraction of receptors in the open-channel state:

$$F_{open} = [\overline{RL_2}]/[R_M] = [\overline{RL_2}]/([R] + [RL] + [RL_2] + [\overline{RL_2}] \quad [1.3D]$$

$$F_{open} = ([R][L]^2/\Phi K_1^2)/ ((([R] + (2[R][L]/K_1) + ([R][L]^2/K_1^2) + ([R][L]^2/\Phi K_1^2)) \quad [1.3E]$$

$$F_{open} = [L]^2/(\Phi K_1^2 + 2[L]\Phi K_1 + [L]^2\Phi + [L]^2) \quad [1.3F]$$

$$F_{open} = [L]^2/(\Phi(K_1 + [L])^2 + [L]^2) \quad [1.3]$$

Both equation [1.3] and [1.4] are based on several assumptions: i) only an active receptor can form an open-channel, ii) although the two GABA binding sites have unique affinities for GABA, the binding of both GABA molecules occurs at rates much faster than the conformational change that leads to an open-channel and faster than the rate of desensitization, thus can be described by two equivalent binding affinities (K_1), iii) all receptors start in an active receptor state in the absence of GABA. The third assumption was revealed by work described in Chapter 3 of this dissertation.

Equation [1.4]

$$F_{open\ t=\infty} = [\overline{RL_2}]_{t=\infty}/[R_M] = ([L]K_{D2})/$$
$$(K_{D2}([L]^2 + \Phi([L] + K_1)^2 + \Phi[L]([L] + 2K_2))$$

This equation is based on the Cash and Hess mechanism (*15*) to estimate the fraction of receptors that are in the open-channel state $\overline{RL_2}$ at infinite time ($t = \infty$), in other words once the Cash and Hess mechanism has reached an equilibrium. The derivation of this equation is quite similar as for [1.3], but has an added layer of complexity due to the desensitized states. Many of the parameters and the assumptions made for this equation are the same as in equation [1.3]. Additional parameters include K_{D2}, which is an equilibrium constant between RL_2 and DL_2 states and K_2 is the binding affinity of the desensitized receptor for GABA. An additional assumption is that receptor desensitization is primarily dictated by a single desensitization equilibrium constant, K_{D2}.

Equation [1.5]

$$I_{obs} = I_M R_M F_{open\ t=0} = I_M R_M ([\overline{RL_2}]_{t=0} / [R_M])$$

This relationship simply describes that the observed current (I_{obs}) is a result of the product of the fraction of receptors in the open-channel state and the amount of current observed if all the functional receptors present were in the open-channel state ($I_M R_M$).

Equation [1.6]

$$I_{obs} = I_M R_M ([\overline{RL_2}]_{t=0} / [R_M]) = E_m g_{channel} N_A [\overline{RL_2}]$$

This equation is derived from equation [1.5] by simply substituting $I_M R_M$ with the channel conductance ($g_{channel}$) and Avogadro's number (N_A). Channel conductance is a parameter that is specific for the receptor examined and must be experimentally determined.

Equation [1.7]

$$I(t) = \sum A_n e^{-t/\tau_n}$$

This equation is a simple exponential function that is used in this dissertation to relate observed current amplitudes (I) to time for specific regions in a current trace. It is used for determining the rate of current decline in the desensitization phase of whole-cell current measurements. It is also used to determine the rate of current rise during the rising phase of flash-photolysis measurements. The number of components used is decided based on the resulting fit using non-linear regression.

Equation [1.8]

$$I_A = (e^{-\Delta t/\tau_n}) \sum_{i=1}^{j} (I_{obs})_{t_i} + (I_{obs})_{t_j}$$

This equation is used to correct current traces for desensitization, i.e. a plot of a current trace from a ligand-gated receptor if the receptor did not undergo desensitization. Essentially this function multiplies an exponential function by the sum of current amplitudes from the start time (i=1) and each time point to be corrected (t=j). This equation uses the time constants that describe the rate of desensitization observed in a current trace obtained by using equation [1.7] for the exponential function shown here.

Equation [2.1]

$$I_P/I_o = I_o + (R_{MAX})(1+(K_d/[Cpd])^h)^{-1}$$

Equation [2.1], which has been used previously to measure barbiturate interactions with $GABA_A$ receptors (*2, 155*), relates the ratio of measured current amplitudes (I_P/I_o) induced by a constant GABA concentration in the presence (I_P) or absence (I_o) of the compound of interest ([Cpd]), JM-II-43A. R_{MAX} is the maximum I_P/I_o ratio observed when the potentiating compound is co-applied with GABA. The empirical parameter h is equivalent to the Hill coefficient.

Equation [2.2]

See equation [1.3]

Equation [2.3]

See equation [1.7]

Equation [3.1]

See equation [1.7]

Equation [3.2]

$$k_{obs} = k_{close} + k_{open}([L]/([L] + K_1))^2$$

This equation is used to describe the relationship between the observed rising phase of current when receptors are activated simultaneously by the release of GABA from a photolabile neurotransmitter derivative. This equation is derived from the sum of a zero order reaction of the closing of the receptor combined with a square of the first order transition of the RL_2 state to the open-channel $\overline{RL_2}$ state.

REFERENCES

1. Ramakrishnan, L., and Hess, G. P. (2004) On the mechanism of a mutated and abnormally functioning gamma-aminobutyric acid (A) receptor linked to epilepsy, *Biochemistry 43*, 7534-7540.

2. Krivoshein, A. V., and Hess, G. P. (2006) On the mechanism of alleviation by phenobarbital of the malfunction of an epilepsy-linked GABA(A) receptor, *Biochemistry 45*, 11632-11641.

3. Dibbens, L. M., Feng, H. J., Richards, M. C., Harkin, L. A., Hodgson, B. L., Scott, D., Jenkins, M., Petrou, S., Sutherland, G. R., Scheffer, I. E., Berkovic, S. F., Macdonald, R. L., and Mulley, J. C. (2004) GABRD encoding a protein for extra- or peri-synaptic GABAA receptors is a susceptibility locus for generalized epilepsies, *Hum Mol Genet 13*, 1315-1319.

4. Feng, H. J., Kang, J. Q., Song, L., Dibbens, L., Mulley, J., and Macdonald, R. L. (2006) Delta subunit susceptibility variants E177A and R220H associated with complex epilepsy alter channel gating and surface expression of alpha4beta2delta GABAA receptors, *J Neurosci 26*, 1499-1506.

5. Hevers, W., Hadley, S. H., Luddens, H., and Amin, J. (2008) Ketamine, but not phencyclidine, selectively modulates cerebellar GABA(A) receptors containing alpha6 and delta subunits, *J Neurosci 28*, 5383-5393.

6. Glykys, J., Peng, Z., Chandra, D., Homanics, G. E., Houser, C. R., and Mody, I. (2007) A new naturally occurring GABA(A) receptor subunit partnership with high sensitivity to ethanol, *Nat Neurosci 10*, 40-48.

7. Sundstrom-Poromaa, I., Smith, D. H., Gong, Q. H., Sabado, T. N., Li, X., Light, A., Wiedmann, M., Williams, K., and Smith, S. S. (2002) Hormonally regulated alpha(4)beta(2)delta GABA(A) receptors are a target for alcohol, *Nat Neurosci 5*, 721-722.

8. Wallner, M., Hanchar, H. J., and Olsen, R. W. (2003) Ethanol enhances alpha 4 beta 3 delta and alpha 6 beta 3 delta gamma-

aminobutyric acid type A receptors at low concentrations known to affect humans, *Proc Natl Acad Sci U S A 100*, 15218-15223.

9. Borghese, C. M., and Harris, R. A. (2007) Studies of ethanol actions on recombinant delta-containing gamma-aminobutyric acid type A receptors yield contradictory results, *Alcohol 41*, 155-162.

10. Kaur, K. H., Baur, R., and Sigel, E. (2009) Unanticipated structural and functional properties of delta-subunit-containing GABAA receptors, *J Biol Chem 284*, 7889-7896.

11. Wafford, K. A., van Niel, M. B., Ma, Q. P., Horridge, E., Herd, M. B., Peden, D. R., Belelli, D., and Lambert, J. J. (2009) Novel compounds selectively enhance delta subunit containing GABA A receptors and increase tonic currents in thalamus, *Neuropharmacology 56*, 182-189.

12. Katz, B., and Thesleff, S. (1957) A study of the desensitization produced by acetylcholine at the motor end-plate, *J Physiol 138*, 63-80.

13. Sigworth, F. J., and Sine, S. M. (1987) Data transformations for improved display and fitting of single-channel dwell time histograms, *Biophys J 52*, 1047-1054.

14. McManus, O. B., Blatz, A. L., and Magleby, K. L. (1987) Sampling, log binning, fitting, and plotting durations of open and shut intervals from single channels and the effects of noise, *Pflugers Arch 410*, 530-553.

15. Cash, D. J., and Hess, G. P. (1980) Molecular mechanism of acetylcholine receptor-controlled ion translocation across cell membranes, *Proc Natl Acad Sci U S A 77*, 842-846.

16. Cash, D. J., Aoshima, H., and Hess, G. P. (1980) Acetylcholine-induced receptor-controlled ion flux investigated by flow quench techniques, *Biochem Biophys Res Commun 95*, 1010-1016.

17. Mabry, J., and Ganem, B. (2006) Studies on the Biginelli reaction: a mild and selective route to 3,4-dihydropyrimidin-2(1H)-ones via enamine intermediates, *Tetrahedron Letters 47*, 55-56.

18. Udgaonkar, J. B., and Hess, G. P. (1987) Chemical kinetic measurements of a mammalian acetylcholine receptor by a fast-

reaction technique, *Proc Natl Acad Sci U S A 84*, 8758-8762.

19. Krnjevicacute, K. (1974) Chemical Nature of Synaptic Transmission in Vertebrates, *Physiol. Rev. 54*, 418-540.

20. Enna, S. J., and Hanns, M., (Eds.) (2007) *The GABA Receptors*, Third ed., Humana Press, Totowa, New Jersey.

21. Olsen, R. W., and Sieghart, W. (2009) GABA A receptors: subtypes provide diversity of function and pharmacology, *Neuropharmacology 56*, 141-148.

22. Del Castillo, J., and Katz, B. (1957) Interaction at end-plate receptors between different choline derivatives, *Proc R Soc Lond B Biol Sci 146*, 369-381.

23. Skou, J. C. (1998) Nobel Lecture. The identification of the sodium pump, *Biosci Rep 18*, 155-169.

24. Nernst, W. (1888) Zur Kinetik der in Losung befindlichen Korper: Theorie der Diffusion., *Zeitschrift fur Physikalische Chemie*, 613-637.

25. Hodgkin, A. L., and Katz, B. (1949) The effect of sodium ions on the electrical activity of the giant axon of the squid, *J Physiol 108*, 37-77.

26. Goldman, D. E. (1943) Potential, Impedance, and Rectification in Membranes, *J Gen Physiol 27*, 37-60.

27. Jones, M. V., and Westbrook, G. L. (1995) Desensitized states prolong GABAA channel responses to brief agonist pulses, *Neuron 15*, 181-191.

28. Twyman, R. E., and Macdonald, R. L. (1992) Neurosteroid regulation of GABAA receptor single-channel kinetic properties of mouse spinal cord neurons in culture, *J Physiol 456*, 215-245.

29. Hodgkin, A. L., and Huxley, A. F. (1952) A quantitative description of membrane current and its application to conduction and excitation in nerve, *J Physiol 117*, 500-544.

30. Del Castillo, J., and Moore, J. W. (1959) On increasing the velocity of a nerve impulse, *J Physiol 148*, 665-670.

31. Bianchi, M. T., Botzolakis, E. J., Haas, K. F., Fisher, J. L., and Macdonald, R. L. (2007) Microscopic kinetic determinants of macroscopic currents: insights from coupling and uncoupling of GABAA receptor desensitization and deactivation, *J Physiol 584*, 769-787.

32. Persohn, E., Malherbe, P., and Richards, J. G. (1992) Comparative molecular neuroanatomy of cloned GABAA receptor subunits in the rat CNS, *J Comp Neurol 326*, 193-216.

33. Olsen, R. W., and Sieghart, W. (2008) International Union of Pharmacology. LXX. Subtypes of gamma-aminobutyric acid(A) receptors: classification on the basis of subunit composition, pharmacology, and function. Update, *Pharmacol Rev 60*, 243-260.

34. Sieghart, W. (2006) Structure, pharmacology, and function of GABAA receptor subtypes, *Adv Pharmacol 54*, 231-263.

35. Mohler, H. (2006) GABA(A) receptor diversity and pharmacology, *Cell Tissue Res 326*, 505-516.

36. Bianchi, M. T., Haas, K. F., and Macdonald, R. L. (2002) Alpha1 and alpha6 subunits specify distinct desensitization, deactivation and neurosteroid modulation of GABA(A) receptors containing the delta subunit, *Neuropharmacology 43*, 492-502.

37. Sieghart, W., and Sperk, G. (2002) Subunit composition, distribution and function of GABA(A) receptor subtypes, *Curr Top Med Chem 2*, 795-816.

38. Fritschy, J. M., and Mohler, H. (1995) GABAA-receptor heterogeneity in the adult rat brain: differential regional and cellular distribution of seven major subunits, *J Comp Neurol 359*, 154-194.

39. Picton, A. J., and Fisher, J. L. (2007) Effect of the alpha subunit subtype on the macroscopic kinetic properties of recombinant GABA(A) receptors, *Brain Res 1165*, 40-49.

40. Hevers, W., and Luddens, H. (1998) The diversity of GABAA receptors. Pharmacological and electrophysiological properties of GABAA channel subtypes, *Mol Neurobiol 18*, 35-86.

41. Simon, J., Wakimoto, H., Fujita, N., Lalande, M., and Barnard, E. A. (2004) Analysis of the set of GABA(A) receptor genes in the human genome, *J Biol Chem 279*, 41422-41435.

42. McKernan, R. M., and Whiting, P. J. (1996) Which GABAA-receptor subtypes really occur in the brain?, *Trends Neurosci 19*, 139-143.

43. Darlison, M. G., (Ed.) (2008) *Inhibitory Regulation of Excitatory Neurotransmission*, Vol. 44, Springer, Heidelberg, Germany.

44. Jechlinger, M., Pelz, R., Tretter, V., Klausberger, T., and Sieghart, W. (1998) Subunit composition and quantitative importance of hetero-oligomeric receptors: GABAA receptors containing alpha6 subunits, *J Neurosci 18*, 2449-2457.

45. Shivers, B. D., Killisch, I., Sprengel, R., Sontheimer, H., Kohler, M., Schofield, P. R., and Seeburg, P. H. (1989) Two novel GABAA receptor subunits exist in distinct neuronal subpopulations, *Neuron 3*, 327-337.

46. Moragues, N., Ciofi, P., Tramu, G., and Garret, M. (2002) Localisation of GABA(A) receptor epsilon-subunit in cholinergic and aminergic neurones and evidence for co-distribution with the theta-subunit in rat brain, *Neuroscience 111*, 657-669.

47. Waldvogel, H. J., Baer, K., Gai, W. P., Gilbert, R. T., Rees, M. I., Mohler, H., and Faull, R. L. (2008) Differential localization of GABAA receptor subunits within the substantia nigra of the human brain: an immunohistochemical study, *J Comp Neurol 506*, 912-929.

48. Pirker, S., Schwarzer, C., Wieselthaler, A., Sieghart, W., and Sperk, G. (2000) GABA(A) receptors: immunocytochemical distribution of 13 subunits in the adult rat brain, *Neuroscience 101*, 815-850.

49. Nusser, Z., Sieghart, W., and Somogyi, P. (1998) Segregation of different GABAA receptors to synaptic and extrasynaptic membranes of cerebellar granule cells, *J Neurosci 18*, 1693-1703.

50. Moragues, N., Ciofi, P., Lafon, P., Odessa, M. F., Tramu, G., and Garret, M. (2000) cDNA cloning and expression of a gamma-aminobutyric acid A receptor epsilon-subunit in rat brain, *Eur J Neurosci 12*, 4318-4330.

51. Tsang, S. Y., Ng, S. K., Xu, Z., and Xue, H. (2007) The evolution of GABAA receptor-like genes, *Mol Biol Evol 24*, 599-610.

52. Schofield, P. R., Darlison, M. G., Fujita, N., Burt, D. R., Stephenson, F. A., Rodriguez, H., Rhee, L. M., Ramachandran, J., Reale, V., Glencorse, T. A., et al. (1987) Sequence and functional expression of the GABA A receptor shows a ligand-gated receptor super-family, *Nature 328*, 221-227.

53. Ortells, M. O., and Lunt, G. G. (1995) Evolutionary history of the ligand-gated ion-channel superfamily of receptors, *Trends Neurosci 18*, 121-127.

54. Miyazawa, A., Fujiyoshi, Y., and Unwin, N. (2003) Structure and gating mechanism of the acetylcholine receptor pore, *Nature 423*, 949-955.

55. Smit, A. B., Syed, N. I., Schaap, D., van Minnen, J., Klumperman, J., Kits, K. S., Lodder, H., van der Schors, R. C., van Elk, R., Sorgedrager, B., Brejc, K., Sixma, T. K., and Geraerts, W. P. (2001) A glia-derived acetylcholine-binding protein that modulates synaptic transmission, *Nature 411*, 261-268.

56. Brejc, K., van Dijk, W. J., Klaassen, R. V., Schuurmans, M., van Der Oost, J., Smit, A. B., and Sixma, T. K. (2001) Crystal structure of an ACh-binding protein reveals the ligand-binding domain of nicotinic receptors, *Nature 411*, 269-276.

57. Hilf, R. J., and Dutzler, R. (2008) X-ray structure of a prokaryotic pentameric ligand-gated ion channel, *Nature 452*, 375-379.

58. Hilf, R. J., and Dutzler, R. (2009) Structure of a potentially open state of a proton-activated pentameric ligand-gated ion channel, *Nature 457*, 115-118.

59. Bocquet, N., Nury, H., Baaden, M., Le Poupon, C., Changeux, J. P., Delarue, M., and Corringer, P. J. (2009) X-ray structure of a pentameric ligand-gated ion channel in an apparently open conformation, *Nature 457*, 111-114.

60. Ernst, M., Brauchart, D., Boresch, S., and Sieghart, W. (2003) Comparative modeling of GABA(A) receptors: limits, insights, future

developments, *Neuroscience 119*, 933-943.

61. Baumann, S. W., Baur, R., and Sigel, E. (2002) Forced subunit assembly in alpha1beta2gamma2 GABAA receptors. Insight into the absolute arrangement, *J Biol Chem 277*, 46020-46025.

62. Jensen, M. L., Timmermann, D. B., Johansen, T. H., Schousboe, A., Varming, T., and Ahring, P. K. (2002) The beta subunit determines the ion selectivity of the GABAA receptor, *J Biol Chem 277*, 41438-41447.

63. Padgett, C. L., Hanek, A. P., Lester, H. A., Dougherty, D. A., and Lummis, S. C. (2007) Unnatural amino acid mutagenesis of the GABA(A) receptor binding site residues reveals a novel cation-pi interaction between GABA and beta 2Tyr97, *J Neurosci 27*, 886-892.

64. Buhr, A., and Sigel, E. (1997) A point mutation in the gamma2 subunit of gamma-aminobutyric acid type A receptors results in altered benzodiazepine binding site specificity, *Proc Natl Acad Sci U S A 94*, 8824-8829.

65. Hosie, A. M., Wilkins, M. E., da Silva, H. M., and Smart, T. G. (2006) Endogenous neurosteroids regulate GABAA receptors through two discrete transmembrane sites, *Nature 444*, 486-489.

66. Derry, J. M., Dunn, S. M., and Davies, M. (2004) Identification of a residue in the gamma-aminobutyric acid type A receptor alpha subunit that differentially affects diazepam-sensitive and -insensitive benzodiazepine site binding, *J Neurochem 88*, 1431-1438.

67. Knabl, J., Zeilhofer, U. B., Crestani, F., Rudolph, U., and Zeilhofer, H. U. (2009) Genuine antihyperalgesia by systemic diazepam revealed by experiments in GABAA receptor point-mutated mice, *Pain 141*, 233-238.

68. Williams, C. A., Bell, S. V., and Jenkins, A. (2010) A residue in loop 9 of the beta2-subunit stabilizes the closed state of the GABAA receptor, *J Biol Chem 285*, 7281-7287.

69. Baulac, S., Huberfeld, G., Gourfinkel-An, I., Mitropoulou, G., Beranger, A., Prud'homme, J. F., Baulac, M., Brice, A., Bruzzone, R., and LeGuern, E. (2001) First genetic evidence of GABA(A) receptor

dysfunction in epilepsy: a mutation in the gamma2-subunit gene, *Nat Genet 28*, 46-48.

70. Wallace, R. H., Marini, C., Petrou, S., Harkin, L. A., Bowser, D. N., Panchal, R. G., Williams, D. A., Sutherland, G. R., Mulley, J. C., Scheffer, I. E., and Berkovic, S. F. (2001) Mutant GABA(A) receptor gamma2-subunit in childhood absence epilepsy and febrile seizures, *Nat Genet 28*, 49-52.

71. Cossette, P., Liu, L., Brisebois, K., Dong, H., Lortie, A., Vanasse, M., Saint-Hilaire, J. M., Carmant, L., Verner, A., Lu, W. Y., Wang, Y. T., and Rouleau, G. A. (2002) Mutation of GABRA1 in an autosomal dominant form of juvenile myoclonic epilepsy, *Nat Genet 31*, 184-189.

72. Hales, T. G., Tang, H., Bollan, K. A., Johnson, S. J., King, D. P., McDonald, N. A., Cheng, A., and Connolly, C. N. (2005) The epilepsy mutation, gamma2(R43Q) disrupts a highly conserved inter-subunit contact site, perturbing the biogenesis of GABAA receptors, *Mol Cell Neurosci 29*, 120-127.

73. Kang, J. Q., and Macdonald, R. L. (2004) The GABAA receptor gamma2 subunit R43Q mutation linked to childhood absence epilepsy and febrile seizures causes retention of alpha1beta2gamma2S receptors in the endoplasmic reticulum, *J Neurosci 24*, 8672-8677.

74. Gallagher, M. J., Shen, W., Song, L., and Macdonald, R. L. (2005) Endoplasmic reticulum retention and associated degradation of a GABAA receptor epilepsy mutation that inserts an aspartate in the M3 transmembrane segment of the alpha1 subunit, *J Biol Chem 280*, 37995-38004.

75. Mohler, H. (2006) GABAA receptors in central nervous system disease: anxiety, epilepsy, and insomnia, *J Recept Signal Transduct Res 26*, 731-740.

76. Macdonald, R. L., and Kang, J. Q. (2009) Molecular Pathology of Genetic Epilepsies Associated with GABA(A) Receptor Subunit Mutations, *Epilepsy Curr 9*, 18-23.

77. Nutt, D. J., Ballenger, J. C., Sheehan, D., and Wittchen, H. U. (2002) Generalized anxiety disorder: comorbidity, comparative biology and treatment, *Int J Neuropsychopharmacol 5*, 315-325.

78. Kessler, R. C., Chiu, W. T., Jin, R., Ruscio, A. M., Shear, K., and Walters, E. E. (2006) The epidemiology of panic attacks, panic disorder, and agoraphobia in the National Comorbidity Survey Replication, *Arch Gen Psychiatry 63*, 415-424.

79. Rudolph, U., and Mohler, H. (2004) Analysis of GABAA receptor function and dissection of the pharmacology of benzodiazepines and general anesthetics through mouse genetics, *Annu Rev Pharmacol Toxicol 44*, 475-498.

80. Crowe, R. R., Wang, Z., Noyes, R., Jr., Albrecht, B. E., Darlison, M. G., Bailey, M. E., Johnson, K. J., and Zoega, T. (1997) Candidate gene study of eight GABAA receptor subunits in panic disorder, *Am J Psychiatry 154*, 1096-1100.

81. Schmidt, S. M., Zoega, T., and Crowe, R. R. (1993) Excluding linkage between panic disorder and the gamma-aminobutyric acid beta 1 receptor locus in five Icelandic pedigrees, *Acta Psychiatr Scand 88*, 225-228.

82. Bandelow, B., Zohar, J., Hollander, E., Kasper, S., Moller, H. J., Allgulander, C., Ayuso-Gutierrez, J., Baldwin, D. S., Buenvicius, R., Cassano, G., Fineberg, N., Gabriels, L., Hindmarch, I., Kaiya, H., Klein, D. F., Lader, M., Lecrubier, Y., Lepine, J. P., Liebowitz, M. R., Lopez-Ibor, J. J., Marazziti, D., Miguel, E. C., Oh, K. S., Preter, M., Rupprecht, R., Sato, M., Starcevic, V., Stein, D. J., van Ameringen, M., and Vega, J. (2008) World Federation of Societies of Biological Psychiatry (WFSBP) guidelines for the pharmacological treatment of anxiety, obsessive-compulsive and post-traumatic stress disorders - first revision, *World J Biol Psychiatry 9*, 248-312.

83. Cameron, O. G., Huang, G. C., Nichols, T., Koeppe, R. A., Minoshima, S., Rose, D., and Frey, K. A. (2007) Reduced gamma-aminobutyric acid(A)-benzodiazepine binding sites in insular cortex of individuals with panic disorder, *Arch Gen Psychiatry 64*, 793-800.

84. Malizia, A. L., Cunningham, V. J., Bell, C. J., Liddle, P. F., Jones, T., and Nutt, D. J. (1998) Decreased brain GABA(A)-benzodiazepine receptor binding in panic disorder: preliminary results from a quantitative PET study, *Arch Gen Psychiatry 55*, 715-720.

85. Bremner, J. D., Innis, R. B., White, T., Fujita, M., Silbersweig, D., Goddard, A. W., Staib, L., Stern, E., Cappiello, A., Woods, S., Baldwin, R., and Charney, D. S. (2000) SPECT [I-123]iomazenil measurement of the benzodiazepine receptor in panic disorder, *Biol Psychiatry 47*, 96-106.

86. Goddard, A. W., Mason, G. F., Almai, A., Rothman, D. L., Behar, K. L., Petroff, O. A., Charney, D. S., and Krystal, J. H. (2001) Reductions in occipital cortex GABA levels in panic disorder detected with 1h-magnetic resonance spectroscopy, *Arch Gen Psychiatry 58*, 556-561.

87. Crestani, F., Lorez, M., Baer, K., Essrich, C., Benke, D., Laurent, J. P., Belzung, C., Fritschy, J. M., Luscher, B., and Mohler, H. (1999) Decreased GABAA-receptor clustering results in enhanced anxiety and a bias for threat cues, *Nat Neurosci 2*, 833-839.

88. Folstein, S. E., and Rosen-Sheidley, B. (2001) Genetics of autism: complex aetiology for a heterogeneous disorder, *Nat Rev Genet 2*, 943-955.

89. Maestrini, E., Lai, C., Marlow, A., Matthews, N., Wallace, S., Bailey, A., Cook, E. H., Weeks, D. E., and Monaco, A. P. (1999) Serotonin transporter (5-HTT) and gamma-aminobutyric acid receptor subunit beta3 (GABRB3) gene polymorphisms are not associated with autism in the IMGSA families. The International Molecular Genetic Study of Autism Consortium, *Am J Med Genet 88*, 492-496.

90. Salmon, B., Hallmayer, J., Rogers, T., Kalaydjieva, L., Petersen, P. B., Nicholas, P., Pingree, C., McMahon, W., Spiker, D., Lotspeich, L., Kraemer, H., McCague, P., Dimiceli, S., Nouri, N., Pitts, T., Yang, J., Hinds, D., Myers, R. M., and Risch, N. (1999) Absence of linkage and linkage disequilibrium to chromosome 15q11-q13 markers in 139 multiplex families with autism, *Am J Med Genet 88*, 551-556.

91. Menold, M. M., Shao, Y., Wolpert, C. M., Donnelly, S. L., Raiford, K. L., Martin, E. R., Ravan, S. A., Abramson, R. K., Wright, H. H., Delong, G. R., Cuccaro, M. L., Pericak-Vance, M. A., and Gilbert, J. R. (2001) Association analysis of chromosome 15 gabaa receptor subunit genes in autistic disorder, *J Neurogenet 15*, 245-259.

92. Cook, E. H., Jr., Courchesne, R. Y., Cox, N. J., Lord, C., Gonen, D.,

Guter, S. J., Lincoln, A., Nix, K., Haas, R., Leventhal, B. L., and Courchesne, E. (1998) Linkage-disequilibrium mapping of autistic disorder, with 15q11-13 markers, *Am J Hum Genet 62*, 1077-1083.

93. Martin, E. R., Menold, M. M., Wolpert, C. M., Bass, M. P., Donnelly, S. L., Ravan, S. A., Zimmerman, A., Gilbert, J. R., Vance, J. M., Maddox, L. O., Wright, H. H., Abramson, R. K., DeLong, G. R., Cuccaro, M. L., and Pericak-Vance, M. A. (2000) Analysis of linkage disequilibrium in gamma-aminobutyric acid receptor subunit genes in autistic disorder, *Am J Med Genet 96*, 43-48.

94. Ashley-Koch, A. E., Mei, H., Jaworski, J., Ma, D. Q., Ritchie, M. D., Menold, M. M., Delong, G. R., Abramson, R. K., Wright, H. H., Hussman, J. P., Cuccaro, M. L., Gilbert, J. R., Martin, E. R., and Pericak-Vance, M. A. (2006) An analysis paradigm for investigating multi-locus effects in complex disease: examination of three GABA receptor subunit genes on 15q11-q13 as risk factors for autistic disorder, *Ann Hum Genet 70*, 281-292.

95. Hogart, A., Wu, D., LaSalle, J. M., and Schanen, N. C. (2010) The comorbidity of autism with the genomic disorders of chromosome 15q11.2-q13, *Neurobiol Dis 38*, 181-191.

96. Oblak, A., Gibbs, T. T., and Blatt, G. J. (2009) Decreased GABAA receptors and benzodiazepine binding sites in the anterior cingulate cortex in autism, *Autism Res 2*, 205-219.

97. Hogart, A., Nagarajan, R. P., Patzel, K. A., Yasui, D. H., and Lasalle, J. M. (2007) 15q11-13 GABAA receptor genes are normally biallelically expressed in brain yet are subject to epigenetic dysregulation in autism-spectrum disorders, *Hum Mol Genet 16*, 691-703.

98. Eagleson, K. L., Gravielle, M. C., Schlueter McFadyen-Ketchum, L. J., Russek, S. J., Farb, D. H., and Levitt, P. (2010) Genetic disruption of the autism spectrum disorder risk gene PLAUR induces GABAA receptor subunit changes, *Neuroscience 168*, 797-810.

99. Campbell, D. B., Li, C., Sutcliffe, J. S., Persico, A. M., and Levitt, P. (2008) Genetic evidence implicating multiple genes in the MET receptor tyrosine kinase pathway in autism spectrum disorder, *Autism*

Res 1, 159-168.

100. Hauser, W. A., Annegers, J. F., and Kurland, L. T. (1993) Incidence of epilepsy and unprovoked seizures in Rochester, Minnesota: 1935-1984, *Epilepsia 34*, 453-468.

101. Leonardi, M., and Ustun, T. B. (2002) The global burden of epilepsy, *Epilepsia 43 Suppl 6*, 21-25.

102. Ma, S., Abou-Khalil, B., Blair, M. A., Sutcliffe, J. S., Haines, J. L., and Hedera, P. (2006) Mutations in GABRA1, GABRA5, GABRG2 and GABRD receptor genes are not a major factor in the pathogenesis of familial focal epilepsy preceded by febrile seizures, *Neurosci Lett 394*, 74-78.

103. Orrico, A., Galli, L., Grosso, S., Buoni, S., Pianigiani, R., Balestri, P., and Sorrentino, V. (2009) Mutational analysis of the SCN1A, SCN1B and GABRG2 genes in 150 Italian patients with idiopathic childhood epilepsies, *Clin Genet 75*, 579-581.

104. Ma, S., Blair, M. A., Abou-Khalil, B., Lagrange, A. H., Gurnett, C. A., and Hedera, P. (2006) Mutations in the GABRA1 and EFHC1 genes are rare in familial juvenile myoclonic epilepsy, *Epilepsy Res 71*, 129-134.

105. Kapoor, A., Vijai, J., Ravishankar, H. M., Satishchandra, P., Radhakrishnan, K., and Anand, A. (2003) Absence of GABRA1 Ala322Asp mutation in juvenile myoclonic epilepsy families from India, *J Genet 82*, 17-21.

106. Marini, C., Scheffer, I. E., Crossland, K. M., Grinton, B. E., Phillips, F. L., McMahon, J. M., Turner, S. J., Dean, J. T., Kivity, S., Mazarib, A., Neufeld, M. Y., Korczyn, A. D., Harkin, L. A., Dibbens, L. M., Wallace, R. H., Mulley, J. C., and Berkovic, S. F. (2004) Genetic architecture of idiopathic generalized epilepsy: clinical genetic analysis of 55 multiplex families, *Epilepsia 45*, 467-478.

107. Fisher, J. L., and Macdonald, R. L. (1998) The role of an alpha subtype M2-M3 His in regulating inhibition of GABAA receptor current by zinc and other divalent cations, *J Neurosci 18*, 2944-2953.

108. Macdonald, R. L., Bianchi, M. T., and Feng, H. (2003) Mutations

linked to generalized epilepsy in humans reduce GABA(A) receptor current, *Exp Neurol 184 Suppl 1*, S58-67.

109. Bianchi, M. T., Song, L., Zhang, H., and Macdonald, R. L. (2002) Two different mechanisms of disinhibition produced by GABAA receptor mutations linked to epilepsy in humans, *J Neurosci 22*, 5321-5327.

110. Audenaert, D., Schwartz, E., Claeys, K. G., Claes, L., Deprez, L., Suls, A., Van Dyck, T., Lagae, L., Van Broeckhoven, C., Macdonald, R. L., and De Jonghe, P. (2006) A novel GABRG2 mutation associated with febrile seizures, *Neurology 67*, 687-690.

111. Kananura, C., Haug, K., Sander, T., Runge, U., Gu, W., Hallmann, K., Rebstock, J., Heils, A., and Steinlein, O. K. (2002) A splice-site mutation in GABRG2 associated with childhood absence epilepsy and febrile convulsions, *Arch Neurol 59*, 1137-1141.

112. Harkin, L. A., Bowser, D. N., Dibbens, L. M., Singh, R., Phillips, F., Wallace, R. H., Richards, M. C., Williams, D. A., Mulley, J. C., Berkovic, S. F., Scheffer, I. E., and Petrou, S. (2002) Truncation of the GABA(A)-receptor gamma2 subunit in a family with generalized epilepsy with febrile seizures plus, *Am J Hum Genet 70*, 530-536.

113. Kang, J. Q., Shen, W., and Macdonald, R. L. (2009) The GABRG2 mutation, Q351X, associated with generalized epilepsy with febrile seizures plus, has both loss of function and dominant-negative suppression, *J Neurosci 29*, 2845-2856.

114. Kang, J. Q., Shen, W., and Macdonald, R. L. (2009) Two molecular pathways (NMD and ERAD) contribute to a genetic epilepsy associated with the GABA(A) receptor GABRA1 PTC mutation, 975delC, S326fs328X, *J Neurosci 29*, 2833-2844.

115. Sun, H., Zhang, Y., Liang, J., Liu, X., Ma, X., Wu, H., Xu, K., Qin, J., Qi, Y., and Wu, X. (2008) SCN1A, SCN1B, and GABRG2 gene mutation analysis in Chinese families with generalized epilepsy with febrile seizures plus, *J Hum Genet 53*, 769-774.

116. Gallagher, M. J., Ding, L., Maheshwari, A., and Macdonald, R. L. (2007) The GABAA receptor alpha1 subunit epilepsy mutation A322D inhibits transmembrane helix formation and causes proteasomal degradation, *Proc Natl Acad Sci U S A 104*, 12999-13004.

117. Fisher, J. L. (2004) A mutation in the GABAA receptor alpha 1 subunit linked to human epilepsy affects channel gating properties, *Neuropharmacology 46*, 629-637.

118. Gallagher, M. J., Song, L., Arain, F., and Macdonald, R. L. (2004) The juvenile myoclonic epilepsy GABA(A) receptor alpha1 subunit mutation A322D produces asymmetrical, subunit position-dependent reduction of heterozygous receptor currents and alpha1 subunit protein expression, *J Neurosci 24*, 5570-5578.

119. Bradley, C. A., Taghibiglou, C., Collingridge, G. L., and Wang, Y. T. (2008) Mechanisms involved in the reduction of GABAA receptor alpha1-subunit expression caused by the epilepsy mutation A322D in the trafficking-competent receptor, *J Biol Chem 283*, 22043-22050.

120. Maljevic, S., Krampfl, K., Cobilanschi, J., Tilgen, N., Beyer, S., Weber, Y. G., Schlesinger, F., Ursu, D., Melzer, W., Cossette, P., Bufler, J., Lerche, H., and Heils, A. (2006) A mutation in the GABA(A) receptor alpha(1)-subunit is associated with absence epilepsy, *Ann Neurol 59*, 983-987.

121. Tanaka, M., Olsen, R. W., Medina, M. T., Schwartz, E., Alonso, M. E., Duron, R. M., Castro-Ortega, R., Martinez-Juarez, I. E., Pascual-Castroviejo, I., Machado-Salas, J., Silva, R., Bailey, J. N., Bai, D., Ochoa, A., Jara-Prado, A., Pineda, G., Macdonald, R. L., and Delgado-Escueta, A. V. (2008) Hyperglycosylation and reduced GABA currents of mutated GABRB3 polypeptide in remitting childhood absence epilepsy, *Am J Hum Genet 82*, 1249-1261.

122. Lo, W. Y., Lagrange, A. H., Hernandez, C. C., Harrison, R., Dell, A., Haslam, S. M., Sheehan, J. H., and Macdonald, R. L. (2010) Glycosylation of beta2 subunits regulates GABAA receptor biogenesis and channel gating, *J Biol Chem*.

123. Neher, E., and Sakmann, B. (1976) Single-channel currents recorded from membrane of denervated frog muscle fibres, *Nature 260*, 799-802.

124. Neher, E., and Sakmann, B. (1992) The patch clamp technique, *Sci Am 266*, 44-51.

125. Sakmann, B., and Neher, E., (Eds.) (1995) *Single-Channel Recording*, 2nd

ed., Plenum Press, New York.

126. Keramidas, A., and Harrison, N. L. (2008) Agonist-dependent single channel current and gating in alpha4beta2delta and alpha1beta2gamma2S GABAA receptors, *J Gen Physiol 131*, 163-181.

127. Lema, G. M., and Auerbach, A. (2006) Modes and models of GABA(A) receptor gating, *J Physiol 572*, 183-200.

128. Campo-Soria, C., Chang, Y., and Weiss, D. S. (2006) Mechanism of action of benzodiazepines on GABAA receptors, *Br J Pharmacol 148*, 984-990.

129. Conti-Tronconi, B. M., and Raftery, M. A. (1982) The nicotinic cholinergic receptor: correlation of molecular structure with functional properties, *Annu Rev Biochem 51*, 491-530.

130. Sigel, E., Stephenson, F. A., Mamalaki, C., and Barnard, E. A. (1983) A gamma-aminobutyric acid/benzodiazepine receptor complex of bovine cerebral cortex, *J Biol Chem 258*, 6965-6971.

131. Stauber, G. B., Ransom, R. W., Dilber, A. I., and Olsen, R. W. (1987) The gamma-aminobutyric-acid/benzodiazepine-receptor protein from rat brain. Large-scale purification and preparation of antibodies, *Eur J Biochem 167*, 125-133.

132. Macdonald, R. L., and Olsen, R. W. (1994) GABAA receptor channels, *Annu Rev Neurosci 17*, 569-602.

133. Karpen, J. W., Aoshima, H., Abood, L. G., and Hess, G. P. (1982) Cocaine and phencyclidine inhibition of the acetylcholine receptor: analysis of the mechanisms of action based on measurements of ion flux in the millisecond-to-minute time region, *Proc Natl Acad Sci U S A 79*, 2509-2513.

134. Hess, G. P. (2003) Rapid chemical reaction techniques developed for use in investigations of membrane-bound proteins (neurotransmitter receptors), *Biophys Chem 100*, 493-506.

135. Hess, G. P., Gameiro, A. M., Schoenfeld, R. C., Chen, Y., Ulrich, H., Nye, J. A., Sit, B., Carroll, F. I., and Ganem, B. (2003) Reversing the action of noncompetitive inhibitors (MK-801 and cocaine) on a

protein (nicotinic acetylcholine receptor)-mediated reaction, *Biochemistry 42*, 6106-6114.

136. Chen, Y., Banerjee, A., and Hess, G. P. (2004) Mechanism-based discovery of small molecules that prevent noncompetitive inhibition by cocaine and MK-801 mediated by two different sites on the nicotinic acetylcholine receptor, *Biochemistry 43*, 10149-10156.

137. Hess, G. P., Udgaonkar, J. B., and Olbricht, W. L. (1987) Chemical kinetic measurements of transmembrane processes using rapid reaction techniques: acetylcholine receptor, *Annu Rev Biophys Biophys Chem 16*, 507-534.

138. Landau, V. H., and Lifshitz, E. M. (1959) *Fluid Mechanics*, Pergamon Press, Oxford, UK.

139. Johnston, G. A. (1996) GABAA receptor pharmacology, *Pharmacol Ther 69*, 173-198.

140. Kopp, S., Baur, R., Sigel, E., Mohler, H., and Altmann, K. H. (2010) Highly potent modulation of GABA(A) receptors by valerenic acid derivatives, *ChemMedChem 5*, 678-681.

141. Study, R. E., and Barker, J. L. (1981) Diazepam and (--)-pentobarbital: fluctuation analysis reveals different mechanisms for potentiation of gamma-aminobutyric acid responses in cultured central neurons, *Proc Natl Acad Sci U S A 78*, 7180-7184.

142. Twyman, R. E., Rogers, C. J., and Macdonald, R. L. (1989) Differential regulation of gamma-aminobutyric acid receptor channels by diazepam and phenobarbital, *Ann Neurol 25*, 213-220.

143. Bianchi, M. T., and Macdonald, R. L. (2003) Neurosteroids shift partial agonist activation of GABA(A) receptor channels from low- to high-efficacy gating patterns, *J Neurosci 23*, 10934-10943.

144. Meera, P., Olsen, R. W., Otis, T. S., and Wallner, M. (2009) Etomidate, propofol and the neurosteroid THDOC increase the GABA efficacy of recombinant alpha4beta3delta and alpha4beta3 GABA A receptors expressed in HEK cells, *Neuropharmacology 56*, 155-160.

145. Zheleznova, N., Sedelnikova, A., and Weiss, D. S. (2008) alpha1beta2delta, a silent GABAA receptor: recruitment by tracazolate and neurosteroids, *Br J Pharmacol 153*, 1062-1071.

146. Jones-Davis, D. M., Song, L., Gallagher, M. J., and Macdonald, R. L. (2005) Structural determinants of benzodiazepine allosteric regulation of GABA(A) receptor currents, *J Neurosci 25*, 8056-8065.

147. Rudolph, U., and Mohler, H. (2006) GABA-based therapeutic approaches: GABAA receptor subtype functions, *Curr Opin Pharmacol 6*, 18-23.

148. Khong, E., Sim, M. G., and Hulse, G. (2004) Benzodiazepine dependence, *Aust Fam Physician 33*, 923-926.

149. Tone, A. (2005) Listening to the past: history, psychiatry, and anxiety, *Can J Psychiatry 50*, 373-380.

150. Smith, M. C., and Riskin, B. J. (1991) The clinical use of barbiturates in neurological disorders, *Drugs 42*, 365-378.

151. Peters, J. A., Kirkness, E. F., Callachan, H., Lambert, J. J., and Turner, A. J. (1988) Modulation of the GABAA receptor by depressant barbiturates and pregnane steroids, *Br J Pharmacol 94*, 1257-1269.

152. Leeb-Lundberg, F., Snowman, A., and Olsen, R. W. (1980) Barbiturate receptor sites are coupled to benzodiazepine receptors, *Proc Natl Acad Sci U S A 77*, 7468-7472.

153. MacDonald, R. L., Rogers, C. J., and Twyman, R. E. (1989) Barbiturate regulation of kinetic properties of the GABAA receptor channel of mouse spinal neurones in culture, *J Physiol 417*, 483-500.

154. Fisher, M. T., and Fisher, J. L. (2010) Activation of alpha6-containing GABAA receptors by pentobarbital occurs through a different mechanism than activation by GABA, *Neurosci Lett 471*, 195-199.

155. Rho, J. M., Donevan, S. D., and Rogawski, M. A. (1996) Direct activation of GABAA receptors by barbiturates in cultured rat hippocampal neurons, *J Physiol 497 (Pt 2)*, 509-522.

156. Steinbach, J. H., and Akk, G. (2001) Modulation of GABA(A)

receptor channel gating by pentobarbital, *J Physiol 537*, 715-733.

157. Macdonald, R. L., and Barker, J. L. (1979) Anticonvulsant and anesthetic barbiturates: different postsynaptic actions in cultured mammalian neurons, *Neurology 29*, 432-447.

158. Callachan, H., Cottrell, G. A., Hather, N. Y., Lambert, J. J., Nooney, J. M., and Peters, J. A. (1987) Modulation of the GABAA receptor by progesterone metabolites, *Proc R Soc Lond B Biol Sci 231*, 359-369.

159. Atack, J. R. (2008) GABA(A) receptor subtype-selective efficacy: TPA023, an alpha2/alpha3 selective non-sedating anxiolytic and alpha5IA, an alpha5 selective cognition enhancer, *CNS Neurosci Ther 14*, 25-35.

160. Atack, J. R., Wafford, K. A., Tye, S. J., Cook, S. M., Sohal, B., Pike, A., Sur, C., Melillo, D., Bristow, L., Bromidge, F., Ragan, I., Kerby, J., Street, L., Carling, R., Castro, J. L., Whiting, P., Dawson, G. R., and McKernan, R. M. (2006) TPA023 [7-(1,1-dimethylethyl)-6-(2-ethyl-2H-1,2,4-triazol-3-ylmethoxy)-3-(2-fluor ophenyl)-1,2,4-triazolo[4,3-b]pyridazine], an agonist selective for alpha2- and alpha3-containing GABAA receptors, is a nonsedating anxiolytic in rodents and primates, *J Pharmacol Exp Ther 316*, 410-422.

161. Mirza, N. R., Larsen, J. S., Mathiasen, C., Jacobsen, T. A., Munro, G., Erichsen, H. K., Nielsen, A. N., Troelsen, K. B., Nielsen, E. O., and Ahring, P. K. (2008) NS11394 [3'-[5-(1-hydroxy-1-methyl-ethyl)-benzoimidazol-1-yl]-biphenyl-2-carbonitr ile], a unique subtype-selective GABAA receptor positive allosteric modulator: in vitro actions, pharmacokinetic properties and in vivo anxiolytic efficacy, *J Pharmacol Exp Ther 327*, 954-968.

162. Fahey, J. M., Grassi, J. M., Reddi, J. M., and Greenblatt, D. J. (2006) Acute zolpidem administration produces pharmacodynamic and receptor occupancy changes at similar doses, *Pharmacol Biochem Behav 83*, 21-27.

163. Lewis, R. W., Mabry, J., Polisar, J. G., Eagen, K. P., Ganem, B., and Hess, G. P. (2010) Dihydropyrimidinone positive modulation of delta-subunit-containing gamma-aminobutyric acid type a receptors, including an epilepsy-linked mutant variant, *Biochemistry 49*, 4841-4851.

164. Benke, D., Mertens, S., Trzeciak, A., Gillessen, D., and Mohler, H. (1991) Identification and immunohistochemical mapping of GABAA receptor subtypes containing the delta-subunit in rat brain, *FEBS Lett 283*, 145-149.

165. Laurie, D. J., Seeburg, P. H., and Wisden, W. (1992) The distribution of 13 GABAA receptor subunit mRNAs in the rat brain. II. Olfactory bulb and cerebellum, *J Neurosci 12*, 1063-1076.

166. Korpi, E. R., Mihalek, R. M., Sinkkonen, S. T., Hauer, B., Hevers, W., Homanics, G. E., Sieghart, W., and Luddens, H. (2002) Altered receptor subtypes in the forebrain of GABA(A) receptor delta subunit-deficient mice: recruitment of gamma 2 subunits, *Neuroscience 109*, 733-743.

167. Mertens, S., Benke, D., and Mohler, H. (1993) GABAA receptor populations with novel subunit combinations and drug binding profiles identified in brain by alpha 5- and delta-subunit-specific immunopurification, *J Biol Chem 268*, 5965-5973.

168. Araujo, F., Ruano, D., and Vitorica, J. (1998) Absence of association between delta and gamma2 subunits in native GABA(A) receptors from rat brain, *Eur J Pharmacol 347*, 347-353.

169. Quirk, K., Whiting, P. J., Ragan, C. I., and McKernan, R. M. (1995) Characterisation of delta-subunit containing GABAA receptors from rat brain, *Eur J Pharmacol 290*, 175-181.

170. Saxena, N. C., and Macdonald, R. L. (1994) Assembly of GABAA receptor subunits: role of the delta subunit, *J Neurosci 14*, 7077-7086.

171. Storustovu, S. I., and Ebert, B. (2006) Pharmacological characterization of agonists at delta-containing GABAA receptors: Functional selectivity for extrasynaptic receptors is dependent on the absence of gamma2, *J Pharmacol Exp Ther 316*, 1351-1359.

172. Thompson, S. A., Wingrove, P. B., Connelly, L., Whiting, P. J., and Wafford, K. A. (2002) Tracazolate reveals a novel type of allosteric interaction with recombinant gamma-aminobutyric acid(A) receptors, *Mol Pharmacol 61*, 861-869.

173. Boehm, S. L., 2nd, Homanics, G. E., Blednov, Y. A., and Harris, R. A.

(2006) delta-Subunit containing GABAA receptor knockout mice are less sensitive to the actions of 4,5,6,7-tetrahydroisoxazolo-[5,4-c]pyridin-3-ol, *Eur J Pharmacol 541*, 158-162.

174. Wohlfarth, K. M., Bianchi, M. T., and Macdonald, R. L. (2002) Enhanced neurosteroid potentiation of ternary GABA(A) receptors containing the delta subunit, *J Neurosci 22*, 1541-1549.

175. Mtchedlishvili, Z., and Kapur, J. (2006) High-affinity, slowly desensitizing GABAA receptors mediate tonic inhibition in hippocampal dentate granule cells, *Mol Pharmacol 69*, 564-575.

176. Glykys, J., and Mody, I. (2007) Activation of GABAA receptors: views from outside the synaptic cleft, *Neuron 56*, 763-770.

177. Mihalek, R. M., Banerjee, P. K., Korpi, E. R., Quinlan, J. J., Firestone, L. L., Mi, Z. P., Lagenaur, C., Tretter, V., Sieghart, W., Anagnostaras, S. G., Sage, J. R., Fanselow, M. S., Guidotti, A., Spigelman, I., Li, Z., DeLorey, T. M., Olsen, R. W., and Homanics, G. E. (1999) Attenuated sensitivity to neuroactive steroids in gamma-aminobutyrate type A receptor delta subunit knockout mice, *Proc Natl Acad Sci U S A 96*, 12905-12910.

178. Spigelman, I., Li, Z., Banerjee, P. K., Mihalek, R. M., Homanics, G. E., and Olsen, R. W. (2002) Behavior and physiology of mice lacking the GABAA-receptor delta subunit, *Epilepsia 43 Suppl 5*, 3-8.

179. Vicini, S., Losi, G., and Homanics, G. E. (2002) GABA(A) receptor delta subunit deletion prevents neurosteroid modulation of inhibitory synaptic currents in cerebellar neurons, *Neuropharmacology 43*, 646-650.

180. Porcello, D. M., Huntsman, M. M., Mihalek, R. M., Homanics, G. E., and Huguenard, J. R. (2003) Intact synaptic GABAergic inhibition and altered neurosteroid modulation of thalamic relay neurons in mice lacking delta subunit, *J Neurophysiol 89*, 1378-1386.

181. Del Castillo, J., and Katz, B. (1955) Production of membrane potential changes in the frog's heart by inhibitory nerve impulses, *Nature 175*, 1035.

182. Marmont, G. (1949) Studies on the axon membrane; a new method, *J Cell Physiol 34*, 351-382.

183. Hodgkin, A. L., and Huxley, A. F. (1952) Movement of sodium and potassium ions during nervous activity, *Cold Spring Harb Symp Quant Biol 17*, 43-52.

184. Neher, E., Sakmann, B., and Steinbach, J. H. (1978) The extracellular patch clamp: a method for resolving currents through individual open channels in biological membranes, *Pflugers Arch 375*, 219-228.

185. Sigworth, F. J., and Neher, E. (1980) Single Na+ channel currents observed in cultured rat muscle cells, *Nature 287*, 447-449.

186. Hamill, O. P., Marty, A., Neher, E., Sakmann, B., and Sigworth, F. J. (1981) Improved patch-clamp techniques for high-resolution current recording from cells and cell-free membrane patches, *Pflugers Arch 391*, 85-100.

187. Hille, B. (2001) *Ion Channels of Excitable Membranes*, Third Edition ed., Sinauer Associates, Inc., Sunderland, MA.

188. Walz, W., Boulton, A. A., and Baker, G. B., (Eds.) (2002) *Patch-Clamp Analysis Advanced Techniques*, Vol. 35, Humana Press, Totowa, New Jersey.

189. Mortensen, M., and Smart, T. G. (2007) Single-channel recording of ligand-gated ion channels, *Nat Protoc 2*, 2826-2841.

190. Krishtal, O. A., and Pidoplichko, V. I. (1980) A receptor for protons in the nerve cell membrane, *Neuroscience 5*, 2325-2327.

191. Trussell, L. O., and Fischbach, G. D. (1989) Glutamate receptor desensitization and its role in synaptic transmission, *Neuron 3*, 209-218.

192. Vyklicky, L., Jr., Benveniste, M., and Mayer, M. L. (1990) Modulation of N-methyl-D-aspartic acid receptor desensitization by glycine in mouse cultured hippocampal neurones, *J Physiol 428*, 313-331.

193. Franke, C., Hatt, H., and Dudel, J. (1987) Liquid filament switch for ultra-fast exchanges of solutions at excised patches of synaptic membrane of crayfish muscle, *Neurosci Lett 77*, 199-204.

194. Edmonds, B., Gibb, A. J., and Colquhoun, D. (1995) Mechanisms of

activation of muscle nicotinic acetylcholine receptors and the time course of endplate currents, *Annu Rev Physiol 57*, 469-493.

195. Botzolakis, E. J., Maheshwari, A., Feng, H. J., Lagrange, A. H., Shaver, J. H., Kassebaum, N. J., Venkataraman, R., Baudenbacher, F., and Macdonald, R. L. (2009) Achieving synaptically relevant pulses of neurotransmitter using PDMS microfluidics, *J Neurosci Methods 177*, 294-302.

196. Sigel, E. (1987) Properties of single sodium channels translated by Xenopus oocytes after injection with messenger ribonucleic acid, *J Physiol 386*, 73-90.

197. Niu, L., Grewer, C., and Hess, G. P. (1996) Chemical kinetic investigations of neurotransmitter receptors on a cell surface in the ms time region., *Tech. Protein Chem. 7*, 139-149.

198. Milburn, T., Matsubara, N., Billington, A. P., Udgaonkar, J. B., Walker, J. W., Carpenter, B. K., Webb, W. W., Marque, J., Denk, W., McCray, J. A., and et al. (1989) Synthesis, photochemistry, and biological activity of a caged photolabile acetylcholine receptor ligand, *Biochemistry 28*, 49-55.

199. Matsubara, N., Billington, A. P., and Hess, G. P. (1992) How fast does an acetylcholine receptor channel open? Laser-pulse photolysis of an inactive precursor of carbamoylcholine in the microsecond time region with BC3H1 cells, *Biochemistry 31*, 5507-5514.

200. Kaplan, J. H., Forbush, B., 3rd, and Hoffman, J. F. (1978) Rapid photolytic release of adenosine 5'-triphosphate from a protected analogue: utilization by the Na:K pump of human red blood cell ghosts, *Biochemistry 17*, 1929-1935.

201. Adams, S. R., and Tsien, R. Y. (1993) Controlling cell chemistry with caged compounds, *Annu Rev Physiol 55*, 755-784.

202. Corrie, J. E. T., and Trentham, D. R., (Eds.) (1993) *Bioorganic Photochemistry 2*, Wiley, New York.

203. Hess, G. P. (1993) Determination of the chemical mechanism of neurotransmitter receptor-mediated reactions by rapid chemical kinetic techniques, *Biochemistry 32*, 989-1000.

204. Nerbonne, J. M. (1996) Caged compounds: tools for illuminating neuronal responses and connections, *Curr Opin Neurobiol 6*, 379-386.

205. Marriott, G., (Ed.) (1998) *Caged Compounds*, Academic Press, New York.

206. Mayer, G., and Heckel, A. (2006) Biologically active molecules with a "light switch", *Angew Chem Int Ed Engl 45*, 4900-4921.

207. Denk, W., Strickler, J. H., and Webb, W. W. (1990) Two-photon laser scanning fluorescence microscopy, *Science 248*, 73-76.

208. Kotter, R., Schubert, D., Dyhrfjeld-Johnsen, J., Luhmann, H. J., and Staiger, J. F. (2005) Optical release of caged glutamate for stimulation of neurons in the in vitro slice preparation, *J Biomed Opt 10*, 11003.

209. Wang, S. S., and Augustine, G. J. (1995) Confocal imaging and local photolysis of caged compounds: dual probes of synaptic function, *Neuron 15*, 755-760.

210. Li, H., Avery, L., Denk, W., and Hess, G. P. (1997) Identification of chemical synapses in the pharynx of Caenorhabditis elegans, *Proc Natl Acad Sci U S A 94*, 5912-5916.

211. Bochet, C. G. (2002) Photolabile protecting groups and linkers, *J. Chem. Soc., Perkin Trans. 1*, 125-142.

212. Ramesh, D., Wieboldt, R., Niu, L., Carpenter, B. K., and Hess, G. P. (1993) Photolysis of a protecting group for the carboxyl function of neurotransmitters within 3 microseconds and with product quantum yield of 0.2, *Proc Natl Acad Sci U S A 90*, 11074-11078.

213. Niu, L., Wieboldt, R., Ramesh, D., Carpenter, B. K., and Hess, G. P. (1996) Synthesis and characterization of a caged receptor ligand suitable for chemical kinetic investigations of the glycine receptor in the 3-microseconds time domain, *Biochemistry 35*, 8136-8142.

214. Park, C. H., and Givens, R. S. (1997) New photoactivated protecting groups. 6. *p*-Hydroxyphenacyl: A phototrigger for chemical and biobhemical probes., *J. Am. Chem. Soc. 119*, 2453-2463.

215. Givens, R. S., Weber, J. F., Jung, A. H., and Park, C. H. (1998) New

photoprotecting groups: desyl and p-hydroxyphenacyl phosphate and carboxylate esters, *Methods Enzymol 291*, 1-29.

216. Bendig, J., Helm, S., and Hagen, V. (1997) (Coumarin-4-yl)Methyl Ester of cGMP and 8-Br-cGMP: Photochemical fluorescence enhancement., *J. Fluorescence 7*, 357-361.

217. Furuta, T., and Iwamura, M. (1998) New caged groups: 7-substituted coumarinylmethyl phosphate esters, *Methods Enzymol 291*, 50-63.

218. Rial Verde, E. M., Zayat, L., Etchenique, R., and Yuste, R. (2008) Photorelease of GABA with Visible Light Using an Inorganic Caging Group, *Front Neural Circuits 2*, 2.

219. Breitinger, H. G., Wieboldt, R., Ramesh, D., Carpenter, B. K., and Hess, G. P. (2000) Synthesis and characterization of photolabile derivatives of serotonin for chemical kinetic investigations of the serotonin 5-HT(3) receptor, *Biochemistry 39*, 5500-5508.

220. Murov, S., Carmichael, I., and Hug, G. (1993) *Handbook of Photochemistry*, 2nd ed., Marcel Dekker, New York, NY.

221. Hatchard, C. G., and Parker, C. A. (1956) A New Sensitive Chemical Actinometer. II. Potassium Ferrioxalate as a Standard Chemical Actinometer, *Proceedings of the Royal Society of London. Series A. Mathematical and Physical Sciences 235*, 518-536.

222. Walker, J. W., McCray, J. A., and Hess, G. P. (1986) Photolabile protecting groups for an acetylcholine receptor ligand. Synthesis and photochemistry of a new class of o-nitrobenzyl derivatives and their effects on receptor function, *Biochemistry 25*, 1799-1805.

223. McCray, J. A., Herbette, L., Kihara, T., and Trentham, D. R. (1980) A new approach to time-resolved studies of ATP-requiring biological systems; laser flash photolysis of caged ATP, *Proc Natl Acad Sci U S A 77*, 7237-7241.

224. Walker, J. W., Reid, G. P., McCray, J. A., and Trentham, D. R. (2002) Photolabile 1-(2-nitrophenyl)ethyl phosphate esters of adenine nucleotide analogs. Synthesis and mechanism of photolysis, *Journal of the American Chemical Society 110*, 7170-7177.

225. Ramakrishnan, L., and Hess, G. P. (2005) Picrotoxin inhibition mechanism of a gamma-aminobutyric acid A receptor investigated by a laser-pulse photolysis technique, *Biochemistry 44*, 8523-8532.

226. Gee, K. R., Wieboldt, R., and Hess, G. P. (1994) Synthesis and photochemistry of a new photolabile derivative of GABA. Neurotransmitter release and receptor activation in the ms time region., *J. Am. Chem. Soc. 116*, 8366-8367.

227. Mehta, A. K., and Ticku, M. K. (1999) An update on GABAA receptors, *Brain Res Brain Res Rev 29*, 196-217.

228. Mohler, H., Benke, D., Benson, J., Luscher, B., and Fritschy, J. M. (1995) GABAA-receptor subtypes in vivo: cellular localization, pharmacology and regulation, *Adv Biochem Psychopharmacol 48*, 41-56.

229. Macdonald, R. L., Gallagher, M. J., Feng, H. J., and Kang, J. (2004) GABA(A) receptor epilepsy mutations, *Biochem Pharmacol 68*, 1497-1506.

230. Zeller, A., Jurd, R., Lambert, S., Arras, M., Drexler, B., Grashoff, C., Antkowiak, B., and Rudolph, U. (2008) Inhibitory ligand-gated ion channels as substrates for general anesthetic actions, *Handb Exp Pharmacol*, 31-51.

231. Meldrum, B. S., and Rogawski, M. A. (2007) Molecular targets for antiepileptic drug development, *Neurotherapeutics 4*, 18-61.

232. Atack, J. R. (2005) The benzodiazepine binding site of GABA(A) receptors as a target for the development of novel anxiolytics, *Expert Opin Investig Drugs 14*, 601-618.

233. Agid, Y., Buzsaki, G., Diamond, D. M., Frackowiak, R., Giedd, J., Girault, J. A., Grace, A., Lambert, J. J., Manji, H., Mayberg, H., Popoli, M., Prochiantz, A., Richter-Levin, G., Somogyi, P., Spedding, M., Svenningsson, P., and Weinberger, D. (2007) How can drug discovery for psychiatric disorders be improved?, *Nat Rev Drug Discov 6*, 189-201.

234. Mody, I., Glykys, J., and Wei, W. (2007) A new meaning for "Gin & Tonic": tonic inhibition as the target for ethanol action in the brain, *Alcohol 41*, 145-153.

235. Boussif, O., Lezoualc'h, F., Zanta, M. A., Mergny, M. D., Scherman, D., Demeneix, B., and Behr, J. P. (1995) A versatile vector for gene and oligonucleotide transfer into cells in culture and in vivo: polyethylenimine, *Proc Natl Acad Sci U S A 92*, 7297-7301.

236. Matsubara, N., and Hess, G. P. (1992) On the mechanism of a mammalian neuronal type nicotinic acetylcholine receptor investigated by a rapid chemical kinetic technique. Detection and characterization of a short-lived, previously unobserved, main receptor form in PC12 cells, *Biochemistry 31*, 5477-5487.

237. Haas, K. F., and Macdonald, R. L. (1999) GABAA receptor subunit gamma2 and delta subtypes confer unique kinetic properties on recombinant GABAA receptor currents in mouse fibroblasts, *J Physiol 514 (Pt 1)*, 27-45.

238. Hadley, S. H., and Amin, J. (2007) Rat alpha6beta2delta GABAA receptors exhibit two distinct and separable agonist affinities, *J Physiol 581*, 1001-1018.

239. Neelands, T. R., Greenfield, L. J., Jr., Zhang, J., Turner, R. S., and Macdonald, R. L. (1998) GABAA receptor pharmacology and subtype mRNA expression in human neuronal NT2-N cells, *J Neurosci 18*, 4993-5007.

240. Orser, B. A., McAdam, L. C., Roder, S., and MacDonald, J. F. (1998) General anaesthetics and their effects on GABA(A) receptor desensitization, *Toxicol Lett 100-101*, 217-224.

241. Yang, P., Jones, B. L., and Henderson, L. P. (2005) Role of the alpha subunit in the modulation of GABA(A) receptors by anabolic androgenic steroids, *Neuropharmacology 49*, 300-316.

242. Kapoor, T. M., Mayer, T. U., Coughlin, M. L., and Mitchison, T. J. (2000) Probing spindle assembly mechanisms with monastrol, a small molecule inhibitor of the mitotic kinesin, Eg5, *J Cell Biol 150*, 975-988.

243. Maliga, Z., and Mitchison, T. J. (2006) Small-molecule and mutational analysis of allosteric Eg5 inhibition by monastrol, *BMC Chem Biol 6*, 2.

244. Kappe, C. O. (2000) Biologically active dihydropyrimidones of the Biginelli-type--a literature survey, *Eur J Med Chem 35*, 1043-1052.

245. Cho, H., Ueda, M., Shima, K., Mizuno, A., Hayashimatsu, M., Ohnaka, Y., Takeuchi, Y., Hamaguchi, M., Aisaka, K., Hidaka, T., and et al. (1989) Dihydropyrimidines: novel calcium antagonists with potent and long-lasting vasodilative and antihypertensive activity, *J Med Chem 32*, 2399-2406.

246. Atwal, K. S., Rovnyak, G. C., Kimball, S. D., Floyd, D. M., Moreland, S., Swanson, B. N., Gougoutas, J. Z., Schwartz, J., Smillie, K. M., and Malley, M. F. (1990) Dihydropyrimidine calcium channel blockers. 2. 3-substituted-4-aryl-1,4-dihydro-6-methyl-5-pyrimidinecarboxylic acid esters as potent mimics of dihydropyridines, *J Med Chem 33*, 2629-2635.

247. Arias, H. R., Bhumireddy, P., and Bouzat, C. (2006) Molecular mechanisms and binding site locations for noncompetitive antagonists of nicotinic acetylcholine receptors, *Int J Biochem Cell Biol 38*, 1254-1276.

248. Dilger, J. P., Boguslavsky, R., Barann, M., Katz, T., and Vidal, A. M. (1997) Mechanisms of barbiturate inhibition of acetylcholine receptor channels, *J Gen Physiol 109*, 401-414.

249. Khanetskyy, B., Dallinger, D., and Kappe, C. O. (2004) Combining Biginelli multicomponent and click chemistry: generation of 6-(1,2,3-triazol-1-yl)-dihydropyrimidone libraries, *J Comb Chem 6*, 884-892.

250. Stroud, R. M., McCarthy, M. P., and Shuster, M. (1990) Nicotinic acetylcholine receptor superfamily of ligand-gated ion channels, *Biochemistry 29*, 11009-11023.

251. Bianchi, M. T., and Macdonald, R. L. (2002) Slow phases of GABA(A) receptor desensitization: structural determinants and possible relevance for synaptic function, *J Physiol 544*, 3-18.

252. Shembekar, V. R., Chen, Y., Carpenter, B. K., and Hess, G. P. (2007) Coumarin-caged glycine that can be photolyzed within 3 microseconds by visible light, *Biochemistry 46*, 5479-5484.

253. Ramakrishnan, L., and Hess, G. P. (2010) Mechanism of Potentiation of a Dysfunctional Epilepsy-Linked Mutated GABA(A) Receptor by a Neurosteroid (3alpha, 21-Dihydroxy-5alpha-pregnan-20-one): Transient Kinetic Investigations, *Biochemistry*.

254. Trigo, F. F., Papageorgiou, G., Corrie, J. E., and Ogden, D. (2009) Laser photolysis of DPNI-GABA, a tool for investigating the properties and distribution of GABA receptors and for silencing neurons in situ, *J Neurosci Methods 181*, 159-169.

255. Herd, M. B., Belelli, D., and Lambert, J. J. (2007) Neurosteroid modulation of synaptic and extrasynaptic GABA(A) receptors, *Pharmacol Ther 116*, 20-34.

256. Feng, H. J., Bianchi, M. T., and Macdonald, R. L. (2004) Pentobarbital differentially modulates alpha1beta3delta and alpha1beta3gamma2L GABAA receptor currents, *Mol Pharmacol 66*, 988-1003.

257. Wafford, K. A., and Ebert, B. (2006) Gaboxadol--a new awakening in sleep, *Curr Opin Pharmacol 6*, 30-36.

258. Hess, G. P., and Grewer, C. (1998) Development and application of caged ligands for neurotransmitter receptors in transient kinetic and neuronal circuit mapping studies, *Methods Enzymol 291*, 443-473.

259. Denk, W. (1994) Two-photon scanning photochemical microscopy: mapping ligand-gated ion channel distributions, *Proc Natl Acad Sci U S A 91*, 6629-6633.

260. Szobota, S., and Isacoff, E. Y. (2010) Optical control of neuronal activity, *Annu Rev Biophys 39*, 329-348.

261. Engels, J., and Schlaeger, E. J. (1977) Synthesis, structure, and reactivity of adenosine cyclic 3',5'-phosphate benzyl triesters, *J Med Chem 20*, 907-911.

262. McCray, J. A., and Trentham, D. R. (1989) Properties and uses of photoreactive caged compounds., *Ann. Rev. Biophys. Biophys. Chem.*, 239-270.

263. De Mayo, P. (1960) Ultraviolet photochemistry of simple unsaturated systems., *Adv. Org. Chem. 2*, 367-425.

264. Barltrop, J. A., Plant, P. J., and Schofield, P. (1966) Photosensitive protecting group, *J. Chem. Soc. Chem. Commun.*, 822-823.

265. Fan, L., Lewis, R. W., Hess, G. P., and Ganem, B. (2009) A new

synthesis of caged GABA compounds for studying GABAA receptors, *Bioorg Med Chem Lett 19*, 3932-3933.

266. Matsuzaki, M., Hayama, T., Kasai, H., and Ellis-Davies, G. C. (2010) Two-photon uncaging of gamma-aminobutyric acid in intact brain tissue, *Nat Chem Biol 6*, 255-257.

267. Wieboldt, R., Ramesh, D., Carpenter, B. K., and Hess, G. P. (1994) Synthesis and photochemistry of photolabile derivatives of gamma-aminobutyric acid for chemical kinetic investigations of the gamma-aminobutyric acid receptor in the millisecond time region, *Biochemistry 33*, 1526-1533.

268. Canepari, M., Nelson, L., Papageorgiou, G., Corrie, J. E., and Ogden, D. (2001) Photochemical and pharmacological evaluation of 7-nitroindolinyl-and 4-methoxy-7-nitroindolinyl-amino acids as novel, fast caged neurotransmitters, *J Neurosci Methods 112*, 29-42.

269. Curten, B., Kullmann, P. H., Bier, M. E., Kandler, K., and Schmidt, B. F. (2005) Synthesis, photophysical, photochemical and biological properties of caged GABA, 4-[[(2H-1-benzopyran-2-one-7-amino-4-methoxy) carbonyl] amino] butanoic acid, *Photochem Photobiol 81*, 641-648.

270. Walker, J. W., Reid, G. P., McCray, J. A., and Trentham, D. R. (1988) Photolabile 1-(2-nitrophenyl)ethyl phosphate esters of adenine nucleotide analogs. Synthesis and mechanism of photolysis, *Journal of the American Chemical Society 110*, 7170-7177.

271. Feng, H. J., and Macdonald, R. L. (2004) Proton modulation of alpha 1 beta 3 delta GABAA receptor channel gating and desensitization, *J Neurophysiol 92*, 1577-1585.

272. Gee, K. R., Carpenter, B. K., and Hess, G. P. (1998) Synthesis, photochemistry, and biological characterization of photolabile protecting groups for carboxylic acids and neurotransmitters, *Methods Enzymol 291*, 30-50.

273. Lewis, C. A. (1979) Ion-concentration dependence of the reversal potential and the single channel conductance of ion channels at the frog neuromuscular junction, *J Physiol 286*, 417-445.

274. Spangler, S. G. (1972) Expansion of the constant field equation to include both divalent and monovalent ions, *Ala J Med Sci 9*, 218-223.